10-5-2017

Analysis of the Radius of Convergence of the Perturbation Expansion for the Ground State Energy of Two-Electron Atoms

Ryan Louis Peck
University of Windsor

Analysis of the Perturbation Expansion for the Ground State Energy of Two-Electron Atoms

by

Ryan Peck

A Thesis
Submitted to the Faculty of Graduate Studies
through the Department of Physics
in Partial Fulfillment of the Requirements for
the Degree of Master of Science
at the University of Windsor

Windsor, Ontario, Canada

Analysis of the Perturbation Expansion for the Ground State Energy of Two-Electron Atoms

by

Ryan Peck

APPROVED BY:

_____

M. Hlynka
Department of Mathematics & Statistics

_____

C. Rangan
Department of Physics

_____

G. W. F. Drake, Advisor
Department of Physics

Aug. 17, 2017

Author's Declaration of Originality

I hereby certify that I am the sole author of this thesis and that no part of this thesis has been published or submitted for publication.

I certify that, to the best of my knowledge, my thesis does not infringe upon anyones copyright nor violate any proprietary rights and that any ideas, techniques, quotations, or any other material from the work of other people included in my thesis, published or otherwise, are fully acknowledged in accordance with the standard referencing practices. Furthermore, to the extent that I have included copyrighted material that surpasses the bounds of fair dealing within the meaning of the Canada Copyright Act, I certify that I have obtained a written permission from the copyright owner(s) to include such material(s) in my thesis and have included copies of such copyright clearances to my Appendix.

I declare that this is a true copy of my thesis, including any final revisions, as approved by my thesis committee and the Graduate Studies office, and that this thesis has not been submitted for a higher degree to any other University or Institution.

Abstract

This thesis solves a controversial physics problem that has existed in the literature for nearly a century – finding the radius of convergence of the perturbation expansion for the ground state energy of the two-electron atom. This problem is important to study because it makes progress towards finding the possible structures that can exist in the quantum mechanical three-body problem. This perturbation expansion is a convergent series and in physics these are rare to work with. We usually refer to this perturbation expansion as the "$1/Z$ expansion". There is still much to learn about finding effective methods of determining the radii of convergence for convergent series. The first 1000 coefficients of the $1/Z$ expansion are calculated with very high precision and are compared to previous values in the literature. These coefficients are determined by using a new type of basis set that is introduced in this work, the pyramidal basis set, which is very useful in describing high-order wave functions generated by perturbation theory. Using the series of ratios of the resulting coefficients along with a series acceleration technique, the radius of convergence of the $1/Z$ expansion is found to be $\lambda^* = 1.0975(2)$.

Dedication

Dedicated to my family.

Acknowledgments

I would like to thank my supervisor Dr.Drake for giving me the opportunity to work for him, for funding my research, and for sharing his knowledge of atomic physics with me. I would also like to thank the Drake research group for making the office a fun place to be. Thank you to my family in Windsor for the countless meals we shared. I will definitely miss those! Last but not least, thanks to my mom, dad and sister for all of the long-distance chats that always brightened my days. This work would not be possible without the support I received from all of these amazing people.

Table of Contents

Author's Declaration of Originality **iii**

Abstract **iv**

Dedication **v**

Acknowledgments **vi**

List of Figures **ix**

List of Tables **xi**

1 Introduction **1**

2 Literature Review **6**

3 Theory **14**

3.1 The Hamiltonian 14

3.2 Variational Method 18

3.3 Basis Sets 22

3.3.1 Hylleraas Coordinates 22

3.3.2 Hylleraas Basis Sets 23

3.3.3 Pyramidal Basis Sets 27

3.4 Rayleigh-Schrödinger Perturbation Theory 30

3.5 Neville-Richardson Extrapolation 34

4 Results **37**

4.1 The Procedure 37

4.2 Calculations 43

4.3 Interesting Findings 101

4.3.1 Diagonalization Scheme Comparison 101

4.3.2 Oscillating Coefficients 101

4.3.3 Decay of Coefficients 105

5 Conclusion **108**

6 Future Work **110**

Appendices **111**

A Linear Variational Method 111

B Hylleraas Undheim Macdonald Theorem 113

C Matrix Diagonalization 116

C.1 Jacobi Method 117

C.2 Tridiagonalization 120

C.3 Power Method and Inverse Iteration Method 126

D Givens' Method 129

E Number of terms in a single Hylleraas basis set 132

Bibliography **135**

Vita Auctoris **138**

List of Figures

3.1 Interleaving of variational energies as basis size is increased . . . 21
3.2 Image of Hylleraas coordinates taken from reference [26] 22
3.3 Comparison of the triple and double basis sets' rates of convergence to the true energy E for the $1s2p^1P$ state of neutral helium. 25
3.4 Spread of nonlinear parameters with increasing basis size 28

4.1 Least squares fit to the ratios from $n = 100$ to 999 87
4.2 Least squares fit to the ratios from $n = 100$ to 400 88
4.3 Least squares fit to the s_n from $n = 100$ to 800 89
4.4 Least squares fit to the s_n from $n = 100$ to 300 90
4.5 Least squares fit to the s_n from $n = 100$ to 400 91
4.6 Least squares fit to the s_n from $n = 100$ to 500 92
4.7 Least squares fit to the t_n from $n = 100$ to 800 93
4.8 Least squares fit to the t_n from $n = 100$ to 300 94
4.9 Least squares fit to the t_n from $n = 100$ to 400 95
4.10 Least squares fit to the t_n from $n = 100$ to 500 96
4.11 Least squares fit to the v_n from $n = 100$ to 400 97
4.12 Least squares fit to the v_n from $n = 100$ to 150 98
4.13 The v_n from $n = 100$ to 200 99
4.14 Runtime for dall2016.f and dtridlz2016.f 102
4.15 PYC5TG974 vs. PYC5TGC68 103
4.16 Baker vs. PYC5TG974 104
4.17 Baker vs. PYC5TGC68 104

4.18 Helium E_n rapid decrease 106
4.19 s_n decay for different H^- triple basis set sizes 107

List of Tables

2.1 Important estimates of the radius of convergence of the $1/Z$ expansion 13

3.1 number of terms N in a typical triple basis set for various Ω. . . 26

3.2 Construction of a pyramidal basis set 29

4.1 Highly accurate energies for helium ^1P states achieved by double basis sets 40

4.2 Triple basis set optimized for H^- 45

4.3 Triple basis set optimized for He 45

4.4 Pyramidal basis with $\alpha_0 = 1.300$, $\beta_0 = 1.450$ and $M = 2.2$ 46

4.5 A special pyramidal basis set with $\alpha_0 = 2.000$, $\beta_0 = 2.200$ and $M = 2.0$ containing a double basis set $(\alpha_1 = 0.500, \beta_1 = 0.500), (\alpha_2 = 0.950, \beta_2 = 0.200)$ 46

4.6 E_2 for the He triple basis set in table 4.3 47

4.7 E_2 for the optimized pyramidal basis set in table 4.4 48

4.8 Comparison of different E_n. D+01 represents 10^1. 50

4.9 Accuracy of the series coefficients 86

5.1 Important estimates of the radius of convergence of the $1/Z$ expansion 109

Chapter 1

Introduction

It is important to know the basics of convergent series in order to understand what a radius of convergence is. A convergent power series is a series of the form

$$\sum_{n=0}^{\infty} a_n (x - x_0)^n \tag{1.1}$$

in which the coefficients a_n are getting progressively smaller at a fast enough rate with increasing n, such that when the entire series is added together the sum is a finite number for some range of values $a < x < b$. x_0 is referred to as the point of expansion of the series and choosing different x_0 will result in different ranges of convergence for the series. Outside of the range of convergence, the series will sum to ∞ and so the series diverges.

The range in which a power series converges is always symmetric about the point of expansion – a convergent power series always converges within some radius, determined by the singularity nearest to the expansion point of the series. For example, the Taylor series for the function $f(x) = \dfrac{1}{x - a}$ expanded about the point $x_0 = a+1$ will converge for all values of x in the range $x_0 - 1 < x < x_0 + 1$. We can think of this range of values as if it were the diameter of a circle. Thus the diameter of the range $x_0 - 1 < x < x_0 + 1$ is 2 and so the power series

expansion for $f(x) = \dfrac{1}{x-a}$ at $x_0 = a+1$ has a radius of convergence of 1.

This symmetric behaviour remains even for complex power series. A convergent complex series will converge within some disc in the complex plane. Thus, the radius of convergence for a general power series expanded about a point z_0 in the complex plane is simply the radius of this disc. It is important to know the radius of convergence of a power series because beyond the radius of convergence, the power series becomes divergent and mathematical techniques must be used to make sense of the series. Usually it is the singular points of a function that are the subject of interest and finding these points can be a difficult task. Knowledge of the radius of convergence of the Taylor series expansion of a function helps to locate the singular points of the function in the complex plane.

The perturbation expansion for the ground state energy of a two-electron atom is a convergent power series and so all of the logic above applies to this series. However, before we can define the perturbation expansion for the ground state energy of a two-electron atom, we must first explain how systems of particles are analyzed in quantum mechanics. For any quantum mechanical system, we are interested in solving the time independent Schrödinger equation (TISE)

$$H\psi_i = E_n\psi_i \tag{1.2}$$

(where H is the quantum mechanical energy operator called the Hamiltonian and will be explained more in section 3.1). To solve the TISE is to find the energy eigenfunctions ψ_i (also referred to as eigenstates or eigenvectors) and the energy eigenvalues E_i of a system of particles under the influence of a specific potential energy field (such as a constant magnetic field). The eigenfunctions are the possible states that the system can exist in after a measurement. The eigenvalues are the energies of each of these states. Once the TISE is solved, the time evolution of the system can be found by using the time dependent Schrödinger equation (TDSE).

$$i\hbar\frac{\partial\Psi}{\partial t} = H\Psi \tag{1.3}$$

in which i is the imaginary unit, $\hbar$ is Planck's constant divided by 2π, and Ψ is the wave function representing the state of the system of particles.

The full time-dependent wave function Ψ can be expanded as a linear combination of the TISE eigenfunctions ψ_i. The ψ_i do not change with time (for this reason they are also commonly referred to as stationary states) and so

$$\Psi(t) = \sum_{i=1}^{\infty} a_i(t)\psi_i \tag{1.4}$$

where all of the time dependence of $\Psi(t)$ comes from the coefficients of the stationary states $a_i(t)$. If the Hamiltonian is assumed to be independent of time then the solution to the TDSE is

$$\Psi(t) = e^{\left(\frac{-iHt}{\hbar}\right)}\Psi(t_0) \tag{1.5}$$

which shows explicitly how the initial state $\Psi(t_0)$ evolves into the state $\Psi(t)$ at a later time t.

The largest success of the Schrödinger equation is in its ability to accurately describe the energy spectrum of the hydrogen atom. The Schrödinger equation for the hydrogen atom can be solved analytically and the resulting spectrum of eigenvalues agreed very well with the observed spectrum which was determined experimentally in the early 20th century. The TISE was able to describe the Lyman, Balmer, Paschen, etc. series of hydrogen (in fact some of these series were observed after the Schrödinger equation predicted their existence). Solving the TISE becomes rapidly more difficult as more complicated atoms and ions are considered. Atomic physicists have been analyzing the TISE for the helium atom ever since the late 1920's and still today the helium atom remains a popular system to study.

Neutral helium consists of two electrons electromagnetically bound to a nucleus containing two protons and two neutrons. Treating the nucleus as a single body, the TISE for a helium atom is reduced to a three-body problem. It is a well known fact that three-body problems do not have closed-form solutions

– the motion of the bodies cannot be expressed in terms of elementary mathematical functions. This is why helium is the subject of so much study – it is the simplest atom which has no closed-form to its corresponding Schrödinger equation. By studying helium, we hope to learn more about the complications that arise from inter-electron correlations and ultimately wish to find highly accurate solutions to the Schrödinger equation for atoms with many electrons.

Today, we can find the eigenvalues for the nonrelativistic, infinite nuclear mass (these simplifications will be explained in section 3.1) TISE for helium to astonishing accuracy. Recent calculations of the eigenvalues of this equation in reference [30] contain up to 20 significant decimal digits. However, there is more to analyzing the helium atom than knowing the energy eigenstates and eigenvalues for the TISE. If we were to continuously lower the nuclear charge Z of a helium atom in its ground state (the state ψ_n with the lowest energy) down from $Z = 2$, at what value of Z would the total energy of the system be equivalent to a hydrogen atom of the same nuclear charge in its ground state? This value of Z is deemed the critical nuclear charge Z_c and has been recently found to very high precision (see reference [23]). Another interesting question is if we were again to continuously lower Z of a helium atom in its ground state, at what point would one of the electrons become unbound from the helium atom? This value of Z is denoted Z^* and we usually refer to the inverse of Z^* rather than Z^* itself. $\lambda^* = 1/Z^*$ denotes the radius of convergence of the $1/Z$ expansion of the energy for two-electron atoms and accurately determining this value is the main purpose of this work.

Finally, it would be interesting to compare the two values Z_c and Z^*. Intuitively, it would make sense that they may be equivalent, but this relationship is not the only possibility. For the two-electron atom, $Z_c \neq Z^*$ would imply that there is a continuous range $Z^* < Z < Z_c$ in which the outer electron would have enough energy to escape the atom, yet still would have a completely normalizable wave function and thus remain bounded to the nucleus. Such a state is called a bound state in the continuum. This work answers the question of whether or not the ground state of a two-electron atom becomes a bound state

in the continuum as the nuclear charge Z is reduced below the critical charge Z_c.

Chapter 2

Literature Review

Finding the radius of convergence λ^* of the $1/Z$ expansion for two-electron atoms has been a challenging problem dating back to the early 1930's. Baker *et al.* in reference [1] provide a very accurate account of the history of this problem up to 1990. The first half of this literature review will be a simplified summary of the history of λ^* as described in their work.

The problem of finding λ^* began with Hylleraas in the 1930's from reference [2]. He was the first to analyze the expansion

$$E(Z) = \sum_{n=0}^{\infty} E_n \frac{1}{Z^n} \tag{2.1}$$

or equivalently

$$E(\lambda) = \sum_{n=0}^{\infty} E_n \lambda^n \tag{2.2}$$

($\lambda = \frac{1}{Z}$) and calculated approximations to the first five E_n. This series is formally known as "the $1/Z$ expansion of the energy for two-electron atoms" but will be referred to as "the $1/Z$ expansion" in this thesis.

The $1/Z$ expansion is derived from the application of perturbation theory to the Z-scaled two-electron atom Schrödinger equation (perturbation theory is explained in section 3.4 and the derivation of the $1/Z$ expansion is covered in

section 4.1). Once the E_n are known, equation (2.2) provides an approximation to the true energy of a particular eigenstate for any value of Z which the series remains convergent.

In 1951 in reference [3], Kato proved that the $1/Z$ expansion is convergent. This proof can also be found in reference [4]. Convergent series are rare in physics, so after Kato proved the convergence of the $1/Z$ expansion, there came a great interest among many physicists to analyze the series and try to determine λ^* as accurately as possible.

The first attempt of finding a value for λ^* came from Knight and Scherr's work in reference [5]. In 1962 Knight and Scherr calculated the coefficients in 2.2 from E_2 up to E_{11} (E_0 and E_1 can be found analytically and are exactly -1 and $5/8$ respectively). From these coefficients, they constructed the ratios

$$r_n = \frac{E_{n+1}}{E_n} \tag{2.3}$$

The r_n's approach $\dfrac{1}{\lambda^*}$ as $n \to \infty$. Based off the observed behaviour of these first few ratios Knight and Scherr supposed that $\lambda^* \sim 1.33$.

In 1965 Midtdal calculated the first 22 coefficients of 2.2 in reference [7]. Stillinger noticed that the series of ratios r_n of Midtdal's coefficients appeared to be linear with respect to $1/n$ and so he performed a linear least squares fit to the last 8 r_n's, concluding that

$$\lambda^* = 1.1184 \tag{2.4}$$

(see reference [8]). Midtdal later calculated the first 81 E_n's in reference [11], however, it was eventually discovered that only the first 20-30 of these coefficients are reliable. As Baker *et al.* stated in reference [1], this was most likely due to the fact that the basis functions (basis functions and basis sets are explained in section 3.3) used to find the E_n's were not in the correct region of configuration space needed to describe the high-order behaviour of the $1/Z$ expansion. This phenomenon is briefly discussed in section 4.2.

In 1970 Brändas and Goscinski used the first 20 coefficients calculated by

Midtdal *et al.* to find

$$\lambda^* = 1.118 \tag{2.5}$$

(see reference [12]). This was done by using a method known as Padé analysis in which the power series expansion from equation (2.2) is replaced with the more general expression

$$E[M/N](\lambda) = \frac{\sum_{i=0}^{M} a_i \lambda^i}{1 + \sum_{j=1}^{N} b_j \lambda^j} \tag{2.6}$$

where $[M/N]$ is the order of the Padé approximant. In 1972, Brändas and Goscinski used a slightly different analysis of the first 27 coefficients from Midtdal *et al.* to find

$$\lambda^* = 1.119 \tag{2.7}$$

(see reference [13]).

In 1977 in reference [16], Reinhardt proved that if λ^* for a series E(λ) describing a normalizable eigenstate is determined by a singularity on the real Z axis, then this singularity must occur at the exact point where E(λ) becomes degenerate with a threshold. This means that if the singularity determining λ^* for a given eigenstate is found to be on the real Z axis and further that the eigenstate is normalizable at λ_c, then $\lambda^* = \lambda_c$.

Arteca *et al.* in reference [18] analyzed the $1/Z$ expansion in 1986 using the 22 coefficients calculated by Midtdal from reference [7]. The technique they used replaces equation (2.2) with a more general mathematical form, similar to the Padé analysis used in reference [12]. $E(\lambda)$ was assumed to behave like

$$E(\lambda) = f(\lambda)(1 - \frac{\lambda}{\lambda_0})^a + h(\lambda) \tag{2.8}$$

where $f(\lambda)$ and $h(\lambda)$ are analytic functions in the range $|\lambda| < R$ with $R > |\lambda_0|$. λ_0 is the location of the singularity which determines the radius of convergence

of the $1/Z$ expansion; $|\lambda_0| = \lambda^*$. They found that

$$\begin{aligned} a &= 1.07 \pm 0.01 \\ \lambda_0 &= 1.107 \pm 0.003 \\ h(\lambda_0) &= -0.995 \pm 0.001 \\ f(\lambda_0) &= -0.72 \pm 0.01 \end{aligned} \tag{2.9}$$

(so their estimate to the radius of convergence was $\lambda^* = \lambda_0 = 1.107 \pm 0.003$). Arteca *et al.* also revisited Stillinger's analysis of Midtdal's 22 E_n's from reference [8]. They performed a least squares fit to the r_n's that was parabolic in $1/n$ (Stillinger's fit was only linear in $1/n$) which yielded

$$\lambda^* = 1.1056 \pm 0.0040 \tag{2.10}$$

Baker, Freund, Morgan and Hill, made huge progress towards finding λ^* in reference [1]. They used variational calculations (see section 3.2) with basis sets consisting of 476 basis functions in conjunction with the HKS variational perturbation method described in reference [6] to find the $1/Z$ expansion coefficients up to 401st order. The last E_n's before the work of Baker *et al.* were calculated only up to 80th order by Midtdal *et al.* in reference [11] and were shown to be unreliable for $n > 30$. In contrast, Baker *et al.* state in their work "even our higher-order E_n's are accurate to a few parts in 10^5 and our high-order r_n's to a few parts in 10^6. The lower-order E_n's are of course much more accurate." The convergence of the series of r_n's is very slow and so Baker *et al.* used Neville-Richardson extrapolation (see section 3.5) to accelerate the convergence of the series.

They calculated the critical nuclear charge to be $Z_c = 0.911\,028$ using simple variational calculations. They also stated that their results from the Neville-Richardson extrapolations of the r_n series indicated $\lambda^* = 1/Z_c$. It should be noted that a direct calculation of λ^* was never performed in their work and most of their results were obtained under the assumption that $\lambda^* = 1/Z_c$. Their estimate of λ^* was

$$\lambda^* = \frac{1}{Z_c} = 1.097\,66(3) \tag{2.11}$$

Finally, Baker *et al.* deduced that the $1/Z$ expansion has both a branch point singularity and an essential singularity located at $\lambda = \frac{1}{Z_c}$ on the real axis, in agreement with Reinhardt's analysis in reference [16].

After the work of Baker *et al.* research into the $1/Z$ expansion continued with the hopes of being able to find an even more precise estimate to λ^*. In 1995 Ivanov analyzed the coefficients of Baker *et al.* and found the most precise estimate of λ^* in the literature to date in reference [19]. Rather than finding the radius of convergence of the series $E(\lambda)$ directly, he constructed the function

$$f(\lambda) = \frac{E(\lambda) - E_0}{E_1} = \sum_{i=1}^{\infty} \frac{E_i}{E_1} \lambda^i \tag{2.12}$$

then analyzed the inverse function

$$\lambda(f) = \sum_{k=1}^{\infty} \frac{f^k}{k!} \left[\frac{d^{k-1}}{d\lambda^{k-1}} \left(\frac{\lambda}{f(\lambda)} \right)^k \right]_{\lambda=0} = \sum_{k=1}^{\infty} \lambda_k f^k \tag{2.13}$$

Ivanov used a few different techniques to accelerate the convergence of this series and found the value

$$\lambda^* = 1.097\,660\,79(1) \tag{2.14}$$

It is important to notice that Ivanov's result for λ^* depends heavily on the accuracy of the coefficients E_n which were provided by reference [1]. For example, if these coefficients are found to be correct to 5 decimal digits, but are incorrect at 6 decimal digits then Ivanov's estimate to λ^* should only contain 5 significant digits. Ivanov also makes the assumption that the singularity determining λ^* is located on the real axis. However, this assumption is most likely true as the analysis of references [1, 8, 18] all independently provide evidence for this.

Recently, there has been some controversy over the results of Baker *et al.* In 2010 Zamastil *et al.* found

$$\lambda^* = 1.1085(2) \tag{2.15}$$

(see reference [20]) which is distinct from the value of $\lambda^* = 1.097\,66$ that was obtained by both Baker *et al.* and Ivanov. The authors arrive at this value of λ^* by using the first 19 E_n from reference [1] to construct a function describing the large-order behaviour of the E_n. As they stated in reference [20]: "one has to keep in mind that high coefficients of the convergent series are very difficult to determine. Certainly, the coefficients from the interval $n = 13$ to $n = 19$ are much more accurate than the coefficients from the interval $n = 25$ to $n = 401$. Consequently, any analysis made on low coefficients is much more reliable than that made on high coefficients". This is in direct contrast to what Baker *et al.* suggested of the series $E(\lambda)$ in reference [1]. They stated "the range $10 \leq n \leq 20$ is very, very far from the asymptotic region, and it is this circumstance which is responsible for the discrepancy between λ_c and λ^* found by Stillinger, by Brandas and Goscinski, by Anno and Teruya, and by Arteca, Fernandez, and Castro".

In June 2015 in reference [21], Turbiner and Guevara used the 401 coefficients from reference [1] to calculate the ground state energies for two-electron atoms for many different values of Z. They compared these ground state energies with those that were calculated directly by use of the variational method. They found that for $2 \leq Z \leq 10$ the resulting ground state energies from these two different methods agreed up to 12 decimal digits. However, for $Z = 1$ they only agreed to 10 decimal digits and for $Z = Z_c = 0.911028\ldots$ to just 6 decimal digits. From this analysis Turbiner and Guevara concluded that even the first significant digit in all of the coefficients E_n for $n > 135$ are not correct and hence that the asymptotic behaviour of the $1/Z$ expansion in reference [1] cannot be trusted. Turbiner and Guevara requested an independent recalculation of the $1/Z$ expansion coefficients.

In October 2015, Jean-Phillipe Karr found a value of $Z^* = 0.911\,276(12)$ in reference [22], corresponding to

$$\lambda^* = 1.097\,362(15) \tag{2.16}$$

This was accomplished by using the complex scaling method (allowing the en-

ergy $E(\lambda)$ and Hamiltonian H to become complex). He derived a formula for the imaginary part of the energy for values of Z near the singularity Z^*

$$\mathrm{Im}(E) \sim A\left(1-\frac{Z}{Z^*}\right)^P \exp\left(\frac{-c}{1-\frac{Z}{Z^*}}\right) \tag{2.17}$$

with $p=-2b-\dfrac{3}{2}$ and $c=\dfrac{a^2}{4}$. Karr found the value of the parameters a and b to be $a=0.26374$ and $b=-1.9896$ by using a formula for the coefficients

$$E_n \sim C(Z^*)^n n^b e^{-a\sqrt{n}} \tag{2.18}$$

and making a least squares fit of this formula to the coefficients from reference [1]. He then made another least squares fit of equation (2.17) to the imaginary part of $E(Z)$ for 11 different points in the range $0.905 \leq Z \leq 0.91103$ which were calculated using the variational method.

Since the work of Baker *et al.* in 1990, there has been no attempt at re-calculating the $1/Z$ expansion coefficients. Finding these coefficients is a very important task as they have formed the basis of many recent theoretical papers in the literature. This work is dedicated to calculating the $1/Z$ expansion coefficients, using them to find λ^* and testing the hypothesis that $\lambda^* = 1/Z_c$.

Table 2.1: Important estimates of the radius of convergence of the $1/Z$ expansion

year	reference	λ^*
1962	Knight and Scherr [5]	1.33
1966	Stillinger [8]	1.1184
1970	Brändas and Goscinski [12]	1.118
1972	Brändas and Goscinski [13]	1.119
1986	Arteca *et al.* [18]	1.1056(40)
1990	Baker *et al.* [1]	1.097 66(3)
1995*	Ivanov [19]	1.097 660 79(1)
2010*	Zamastil *et al.* [20]	1.1085(2)
2015*	Karr [22]	1.097 362(15)

The * indicates works that depend directly on the $1/Z$ expansion coefficients from reference [1].

Chapter 3

Theory

This chapter explains the main theories and concepts that were used in this work. We derive the Hamiltonian for a two-electron atom and describe the necessary approximation methods that were used to solve the corresponding Schrödinger equation. The theories in this chapter are extremely useful and will allow the reader to understand the procedure for obtaining the main results of this work (section 4.1).

3.1 The Hamiltonian

The time independent Schrödinger equation (TISE) is arguably the most useful equation in quantum mechanics

$$H\Psi_i = E_i\Psi_i \tag{3.1}$$

It is a differential equation (usually second order) with a wide range of possible solutions depending upon the form of the differential operator H. The eigenfunctions and eigenvalues of this differential equation correspond to the states that a given system of particles may be found in and the energy of each of these states, respectively. Physically, the Ψ_i are wave functions that describe how likely it is to find a type of particle (electrons, protons, muons, etc.) to be in

a certain position in space; the square amplitude of a wave function, $\Psi_i^* \Psi_i$, determines the probability of finding that type of particle for each point in space. E_i is the energy a system of particles has if they were measured to be in the corresponding state Ψ_i.

The Hamiltonian, H, in quantum mechanics is constructed the same way as it is in classical mechanics; $H = T + V$ where T is the kinetic energy and V the potential energy of the system. The only difference is that the classical position and momentum variables x and p respectively are replaced with their quantum mechanical operators $x \to x$, $p \to -i\hbar\nabla$.

The TISE can also be treated as an eigenvalue problem with Ψ_i as the eigenvectors and E_i as the eigenvalues by using matrix mechanics in which the Hamiltonian operator is represented by a matrix and the Ψ_i are represented by vectors. The first step to solving the TISE is to construct the Hamiltonian for the system under study.

For instance, the neutral helium atom consists of two electrons, two protons, and two neutrons. The two protons and neutrons make up the nucleus of the atom where most of the mass is located. The size of the nucleus is on the order of femtometers (10^{-15} m) while the distance of the electrons from the nucleus is on the order of Ångströms (10^{-10} m). Due to this large discrepancy between relative distance scales, it is fair to treat the nucleus as a single point-particle of nuclear charge $Z = 2$ in the case of neutral helium.

The protons and neutrons that make up the nucleus are each roughly 2000 times as massive as an electron. The electromagnetic forces that the electrons apply to the nucleus will therefore not result in much movement of the nucleus compared to the motion of the electrons resulting from the forces that the nucleus applies to the electrons. A simple analogy of this situation is that of the gravitational attraction between a person and the earth. Both the person and the earth experience the exact same force due to the gravitational attraction between them, however, the person moves much more than the earth because he/she has much less mass than the earth. We can then justify the assumption that the nucleus is stationary in comparison to the motion of the electrons.

This is called the "infinite nuclear mass" approximation. Finally, the effects of special relativity will be excluded in the Hamiltonian so that we are working in the nonrelativistic regime of electron motion (the electrons are not moving at an appreciable speed relative to the speed of light).

So, the physical situation that we are to describe is a three-body problem consisting of an infinitely massive nucleus which has a nuclear charge Z which we will ultimately allow to vary continuously, along with two nonrelativistic electrons bound to the nucleus by the electromagnetic force. The Hamiltonian which describes this system is

$$H = -\frac{\hbar^2}{2m}(\nabla_1^2 + \nabla_2^2) - \frac{Ze^2}{r_1} - \frac{Ze^2}{r_2} + \frac{e^2}{r_{12}} \tag{3.2}$$

where m and e are the mass and charge of an electron, r_1 and r_2 are the radial positions of electrons 1 and 2 respectively, and finally

$$r_{12} = |\vec{r_1} - \vec{r_2}| \tag{3.3}$$

This is the nonrelativistic, infinite nuclear mass Hamiltonian for a two-electron atom with variable nuclear charge Z in electrostatic units and it can be simplified by making the scale change

$$r' = \frac{Zr}{a_0} \tag{3.4}$$

($a_0 = \dfrac{\hbar^2}{me^2}$ is the Bohr radius)

$$H' = -\frac{Z^2e^2}{a_0}(\nabla_1'^2 + \nabla_2'^2) - \frac{Z^2e^2}{a_0 r_1'} - \frac{Z^2e^2}{a_0 r_2'} + \frac{Ze^2}{a_0 r_{12}'} \tag{3.5}$$

We then convert to atomic units ($m = e = \hbar = \frac{1}{4\pi\epsilon_0} = 1$), divide by Z^2 and remove the primes (with the understanding we are still working with $r' = \dfrac{Zr}{a_0}$ and not r – we have just renamed the variables so that we don't have to use the primes) to arrive at the Z-scaled two-electron Hamiltonian

$$H = -\frac{1}{2}(\nabla_1^2 + \nabla_2^2) - \frac{1}{r_1} - \frac{1}{r_2} + \frac{Z^{-1}}{r_{12}} \tag{3.6}$$

The Schrödinger equation for this Hamiltonian is

$$H\psi = \frac{E}{Z^2}\psi \tag{3.7}$$

where the Energy E is in atomic units (a.u.) and the factor of $\frac{1}{Z^2}$ comes from the division by Z^2 that we applied in order to derive the Z-scaled two-electron Hamiltonian. If we work in a set of units known as "Z-scaled atomic units" we can get rid of the Z^2 term in the Schrödinger equation. The energy in Z-scaled atomic units ϵ is related to the energy in atomic units E by

$$\epsilon = \frac{E}{Z^2} \tag{3.8}$$

and so in Z-scaled atomic units we have the more familiar Schrödinger equation

$$H\psi = \epsilon\psi \tag{3.9}$$

Now, we are interested in the behaviour of the electrons as the nuclear charge is continuously varied down from $Z = 2$. From equation (3.6) it is seen that decreasing Z will increase the strength of the repulsive Coulomb interaction between the two electrons while the strength of the attractive nucleus-electron interactions will not change. Eventually the repulsion between the two electrons will dominate and the outer electron will be pushed away from the nucleus, becoming unbound. At this point, the outer-electron is a free particle and so the energy calculated by equation (3.9) should just be the energy of the remaining electron-nucleus system in Z-scaled atomic units.

Z_c is the critical nuclear charge and is defined to be the Z at which $\epsilon = -\frac{1}{2}$ in equation (3.6). This definition comes from the ground state energy of hydrogen-like atoms (atoms with one electron). The energy eigenvalues of a hydrogen-like atom with variable nuclear charge Z are $E_n = -\frac{Z^2}{n^2}$. Thus, the ground state energy ($n = 1$) of a hydrogen-like atom is $E_1 = -\frac{1}{2}$ in Z-scaled atomic units. So Z_c is the value of Z for which the ground state energy of the two-electron atom and the hydrogen-like atom have the same energy.

It has been proven by Hill in 1977 in reference [24] that the H^- two-electron atom ($Z = 1$) has only one state with both electrons bound to the nucleus. This means that $Z_c \leq 1$, and also that the only bound state of the two-electron atom as Z is decreased below one is the ground state.

3.2 Variational Method

The three-body problem cannot be solved analytically and so a method of approximating the solutions of the two-electron Hamiltonian is needed. We begin by attempting to solve the TISE

$$H\phi_i = E_i\phi_i \tag{3.10}$$

with the goal of finding the eigenfunctions, ϕ_i and eigenvalues, E_i for a given Hamiltonian, H. From the axioms of quantum mechanics we know that the eigenfunctions must form a complete set of basis functions. This means any trial wave function used to approximate one of the true eigenfunctions can be expressed as a linear combination of the true eigenfunctions. The simple knowledge that we can express the trial wave functions this way even though we may know nothing about the true eigenfunctions themselves turns out to be surprisingly useful.

The true energy eigenfunctions ϕ_i obey

$$E_i = \langle\phi_i|H|\phi_j\rangle\delta_{ij} \tag{3.11}$$

where the E_i are the exact energies. Let ψ_{tr} be a normalizable trial wave function that approximates the true ground state ϕ_0 and let $\tilde{E}_{tr}$ be a variational energy defined by

$$\tilde{E}_{tr} = \frac{\langle\psi_{tr}|H|\psi_{tr}\rangle}{\langle\psi_{tr}|\psi_{tr}\rangle} \tag{3.12}$$

Assuming the trial ground state wave function, ψ_{tr} is normalized then

$$\tilde{E}_{tr} = \langle \psi_{tr} | H | \psi_{tr} \rangle \tag{3.13}$$

Expand the unit operator $\sum_{i=1}^{\infty} |\phi_i\rangle\langle\phi_i| = 1$ on both sides of H

$$\tilde{E}_{tr} = \sum_{ij=1}^{\infty} \langle \psi_{tr} | \phi_i \rangle \langle \phi_i | H | \phi_j \rangle \langle \phi_j | \psi_{tr} \rangle \tag{3.14}$$

Inserting equation (3.11) into equation (3.14) leaves us with

$$\tilde{E}_{tr} = \sum_{i=1}^{\infty} |\langle \psi_{tr} | \phi_i \rangle|^2 E_i \tag{3.15}$$

Since we have assumed ψ_{tr} to be normalized, we can add and subtract E_0 in the following way

$$\tilde{E}_0 = E_0 + \sum_{i=1}^{\infty} |\langle \psi_{tr} | \phi_i \rangle|^2 (E_i - E_0) \tag{3.16}$$

We know that both $|\langle \psi_{tr} | \phi_i \rangle|^2 \geq 0$ and $(E_i - E_0) \geq 0$ which leads us to the conclusion of the variational method

$$\tilde{E}_{tr} \geq E_0 \tag{3.17}$$

Any normalizable trial wave function will yield an upper bound to the exact ground state energy of a given Hamiltonian. The lower the variational ground state energy is, the more accurate it is!

The idea of the variational method is to start with an arbitrary trial wave function with tunable parameters and optimize them to minimize the variational energy, which will result in the best approximation to E_0 that the chosen trial wave function can provide. We usually treat these trial wave functions as vectors in a vector space once we have chosen an appropriate basis set to expand ψ_{tr} in.

A basis set B is complete on a vector space V (V could be Hilbert space or Euclidean space for example) if every element of V can be expressed as a linear combination of elements of B. Therefore, we can always express ψ_{tr} as a finite linear combination of basis functions χ_i as long as we know the set of basis

functions (the basis set) is complete in Hilbert space (the space of solutions ϕ_i to the Schrödinger equation) in the limit $\lim_{N\to\infty}$ (where N is the number of basis functions being used in the basis set). $\chi_i(\alpha, \beta, \dots)$ will denote the ith basis function of a basis set that is complete as $N \to \infty$, with $(\alpha, \beta, \dots)$ appearing as tunable nonlinear parameters.

$$|\psi_{tr}\rangle = \sum_{i=1}^{N} c_i |\chi_i(\alpha, \beta, \dots)\rangle \tag{3.18}$$

Optimizing only the linear parameters c_i in a trial wave function is equivalent to solving

$$\mathbf{Hc} = E\mathbf{Oc} \tag{3.19}$$

(see Appendix A for proof) where $\mathbf{H}$ and $\mathbf{O}$ are the Hamiltonian and overlap matrices respectively. The matrix elements of $\mathbf{H}$ are $H_{ij} = \langle\chi_i|H|\chi_j\rangle$ and the matrix elements of $\mathbf{O}$ are $O_{ij} = \langle\chi_i|\chi_j\rangle$. $\mathbf{c}$ is the ordered column vector of coefficients of the basis functions $c_i = \langle\chi_i|\psi_{tr}\rangle$. Equation (3.19) is the "generalized eigenvalue problem". This equation reduces to the Schrödinger equation when the basis set being used is orthonormal ($\langle\chi_i|H|\chi_j\rangle = \delta_{ij} \implies \mathbf{O} = \mathbf{I}$).

As is explained in reference [27], to find upper bounds to not only the ground state but the excited states as well, we can use the Hylleraas Undheim MacDonald Theorem (HUM) from references [28, 29]. HUM states that as the dimensions of $\mathbf{H}$ and $\mathbf{O}$ are increased, the N old eigenvalues are sandwiched between the new $N + 1$ eigenvalues (See figure 3.1). HUM further states that if the basis set being used is complete and if there is a lower bound E_0 to the energy spectrum, then each of the eigenvalues of the Hamiltonian matrix are upper bounds to the exact energies E_i. This spectrum of energy eigenvalues which approximates the true energy spectrum is called the "pseudospectrum".

To summarize this section, by expanding a trial wave function in a truncated basis set that is complete in Hilbert space as $N \to \infty$, we can solve the TISE and find upper bounds to all of the exact energies in the spectrum. We can improve the accuracy of these upper bounds by introducing adjustable parameters into

Figure 3.1: Interleaving of variational energies as basis size is increased

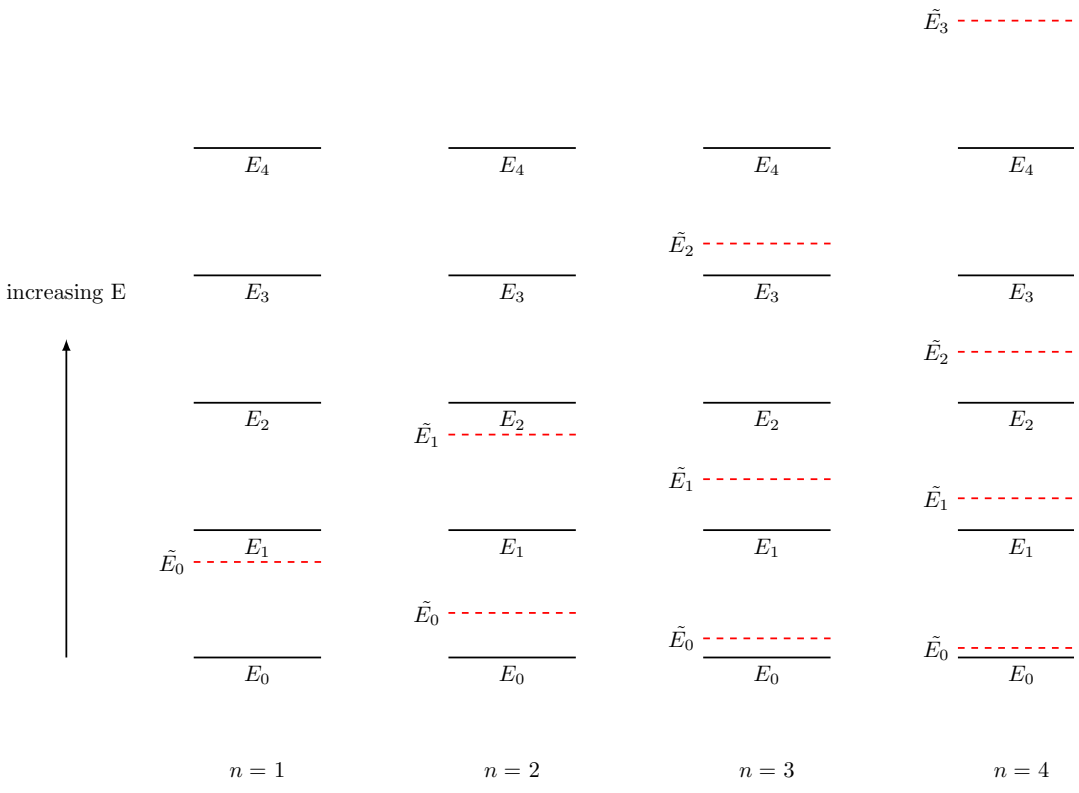

our basis set that can be optimized to minimize these upper bounds.

3.3 Basis Sets

This section describes the two different complete variational basis sets that were used in this work. With these basis sets, the TISE for the two-electron Z-scaled Hamiltonian can be solved with very high precision. Both of these basis sets are expressed in Hylleraas coordinates and so before they are discussed it is important to first understand Hylleraas coordinates.

3.3.1 Hylleraas Coordinates

Figure 3.2: Image of Hylleraas coordinates taken from reference [26]

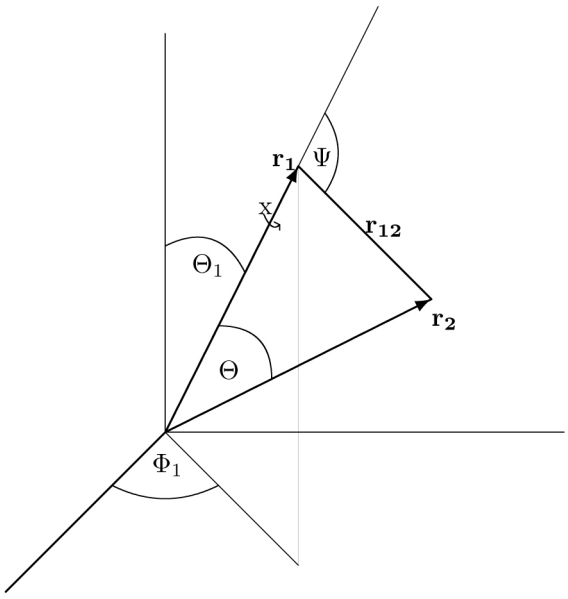

The independent variables in Hylleraas coordinates are

$$(r_1, r_2, r_{12}, \Theta_1, \Phi_1, \chi) \tag{3.20}$$

where r_i corresponds to the distance of electron i from the origin and $r_{12} =$

$|r_1 - r_2|$. When Hylleraas introduced these coordinates to solve the helium atom, he initially used

$s = r_1 + r_2, t = r_{12}, u = r_1 - r_2$ instead of r_1, r_2, r_{12}. However, both of these bases are equivalent because there is an invertible linear transformation relating the two basis sets.

$$\begin{pmatrix} s \\ t \\ u \end{pmatrix} = \begin{pmatrix} 1 & 1 & 0 \\ 0 & 0 & 1 \\ 1 & -1 & 0 \end{pmatrix} \begin{pmatrix} r_1 \\ r_2 \\ r_{12} \end{pmatrix} \tag{3.21}$$

The significance of Hylleraas coordinates is to include the r_{12} term as an independent parameter. The inclusion of powers of r_{12} in the basis set generates much more rapidly converging results compared to those of a configuration interaction calculation (this is a very common method used in quantum chemistry for finding the ground state energies of atoms and molecules).

3.3.2 Hylleraas Basis Sets

The variational basis sets used in this work are modified Hylleraas basis sets

$$\Psi = \sum_{ijk}^{\Omega} c_{ijk}[r_1^i r_2^j r_{12}^k e^{-\alpha r_1} e^{-\beta r_2} \pm r_2^i r_1^j r_{12}^k e^{-\alpha r_2} e^{-\beta r_1}] \tag{3.22}$$

$$i + j + k \leq \Omega \tag{3.23}$$

The above basis set is called a single Hylleraas basis set. The α's and β's that appear in these basis sets are nonlinear parameters. Larger α's and β's will describe states where the electrons are closer to the nucleus while smaller α's and β's will describe states where the electrons are further from the nucleus. The number of terms in a single Hylleraas basis set is

$$N = \frac{(\Omega + 1)(\Omega + 2)(\Omega + 3)}{6} \tag{3.24}$$

(see Appendix E for proof)

so the number of terms in a single basis set grows roughly like Ω^3 which is very rapid!

The term on the right of the $\pm$ in (3.22) is the exchange term. The sign of the exchange term is determined by the required symmetry of the state represented by Ψ. Electrons are fermions and so any wave function describing electrons must be antisymmetric under an interchange of the electrons (switching the states of any two electrons must yield an overall minus sign in the wave function). The total wave function is a product of the spatial and spin wave functions. The ground state of helium $(1s)^2\ ^1S_0$ has the two electrons in a spin singlet configuration, so the spin part of the wave function is antisymmetric. Thus for the ground state of helium the exchange term in Ψ would be added (+) in order to make the spatial part of the wave function symmetric.

An extension of the basis sets used in this work are triple basis sets, which are simply constructed from three individual single Hylleraas basis sets

$$\Psi = \sum_{p=1}^{q} \sum_{i,j,k}^{\Omega_p} c_{ijk}^{p} [r_1^i r_2^j r_{12}^k e^{-\alpha_p r_1} e^{-\beta_p r_2} \pm r_2^i r_1^j r_{12}^k e^{-\alpha_p r_2} e^{-\beta_p r_1}] \tag{3.25}$$

with $i + j + k \leq \Omega_p$ for each basis set in the p sum. $q = 2$ corresponds to a double basis set and $q = 3$ to a triple basis set. For a sufficiently large basis, a triple basis set produces variational energies which converge faster to the true energies than its double basis set counterpart. Figure 3.3 clearly shows this difference in convergence rates.

Diagonalizing the Hamiltonian matrix is equivalent to optimizing the linear coefficients in our Hylleraas basis set, c_{ijk}^{p} (see Appendix A for a proof of this). After diagonalizing the Hamiltonian matrix, only the nonlinear parameters that appear in our basis sets will need to be optimized. However, this turns out to be a time consuming task.

We choose initial nonlinear parameters $\alpha_p = \alpha_{p_0}$ and $\beta_p = \beta_{p_0}$, then solve the generalized eigenvalue problem (equation (3.19)) which yields an entire pseudospectrum of energy eigenvalues which approximates the true energy spectrum. We keep track of the variational eigenvalue we are interested $\tilde{E}_n$ and repeat the process using an adjusted set of nonlinear parameters. Newton's method is used

Figure 3.3: Comparison of the triple and double basis sets' rates of convergence to the true energy E for the $1s2p\,^1P$ state of neutral helium.

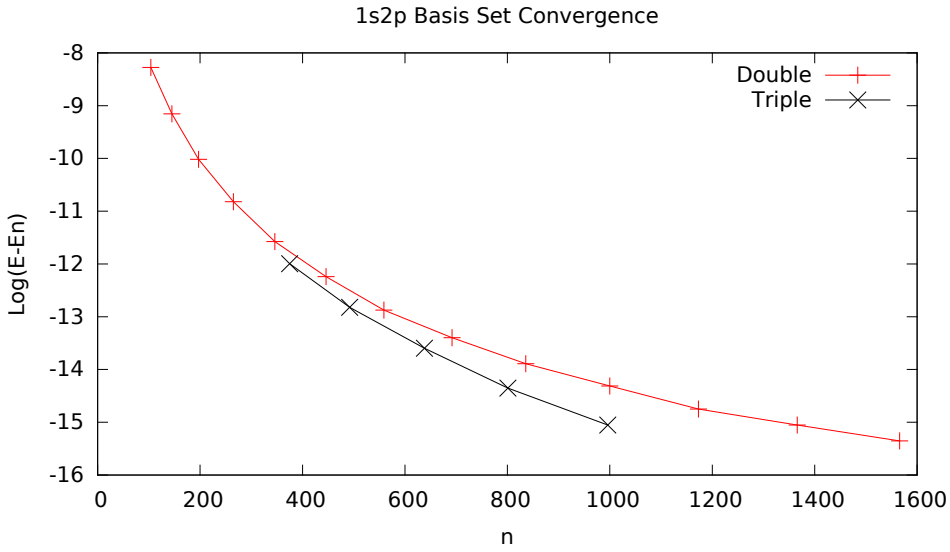

to find the nonlinear parameters that minimize $\tilde{E}_n$ and so the generalized eigenvalue problem needs to be solved multiple times before the optimal nonlinear parameters are found. Luckily, the nonlinear parameters can all be optimized simultaneously so this entire procedure does not need to be repeated for each individual nonlinear parameter one at a time (this is explained in reference [26]).

There is a simple way to increase the accuracy of the upper bounds to the energies that does not involve optimizing the nonlinear parameters. Increasing the size of a basis set by including more basis functions, guarantees lower and thus improved upper bounds to the true energies (see Appendix B). When using a triple basis set, we would generally start with $\Omega_1 = 10$, $\Omega_2 = 10$, $\Omega_3 = 2$ and then end around $\Omega_1 = 18$, $\Omega_2 = 18$, $\Omega_3 = 10$, incrementing all of the Ω_p's by 1 each time. The optimal nonlinear parameter groups, (α_p, β_p), each increase roughly linearly with respect to Ω as Drake *et al.* have explained in reference [30]. In order to understand why this happens, we will analyze just a single

Table 3.1: number of terms N in a typical triple basis set for various Ω.

Ω	N
10	324
11	411
12	512
13	630
14	764
15	918
16	1098
17	1283
18	1495

The triple basis set used to create this table consisted of single basis set sectors of size $\Omega_1 = \Omega_2 = \Omega$, $\Omega_3 = \Omega - 8$

.

Hylleraas basis set

$$\Psi = \sum_{ijk}^{\Omega} c_{ijk} r_1^i r_2^j r_{12}^k e^{-\alpha r_1} e^{-\beta r_2} \tag{3.26}$$

We only need a general idea of how the nonlinear parameters vary with Ω so the exchange term is left out in order to simplify the calculations. Taking the derivative of 3.26 with respect to r_1

$$\frac{\partial \Psi}{\partial r_1} = \sum_{ijk}^{\Omega} c_{ijk} \left(\frac{i}{r_1} - \alpha \right) r_1^i r_2^j r_{12}^k e^{-\alpha r_1} e^{-\beta r_2} \tag{3.27}$$

We will replace the above sum in 3.27 with only the dominant term

$$\frac{\partial \Psi}{\partial r_1} = \left(\frac{\Omega}{r_1} - \alpha \right) r_1^i r_2^j r_{12}^k e^{-\alpha r_1} e^{-\beta r_2} \tag{3.28}$$

Now we can find where Ψ peaks with respect to r_1.

$$\left(\frac{\Omega}{r_1} - \alpha\right) r_1^i r_2^j r_{12}^k e^{-\alpha r_1} e^{-\beta r_2} = 0$$

$$\frac{\Omega}{r_1} - \alpha = 0$$

$$r_1 = \frac{\Omega}{\alpha} \tag{3.29}$$

Ψ will be optimized to describe only a single energy eigenstate. Assuming that the optimized Ψ can accurately approximate the true eigenstate, then a sequence of $\Psi(\Omega_n)$ describing this eigenstate should all have the same peak location $r_1 = \frac{\Omega_n}{\alpha_n}$. This means that if Ω is increased, the corresponding optimal α must increase by the same amount. Exactly the same argument can be used for $\frac{\partial \Psi}{\partial r_2}$ to arrive at an identical conclusion for β. There were some assumptions and simplifications used to arrive at these conclusions and so the final result of this analysis is that the optimized nonlinear parameters for a given wave function should increase roughly linearly with Ω.

It is also interesting to note that the three sets of nonlinear parameters tend to spread out at different rates as can be seen in figure 3.4. As Ω is increased, each of these three sectors of the triple basis set will describe phenomenon at different length scales due to this separation.

3.3.3 Pyramidal Basis Sets

A pyramidal basis stems from the success of the triple basis set, achieved by the inclusion of multiple length scales, α_q, β_q into the basis set. A pyramidal basis set has the form

$$\Psi = \sum_{q=1}^{p_n} \sum_{ijk}^{\Omega_q} c_{ijk}^{(q)} [r_1^i r_2^j r_{12}^k e^{-\alpha_q r_1} e^{-\beta_q r_2} \pm r_2^i r_1^j r_{12}^k e^{-\alpha_q r_2} e^{-\beta_q r_1}] \tag{3.30}$$

A single pyramidal basis set includes p_n single Hylleraas basis sets, each with different numbers of terms determined by the Ω_q and the different nonlinear parameters α_q, β_q. Each of the single Hylleraas basis sets that compose the

Figure 3.4: Spread of nonlinear parameters with increasing basis size

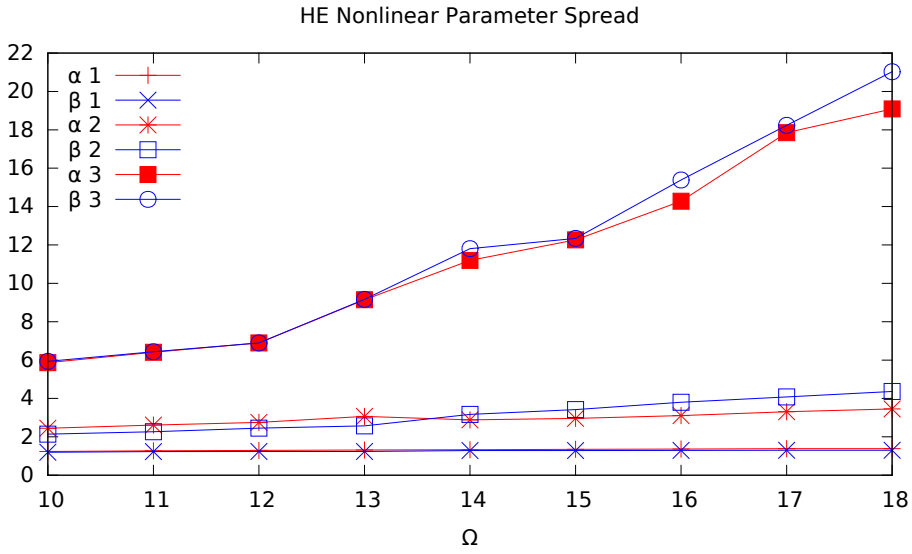

overall pyramidal basis set are arranged in layers like that of a pyramid (see table 3.2).

There are also restrictions on the Ω_q's and α_q β_q to give the basis sets more structure thereby making them more consistent and removing some unnecessary degrees of freedom as the basis size increases. The restrictions are

$$\alpha_{q+1} = M\alpha_q$$
$$\beta_{q+1} = M\beta_q$$
$$\Omega_{q+1} = \Omega_q - 1$$

where M is a constant, predetermined multiplying factor and is a degree of freedom along with α_1, β_1 and Ω_1.

Here is an example to help the reader understand the components of a pyramidal basis set. To construct our very first pyramidal basis set in a pyramidal

Table 3.2: Construction of a pyramidal basis set

			$\Omega = 5; M^3\alpha_0, M^3\beta_0$
		$\Omega = 5; M^2\alpha_0, M^2\beta_0$	$\Omega = 6; M^2\alpha_0, M^2\beta_0$
	$\Omega = 5; M\alpha_0, M\beta_0$	$\Omega = 6; M\alpha_0, M\beta_0$	$\Omega = 7; M\alpha_0, M\beta_0$
$\Omega = 5; \alpha_0, \beta_0$	$\Omega = 6; \alpha_0, \beta_0$	$\Omega = 7; \alpha_0, \beta_0$	$\Omega = 8; \alpha_0, \beta_0$

The columns of this table contain the components of the pyramidal basis set at each stage of its construction. Going from leftmost column to the rightmost we see how each increase in the size of the pyramidal basis set includes another single Hylleraas basis set.

basis set series, the degrees of freedom α_1, β_1 and Ω_1 are chosen and we set $p_n = 1$. To make this example more concrete let's set $\alpha_1 = 1$ $\beta_1 = 2$ $\Omega_1 = 5$ and $M = 2$. The result is a single Hylleraas basis set (Just to clarify, we chose M now, but it does not affect this first basis set. We could have chosen M in the next step instead)

$$\Psi = \sum_{ijk}^{5} c_{ijk}^{(1)} [r_1^i r_2^j r_{12}^k e^{-1r_1} e^{-2r_2} \pm r_2^i r_1^j r_{12}^k e^{-1r_2} e^{-2r_1}]$$

Now, for the next pyramidal basis set in the series, we set $p_n = 2$ and raise Ω_1 up to six from five, With $M = 2$, $\alpha_2 = M \times \alpha_1 = 2$ and $\beta_2 = M \times \beta_1 = 4$. Then the next pyramidal basis set is the following double basis set

$$\begin{aligned}\Psi = &\sum_{ijk}^{6} c_{ijk}^{(1)} [r_1^i r_2^j r_{12}^k e^{-1r_1} e^{-2r_2} \pm r_2^i r_1^j r_{12}^k e^{-1r_2} e^{-2r_1}] \\ &+ \sum_{ijk}^{5} c_{ijk}^{(2)} [r_1^i r_2^j r_{12}^k e^{-2r_1} e^{-4r_2} \pm r_2^i r_1^j r_{12}^k e^{-2r_2} e^{-4r_1}]\end{aligned}$$

For the next basis set, Ω_1 and p_n would be incremented yet again by one, with $\alpha_3 = M \times \alpha_2 = 4$, $\beta_3 = M \times \beta_2 = 8$ resulting in the triple basis set

$$\Psi = \sum_{ijk}^{7} c_{ijk}^{(1)} [r_1^i r_2^j r_{12}^k e^{-1r_1} e^{-2r_2} \pm r_2^i r_1^j r_{12}^k e^{-1r_2} e^{-2r_1}]$$
$$+ \sum_{ijk}^{6} c_{ijk}^{(2)} [r_1^i r_2^j r_{12}^k e^{-2r_1} e^{-4r_2} \pm r_2^i r_1^j r_{12}^k e^{-2r_2} e^{-4r_1}]$$
$$+ \sum_{ijk}^{5} c_{ijk}^{(3)} [r_1^i r_2^j r_{12}^k e^{-4r_1} e^{-8r_2} \pm r_2^i r_1^j r_{12}^k e^{-4ar_2} e^{-8r_1}]$$

The advantage that these pyramidal basis sets have is that they are not restricted to describing just a couple length scales. Each increase in size of a pyramidal basis set includes another single Hylleraas basis set with larger nonlinear parameters. This corresponds to incorporating smaller distance scales into the total wave function Ψ, ideally leading to improved numerical precision for the variational energy eigenvalues once the optimal linear parameters $c_{ijk}^{(q)}$ are found. The presence of these large nonlinear parameter terms in the pyramidal basis sets also results in much larger highest energies in the pseudospectra. Naturally, the question arises as to whether these pyramidal basis sets are any better than the triple basis sets at retrieving accurate eigenvalues for the two-electron TISE – does the inclusion of the extra length scales make a significant difference in the variational energies? The answer to this question will be discussed in the results chapter, section 4.2.

3.4 Rayleigh-Schrödinger Perturbation Theory

Perturbation theory is an important and useful method of finding an approximate solution to a difficult TISE. Most of the time the TISE for the Hamiltonian we are interested in is either very difficult to solve, or it cannot be solved analytically (such is the case with our three-body Z-scaled Hamiltonian). In these very common cases, perturbation theory is used to turn a single very difficult problem (solving the full TISE) into an infinite series of easier problems in the hope that the solutions to the easy problems can be pieced together to form an approximate solution to the difficult problem.

Perturbation theory begins by splitting the Hamiltonian into two parts. The first part H_0 is a known exactly solvable part and the second part is the rest of the Hamiltonian which is denoted by λV where λ is a parameter controlling the strength of the perturbation. The TISE for the latter part of the Hamiltonian usually doesn't have a simple or known solution and is called the "perturbation".

In order to attain accurate results upon application of perturbation theory, the perturbation should not be the dominant part of the Hamiltonian. To clarify this condition, we require that the differences in the energy spectrum of H and H_0 be relatively small. Of course, it is difficult to guess if this condition is met before the spectrum of H is found, so usually perturbation theory is applied first and then the resulting spectrum is compared to the spectrum of H_0 to see if there are any large differences.

The Hamiltonian we have constructed is

$$H = H_0 + \lambda V \tag{3.31}$$

The TISE then becomes

$$(H_0 + \lambda V)|\psi_m\rangle = E_m|\psi_m\rangle \tag{3.32}$$

λ is an auxiliary variable that plays the role of an expansion parameter. In the case of the Z-scaled two-electron Hamiltonian, we set $\lambda = \dfrac{1}{Z}$ at the end of the calculation.

We assume the energies and wave functions have power series solutions

$$E_m = \sum_{i=0}^{\infty} \lambda^i E_m^i \tag{3.33}$$

$$|\psi_m\rangle = \sum_{i=0}^{\infty} \lambda^i |\psi_m^i\rangle \tag{3.34}$$

where the subscript m represents which state we are working with ($m = 1$ would be the ground state) and the superscript i that appears above the coefficients in the two separate series is called the "order" of the coefficient. Expanding

these in equation (3.32) and equating powers of λ to zero gives us the following sequence of equations

$$\lambda^0 : H_0|\psi_m^0\rangle = E_m^0|\psi_m^0\rangle \tag{3.35}$$

$$\lambda^1 : H_0|\psi_m^1\rangle + V|\psi_m^0\rangle = E_m^1|\psi_m^0\rangle + E_m^0|\psi_m^1\rangle \tag{3.36}$$

$$\lambda^2 : H_0|\psi_m^2\rangle + V|\psi_m^1\rangle = E_m^2|\psi_m^0\rangle + E_m^1|\psi_m^1\rangle + E_m^0|\psi_m^2\rangle \tag{3.37}$$

$$\lambda^n : H_0|\psi_m^n\rangle + V|\psi_m^{n-1}\rangle = \sum_{k=0}^{n} E_m^{n-k}|\psi_m^k\rangle \tag{3.38}$$

Equation (3.35) is already solved – it is the Schrödinger equation for the known piece of the Hamiltonian H_0. Equation (3.36) and (3.37) are the first and second order equations respectively. Equation (3.38) is the nth order equation for any general $n \geq 1$.

Now, we must decide how to normalize all of these wave functions. First, we will require that both the zeroth order wave function $|\psi_m^0\rangle$ and the full wave function $|\psi_m\rangle$ be normalized to unity.

$$\langle\psi_m^0|\psi_m^0\rangle = 1 \tag{3.39}$$

$$\langle\psi_m|\psi_m\rangle = \sum_{i=0}^{\infty}\sum_{j=0}^{\infty}\lambda^{i+j}\langle\psi_m^i|\psi_m^j\rangle = 1 \tag{3.40}$$

These equations create a normalization condition to be satisfied for each order of λ.

$$\lambda^n : \sum_{i=0}^{n}\langle\psi_m^{n-i}|\psi_m^i\rangle = \delta_{n0} \tag{3.41}$$

In the absence of degeneracy ($E_i \neq E_j, \forall i \neq j$) the wave function can always be taken to be real. In taking $|\psi_m\rangle$ to be real, equation (3.41) becomes

$$\lambda^0 : \langle \psi_m^0 | \psi_m^0 \rangle = 1 \tag{3.42}$$

$$\lambda^1 : \langle \psi_m^1 | \psi_m^0 \rangle = 0 \tag{3.43}$$

$$\lambda^n, n \geq 2 : \langle \psi_m^n | \psi_m^0 \rangle = -\frac{1}{2} \sum_{i=1}^{n-1} \sum_{l=0}^{N} \langle \psi_m^{n-i} | \psi_l^0 \rangle \langle \psi_l^0 | \psi_m^i \rangle \tag{3.44}$$

The second sum in the above equation is over all of the N members of the variational basis set.

Now, we can apply $\langle \psi_m^0 |$ to both sides of equation (3.38) to get the nth order energy equation.

$$E_m^n = \langle \psi_m^0 | V | \psi_m^{n-1} \rangle - \sum_{i=1}^{n-1} \langle \psi_m^0 | \psi_m^i \rangle E_m^{n-i} \tag{3.45}$$

Finally, we can apply $\langle \psi_{m'}^0 |$ with $m' \neq m$ to equation (3.38) to get the nth order wave function coefficients

$$\langle \psi_{m'}^0 | \psi_m^n \rangle = \frac{\langle \psi_{m'}^0 | V | \psi_m^{n-1} \rangle}{E_m^0 - E_{m'}^0} - \sum_{i=0}^{n-1} \frac{\langle \psi_{m'}^0 | \psi_m^i \rangle E_m^{n-i}}{E_m^0 - E_{m'}^0} \tag{3.46}$$

Once the wave function coefficients $\langle \psi_{m'}^0 | \psi_m^n \rangle$ and the energy coefficients E_m^n are calculated from $n = 0$ up to some integer $n = K$, then the true m'th eigenfunction and eigenvalue of the TISE for the full Hamiltonian H can be approximated by

$$E_m \approx \sum_{i=0}^{K} \lambda^i E_m^i \tag{3.47}$$

$$|\psi_m\rangle \approx \sum_{i=0}^{K} \sum_{j=0}^{N} \lambda^i |\psi_j^0\rangle \langle \psi_j^0 | \psi_m^i \rangle \tag{3.48}$$

where the j sum is over all of the N members of the variational basis set.

To conclude this section it will be shown that the calculated second order energy coefficient for the ground state E_0^2 is always an upper bound to its true value. Using equation (3.45) we have

$$E_0^2 = \langle \psi_0^0 | V | \psi_0^1 \rangle$$
$$= \sum_{m=1}^{N} \langle \psi_0^0 | V | \psi_m^0 \rangle \langle \psi_m^0 | \psi_0^1 \rangle$$

Then we can use equation (3.46) to find

$$\langle \psi_m^0 | \psi_0^1 \rangle = \frac{\langle \psi_m^0 | V | \psi_0^0 \rangle}{E_0^0 - E_m^0} \tag{3.49}$$

so then

$$E_0^2 = \sum_{m=1}^{N} \frac{\langle \psi_0^0 | V | \psi_m^0 \rangle \langle \psi_m^0 | V | \psi_0^0 \rangle}{E_0^0 - E_m^0} \tag{3.50}$$

$\langle \psi_0^0 | V | \psi_m^0 \rangle$ is some complex number denoted by z and $\langle \psi_0^0 | V | \psi_m^0 \rangle \langle \psi_m^0 | V | \psi_0^0 \rangle = zz^*$ which is a positive number for all m. Also, E_0^0 is the ground state energy of the unperturbed Hamiltonian H_0 for which we know that $E_0^0 < E_m^0$ for all m. Therefore, every term in the sum of equation (3.50) is negative. Increasing the basis size N will always lower the value of E_0^2 and so the value of E_0^2 calculated with any finite basis set is always an upper bound to its true value.

3.5 Neville-Richardson Extrapolation

Neville-Richardson extrapolation is a very useful technique for accelerating the convergence of series. Given some series of converging coefficients, r_n^0, we aim to construct a new series, r_n^1 that consists of some combination of the r_n^0 series so that it converges to the same limit as the r_n^0 series but much faster. This technique is usually used to calculate approximate values for derivatives and integrals of functions (Romberg Integration) very accurately. In this work Neville-Richardson extrapolation is used to accelerate the convergence of the $1/Z$ expansion, as was done by Baker *et al.*

Neville-Richardson extrapolation may be used when we can make an assumption of the functional dependence of the series we are trying to accelerate. For example, let

$$r_n^{(0)} = C_0 + \frac{C_1}{n} + \frac{C_2}{n^2} + \dots \tag{3.51}$$

with the 0 in $r_n^{(0)}$ representing the unaltered initial sequence of numbers r_n. Assuming we have guessed the correct dependence for r_n, it is clear that this series converges to C_0 and the dominant dependence on n comes from the $1/n$ term. If we were to somehow drop the $1/n$ dependence in (3.51) then the series would converge to the limit C_0 faster. This can be done simply by finding the right linear combination of the series r_n^0 and $r_{n\prime}^0$ so the $1/n$ term gets canceled out. For example, we can use

$$\begin{aligned} r_{n+1}^{(0)} &= C_0 + \frac{C_1}{n+1} + \frac{C_2}{(n+1)^2} + \dots \\ (n+1)r_{n+1}^{(0)} &= (n+1)C_0 + C_1 + \frac{C_2}{n+1} + \dots \end{aligned} \tag{3.52}$$

along with

$$nr_n^{(0)} = nC_0 + C_1 + \frac{C_2}{n} + \dots \tag{3.53}$$

then by subtracting the two series (3.52),(3.53) we are left with

$$r_n^{(1)} = (n+1)r_{n+1} - nr_n = C_0 - \frac{C_2}{n(n+1)} + \dots$$

where our new series $r_n^{(1)}$ converges to C_0 faster due to the elimination of the $1/n$ term. We can then go a step further by creating the $r_n^{(2)}$ series from the linear combination of $r_n^{(1)}$ and $r_{n+1}^{(1)}$ which cancels out the $\dfrac{1}{n(n+1)}$ dependence. Theoretically this procedure could be repeated indefinitely, resulting in faster convergence each time. However, in practice we lose some significant figures for each higher-order series we find. Each term in a high-order series arises from the accumulation of many subtractions between similar numbers resulting in a net loss of significant figures. If Neville-Richardson extrapolation is carelessly applied too many times without validating the numerical stability of the coefficients in the series, then untrustworthy extrapolations could be mistakenly

assumed to yield accurate results. Thus, the Neville-Richardson extrapolation should be thought of as a way of trading significant figures for enhanced accuracy and should only be used until the desired balance is found.

Chapter 4

Results

This chapter describes the entire process of obtaining an accurate estimate to the radius of convergence of the $1/Z$ expansion in great detail. The meaning of the value of λ^* obtained is also explained.

4.1 The Procedure

As mentioned in the last chapter, the Schrödinger equation for the two-electron atom Hamiltonian cannot be solved analytically and so an approximation method must be used to generate the eigenvalues and eigenvectors. The Z-scaled Hamiltonian can be split into a solvable part H_0 and a perturbation λV according to

$$H = -\frac{1}{2}(\nabla_1^2 + \nabla_2^2) - \frac{1}{r_1} - \frac{1}{r_2} + \frac{Z^{-1}}{r_{12}} \tag{4.1}$$

$$H_0 = -\frac{1}{2}(\nabla_1^2 + \nabla_2^2) - \frac{1}{r_1} - \frac{1}{r_2} \tag{4.2}$$

$$\lambda V = \frac{Z^{-1}}{r_{12}} \tag{4.3}$$

$$\text{where } \lambda = Z^{-1} \text{ and } V = \frac{1}{r_{12}}$$

H_0 consists of two hydrogen atom Hamiltonians added together and V is the potential energy due to the inter-electron Coulomb interaction in Z-scaled atomic units. The TISE for this Hamiltonian is

$$(H_0 + \lambda V)\psi_n = E_n \psi_n \tag{4.4}$$

We assume power series solutions for E_n and ψ_n

$$E_n = \sum_{i=0}^{\infty} \lambda^i E_n^i \tag{4.5}$$

$$\psi_n = \sum_{i=0}^{\infty} \lambda^i \psi_n^i \tag{4.6}$$

which breaks the TISE into an infinite sequence of equations indexed by the "order" i. These equations are

$$\lambda^i : H_0 \psi_n^i + V \psi_n^{i-1} = \sum_{k=0}^{i} E_n^{i-k} \psi_n^k \tag{4.7}$$

which come from section 3.4. We first must solve the zeroth order equation

$$H_0 \psi_n = E_n \psi_n \tag{4.8}$$

which is a separable differential equation with solutions

$$\begin{aligned} \psi_n &= \psi_{n_1 l_1 m_1} \psi_{n_2 l_2 m_2} \\ E_n &= -\frac{1}{n_1^2} - \frac{1}{n_2^2} \end{aligned} \tag{4.9}$$

where the ψ_{nlm} ($n \geq 1$, $l \leq n-1$ and $|m| \leq l$) are the eigenfunctions of the Schrödinger equation for a single hydrogen atom Hamiltonian.

The variational method was used to generate a complete set of pseudostates from the double hydrogenic TISE (4.8). Both the triple and pyramidal variational basis sets described in section 3.2 were used. Table 4.1 shows approximations to the energies for some states of helium after using the variational

method with a double basis set. The calculation of each one of these approximate energies is an arduous process. We would start with a relatively small double basis set of roughly 200 terms and optimize the nonlinear parameters so that the variational energy of interest was minimized (recall that the variational energies are all upper bounds to the true energies). Each optimization involved multiple applications of the inverse iteration method (see Appendix C.3) for different values of the α_i and β_i. Each run of the inverse iteration method takes $O(n^3)$ operations to complete (where n is the number of terms in the basis set). Once the optimal variational energy and nonlinear parameters were found for a given basis set size, Ω_1 and Ω_2 were each incremented by one and the entire process was repeated for the next larger basis set in the sequence. Basis sizes of up to 2000 terms could successfully be used before encountering issues of numerical stability. Finding the optimal nonlinear parameters for a 2000 term basis set took over 8 hours of runtime on a UNIX system with an Intel Core2 quad Q9450 2.66Ghz CPU (all calculations were performed in quadruple precision arithmetic in f77). After the optimized variational energies were obtained for many different basis sizes n these energies were extrapolated to infinite basis size $n \to \infty$. The extrapolated energies are the values displayed in table 4.1.

Table 4.1: Highly accurate energies for helium ^1P states achieved by double basis sets

State	Energy
$1s2p^1P$	-2.123843086498101362(7)
$1s3p^1P$	-2.05514636209194349(1)
$1s4p^1P$	-2.03106965045024067(1)
$1s5p^1P$	-2.019905989900846436(5)
$1s6p^1P$	-2.013833979671740067(8)
$1s7p^1P$	-2.0101693145293889(1)
$1s8p^1P$	-2.00778912713323586(2)
$1s9p^1P$	-2.00615638465285382(3)
$1s10p^1P$	-2.00498798380221815(4)

The numbers in the brackets are the uncertainties in the last recorded significant digits

Neither the triple nor the pyramidal basis sets are orthogonal basis sets. Using an orthogonal basis set reduces the generalized eigenvalue problem to the simpler TISE (see Appendix A) and so these basis sets were orthonormalized. This was done by calculating and diagonalizing the overlap matrix

$$O_{ij} = \langle \phi_i | \phi_j \rangle \tag{4.10}$$

where ϕ_k is the kth member of the chosen basis set. After $\mathbf{O}$ was diagonalized a scale change matrix was applied so that $\mathbf{O} = \mathbf{I}$ in the rescaled basis

$$\mathbf{O} = \begin{pmatrix} \lambda_1 & 0 & \dots & 0 \\ 0 & \lambda_2 & \dots & 0 \\ \vdots & \vdots & \ddots & \vdots \\ 0 & 0 & \dots & \lambda_n \end{pmatrix} \rightarrow \mathbf{S^t O S} = \begin{pmatrix} 1 & 0 & \dots & 0 \\ 0 & 1 & \dots & 0 \\ \vdots & \vdots & \ddots & \vdots \\ 0 & 0 & \dots & 1 \end{pmatrix} \tag{4.11}$$

This new orthonormal basis set is a linear combination of the original basis set elements.

The variational method was used via diagonalizing the double hydrogenic Hamiltonian matrix $\mathbf{H_0}$ expressed in the orthonormalized basis sets. Three

different matrix diagonalization procedures were used and are described in Appendix C. The exact ground state of the zeroth order TISE (equation (4.8))

$$\psi_{100}\psi_{100} = e^{-r_1}e^{-r_2} \tag{4.12}$$

was included in all of the basis sets (it is omitted in the basis set tables). This ensured a very accurate ground state wave function and ground state energy upon application of the variational method.

The next step in the process was to progressively increase the size of the basis sets. For example, for a triple basis set we would usually start with $\Omega_1 = \Omega_2 = 10, \Omega_3 = 2$ and progressively work up to $\Omega_1 = \Omega_2 = 17, \Omega_3 = 9$ in increments of 1. For each of these basis sizes the procedure of orthonormalizing the basis set and then diagonalizing $\mathbf{H_0}$ was done. After the eigenvectors and eigenvalues of $\mathbf{H_0}$ were found for a given basis set, Rayleigh-Schrödinger perturbation theory was used to find E_0^n, of the $1/Z$ expansion. The appropriate equations derived in section 3.4 are

$$E_0^n = \langle\psi_0^0|V|\psi_0^{n-1}\rangle - \sum_{k=1}^{n-1}\langle\psi_0^0|\psi_0^k\rangle E_0^{n-k} \tag{4.13}$$

$$\langle\psi_m^0|\psi_0^n\rangle = \frac{\langle\psi_m^0|V|\psi_0^{n-1}\rangle}{E_0^0 - E_m^0} - \sum_{k=0}^{n-1}\frac{\langle\psi_m^0|\psi_0^k\rangle E_0^{n-k}}{E_0^0 - E_m^0} \tag{4.14}$$

$$\text{where } m \neq 0$$

These equations were used to sequentially calculate the $1/Z$ expansion coefficients for both the ground state energy and the ground state eigenfunction up to 1000th order ($n = 1000$). With the $1/Z$ expansion coefficients calculated, the radius of convergence of the series could be estimated with the ratio test

$$\lambda^* = \lim_{n\to\infty}\frac{1}{r_n} \tag{4.15}$$

where the r_n are the ratios of the $1/Z$ series coefficients

$$r_n = \frac{E_0^{n+1}}{E_0^n} \tag{4.16}$$

The r_n series were very slowly converging and so the Neville-Richardson extrapolation technique (section 3.5) was used to accelerate the rate of convergence. This method was used by Baker *et. al.* and so we could compare our results with theirs. We assumed the r_n had the form

$$r_n = C_0 + \frac{C_{1/2}}{n^{1/2}} + \frac{C_1}{n} + \frac{C_{3/2}}{n^{3/2}} + \frac{C_2}{n^2} + \dots \tag{4.17}$$

because there was convincing evidence for this in reference [1] and also because our own analysis of the r_n's showed agreement with this behaviour. For large n this series converges to $C_0 = Z^*$. Two different first order Neville-Richardson extrapolations were used

$$s_n = (n+1)r_{n+1} - nr_n = C_0 + \frac{C_{1/2}}{2n^{1/2}} - \frac{C_{1/2} + 4C_{3/2}}{8n^{3/2}} - \frac{C_2}{n(n+1)} + O(n^{-5/2}) \tag{4.18}$$

(the $1/n$ dependence is canceled out in the s_n series)

$$t_n = 2[(n+\frac{1}{2})r_{n+1} - nr_n] = C_0 - \frac{C_1}{n+1} - \frac{8C_{3/2} - C_{1/2}}{4n^{3/2}} - \frac{3C_2}{(n+1)^2} + O(n^{-5/2}) \tag{4.19}$$

Both of these series converge to $C_0 = Z^*$ but faster than the original r_n series. A second order Neville-Richardson extrapolation was constructed

$$v_n = (n+2)t_{n+1} - (n+1)t_n = C_0 + \frac{8C_{3/2} - C_{1/2}}{8n^{3/2}} + \frac{3C_2}{(n+1)(n+2)} + O(n^{-5/2}) \tag{4.20}$$

but due to the loss of numerical precision in their calculation, only the v_n which were constructed from our most accurate E_n ($E_n \to r_n \to t_n \to v_n$) could be used to determine λ^*.

A least squares fit was used to extrapolate r_n, s_n, t_n and v_n to $1/n = 0$ ($n \to \infty$). The fits that were applied to each series were

$$r_n = a + \frac{b}{n^{1/2}} + \frac{c}{n}$$
$$s_n = a + \frac{b}{n^{1/2}} + \frac{c}{n}$$
$$t_n = a + \frac{b}{n}$$
$$v_n = a + \frac{b}{n^{3/2}} + \frac{c}{n^2}$$

When these least square fits were plotted with respect to $1/n$ the y-intercept of the best fit line would serve as the estimated value for $a \approx Z^* = \frac{1}{\lambda^*}$ thereby yielding an approximation to the radius of convergence of the $1/Z$ expansion λ^*.

4.2 Calculations

The E_n were calculated up to 1000th order using various different basis sets. Stability checks were used to estimate the precision of the E_n. These stability checks were performed by changing all of the nonlinear parameters in the basis set by a small amount and then recalculating the $1/Z$ expansion coefficients. The two sets of E_n would be compared and the decimal digits that were in agreement were assumed to be correct.

Tables 4.2 – 4.5 display the most important basis sets that were used to calculate the $1/Z$ expansion coefficients. Both triple and pyramidal basis sets were used to solve the Schrödinger equation (4.8) via the variational method. Tables 4.2 and 4.3 display two of the triple basis sets that were used. Tables 4.4 and 4.5 show the two most useful pyramidal basis sets.

The solutions to equation (4.8) are known and the exact ground state is

$$\psi_0 = \frac{1}{\pi} e^{-r_1 - r_2} \tag{4.21}$$

Basis sets that do not include the exact ground state result in inaccurate eigenvectors and eigenvectors and hence inaccurate E_n. The exact ground state was

included in all of the variational basis sets used in this thesis (it is omitted in the relevant tables). The inclusion of the exact ground state in a basis set not only improved the accuracy of the variational eigenvalues and eigenvectors obtained by applying the variational method to equation (4.8), but also provided a way of estimating the numerical precision of the variational eigenvectors. Upon diagonalization of the Hamiltonian matrix $\mathbf{H_0}$ corresponding to the Hamiltonian (4.1), the variational ground state eigenvector ϕ_0 should be exactly

$$\phi_0 = \begin{pmatrix} 1 \\ 0 \\ \vdots \\ 0 \end{pmatrix} \tag{4.22}$$

For small basis sets of only a few hundred terms, ϕ_0 would agree with ψ_0 to roughly 15 decimal digits. As basis sizes increased, the number of arithmetic operations required to diagonalize $\mathbf{H_0}$ would rapidly increase, reducing the number of significant figures in the resulting variational eigenvectors ϕ_n. It was required that ϕ_0 agree with ψ_0 to at least 10 decimal digits in order to achieve appreciably accurate $1/Z$ expansion coefficients. The deviation of the variational energy from the true energy δE is roughly proportional to the square of the deviation of the variational wave function from the true wave function $\delta\psi$. Therefore if the variational wave function is accurate to 10 decimal digits we can be confident that the variational energy is accurate to at least 20 decimal digits.

The first basis set that was used was the H^- triple basis set shown in table 4.2. This basis set used nonlinear parameters that were optimized for the ground state of H^-. The nonlinear parameters were found with a program called dpoldl.f which used the inverse iteration method to find a single eigenvalue and eigenvector pair from a Hamiltonian matrix (see Appendix C.3). After performing a stability check to the largest H^- triple basis set, the resulting E_n were found to be accurate to at least 4 decimal digits up to 200th order. The resulting s_n and t_n series were fitted using $n = 100$ to $n = 200$ which yielded $\lambda^* = 1.10143$ and $\lambda^* = 1.09796$ respectively. The v_n series was numerically

Table 4.2: Triple basis set optimized for H^-

Ω	α_1	β_1	α_2	β_2	α_3	β_3
10	0.94318	0.51190	2.41467	2.52594	5.22424	6.90106
11	0.96783	0.51624	2.32599	2.75018	7.60901	10.04987
12	0.96143	0.51984	2.68549	2.78174	9.11432	7.46344
13	0.98199	0.51904	2.50262	2.90271	10.28485	10.53516
14	0.98279	0.52069	2.56238	3.04138	10.75458	10.78339
15	0.98920	0.52222	2.85748	2.84436	11.00897	11.10162
16	1.00073	0.52576	3.23096	2.78528	13.33142	12.31256
17	1.02875	0.53302	3.03937	3.17322	13.12842	13.87701

Table 4.3: Triple basis set optimized for He

Ω	α_1	β_1	α_2	β_2	α_3	β_3
10	1.23962	1.19568	2.44611	2.13763	5.86517	5.93225
11	1.27502	1.22772	2.61005	2.26721	6.40723	6.43719
12	1.29248	1.23926	2.75348	2.45520	6.89081	6.89404
13	1.31207	1.23779	3.06598	2.57349	9.14484	9.16608
14	1.32660	1.28516	2.88397	3.17126	11.19373	11.80603
15	1.34479	1.28821	2.96136	3.41583	12.26294	12.34119
16	1.36322	1.28998	3.10455	3.79791	14.28326	15.38464
17	1.38293	1.30011	3.30933	4.07678	17.85199	18.23389

unstable and could not be used to estimate λ^*.

The success of the H^- triple basis set in finding accurate E_n necessitated a comparison with the He triple basis set (table 4.3). This basis set used nonlinear parameters optimized for the ground state of helium. It was constructed by Drake *et al.* in reference [30] and so the optimal nonlinear parameters were taken directly from this work. Even though the nonlinear parameters of the H^- and He triple basis sets are almost equivalent, the differences between their E_n are astounding. The He E_n would begin oscillating between positive and

Table 4.4: Pyramidal basis with $\alpha_0 = 1.300$, $\beta_0 = 1.450$ and $M = 2.2$

basis set number:	1	2	3	4	5	6
$\alpha = 147.4, \beta = 164.4$						9
$\alpha = 66.98, \beta = 74.72$					9	10
$\alpha = 30.45, \beta = 33.97$				9	10	11
$\alpha = 13.84, \beta = 15.44$			9	10	11	12
$\alpha = 6.292, \beta = 7.018$		9	10	11	12	13
$\alpha = 2.860, \beta = 3.190$	9	10	11	12	13	14
$\alpha = 1.300, \beta = 1.450$	10	11	12	13	14	15

The values in this table are the Ω's for each of the single Hylleraas basis sets used to construct the pyramidal basis set. The columns of this table show the components of the pyramidal basis set at each stage in its construction. The smallest basis size is represented by the left-most column and the largest basis size is represented by the right-most column of this table

Table 4.5: A special pyramidal basis set with $\alpha_0 = 2.000$, $\beta_0 = 2.200$ and $M = 2.0$ containing a double basis set $(\alpha_1 = 0.500, \beta_1 = 0.500), (\alpha_2 = 0.950, \beta_2 = 0.200)$

basis set number:	1	2	3	4	5	6	7	8
$\alpha = 128.0, \beta = 140.8$								5
$\alpha = 64.00, \beta = 70.40$							5	6
$\alpha = 32.00, \beta = 35.20$						5	6	7
$\alpha = 16.00, \beta = 17.60$					5	6	7	8
$\alpha = 8.000, \beta = 8.800$				5	6	7	8	9
$\alpha = 4.000, \beta = 4.400$			5	6	7	8	9	10
$\alpha = 2.000, \beta = 2.200$		5	6	7	8	9	10	11
$\alpha = 0.950, \beta = 0.200$	5	6	7	8	9	10	11	12
$\alpha = 0.500, \beta = 0.500$	6	7	8	9	10	11	12	13

negative values for $n \geq 100$ while the H^- E_n were all negative. Performing a stability check to these E_n's determined they were not accurate to even one decimal for $n > 50$ which explained these oscillations. Meaningful s_n and t_n series could not be constructed and so no estimation of λ^* could be found from the He basis sets. However, E_2 for the He triple basis set is extremely accurate compared to the E_2 from the H^- triple basis set.

The second order coefficient for the ground state energy E_2 calculated using a finite variational basis set is an upper bound to its true value (see 3.4. The notation E_2 is used and not E_0^2 because only the ground state energy is of interest and so the 0 label is unnecessary and hence is removed). One minor accomplishment of this work was to find a very accurate value of E_2. Using a large He triple basis set (the last row in table 4.3) E_2 was calculated to be

Table 4.6: E_2 for the He triple basis set in table 4.3

basis size	E_2	Difference	Ratio
324	-0.157 666 429 355 860 486		
411	-0.157 666 429 446 395 895	-0.000 000 000 090 535 409	
512	-0.157 666 429 465 780 973	-0.000 000 000 019 385 078	0.214
630	-0.157 666 429 468 841 650	-0.000 000 000 003 060 677	0.158
764	-0.157 666 429 469 129 725	-0.000 000 000 000 288 075	0.094
918	-0.157 666 429 469 147 824	-0.000 000 000 000 018 099	0.063
1089	-0.157 666 429 469 150 371	-0.000 000 000 000 002 547	0.141
1283	-0.157 666 429 469 150 850	-0.000 000 000 000 000 479	0.188

The difference column is simply $d(i) = E(i) - E(i-1)$ and the ratio column is the ratio of the differences $r(i) = \dfrac{d(i)}{d(i-1)}$ where $E(i)$ represents the ith E_2 value in the table.

Therefore the He triple basis set yields the result

$$E_2 = -0.157\,666\,429\,469\,150\,8(1) \tag{4.23}$$

where the error in the 15th decimal digit is estimated from the convergence

behaviour of E_2 in table 4.6.

A pyramidal basis set was used in the attempt to find a more accurate E_2 (table 4.4). The first set of nonlinear parameters used in the pyramidal basis set were found by using Newton's method to minimize the resulting E_2 obtained from a series of different runs using α_1, β_1 in the range $(0.15, 2.00)$. The values $\alpha_1 = 1.3000$ and $\beta_1 = 1.45000$ were optimal. Some trial and error was involved in finding the optimal M in the pyramidal basis set to minimize E_0^2. $M = 1.1$ and $M = 4$ failed to provide E_2 that were smaller than the He triple basis E_2 shown above. These basis sets failed for two different reasons. For $M = 1.1$, the pyramidal basis sets quickly ran into numerical dependence issues when using large basis sizes of 1000 terms or more. This would cause negative eigenvalues in the overlap matrix (these should all be positive) during the diagonalization procedure and would lead to very inaccurate E_n. For the $M = 4$ case it seemed that the nonlinear parameters spread out too quickly and missed some important ranges of values that needed to be included in the basis sets. Thus, M was varied from the range $(2.0, 3.0)$ in steps of 0.1 and it was found that $M = 2.2$ provided the minimal E_2. The E_2 for this basis set can be seen in table 4.7

Table 4.7: E_2 for the optimized pyramidal basis set in table 4.4

basis size	E_2	Difference	Ratio
125	-0.157 666 384 056 843 799		
284	-0.157 666 429 437 046 212	-0.000 000 045 380 202 413	
482	-0.157 666 429 468 960 486	-0.000 000 000 031 914 274	0.000 703
726	-0.157 666 429 469 140 498	-0.000 000 000 000 180 012	0.005 64
1020	-0.157 666 429 469 149 921	-0.000 000 000 000 009 423	0.0523
1372	-0.157 666 429 469 150 846	-0.000 000 000 000 000 925	0.0982
1786	-0.157 666 429 469 150 932	-0.000 000 000 000 000 086	0.093

Therefore our best estimate is

$$E_2 = -0.157\,666\,429\,469\,150\,932 \tag{4.24}$$

which is an improvement to the He basis set upper bound and is likely accurate up to 16 decimal digits based off of the convergence behaviour displayed in table 4.7.

The main result so far is that the nonlinear parameters used in the He triple basis set resulted in more accurate low-order E_n (only for $n = 1$ to 10) while those of the H^- triple basis set yielded more accurate high-order coefficients. The fact that the H^- and He nonlinear parameters are almost equivalent yet yield very different E_n emphasizes the importance of the nonlinear parameters in accurately determining these coefficients. This suggested the use of the pyramidal basis sets with their many adjustable nonlinear parameters.

As was explained in reference [1], the higher order terms in the $1/Z$ expansion correspond to the atomic configuration with one electron localized near the nucleus and the other electron very far from the nucleus. This meant the pyramidal basis sets would need to incorporate a large number of terms with nonlinear parameters $\alpha \sim 1$ and $\beta \sim 0$. In reference [23] a Hylleraas double basis set was used to find the variational eigenvectors and eigenvalues of the full Z-scaled two-electron atom Hamiltonian

$$H = -\frac{1}{2}(\nabla_1^2 + \nabla_2^2) - \frac{1}{r_1} - \frac{1}{r_2} + \frac{Z^{-1}}{r_{12}} \tag{4.25}$$

at the critical charge $Z = Z_c = 0.911\,028\,224\,077$. The nonlinear parameters in the double basis set were optimized to minimize the variational ground state energy. The optimal values are

$$\alpha_1 = 0.95 \qquad \beta_1 = 0.15$$
$$\alpha_2 = 1.20 \qquad \beta_2 = 1.10$$

These values are important because they quantify the configuration of the ground state of the two-electron atom at the critical nuclear charge. Many different Hylleraas double basis sets were constructed using nonlinear parameters in the range of $\alpha_1, \beta_1 \in (0.1, 1.5)$ and $\alpha_2, \beta_2 \in (0.5, 2.0)$ and their resulting E_n were compared with stability checks. After much trial and error, it was

found that the double basis set yielding the most numerically stable coefficients had nonlinear parameters

$$\alpha_1 = 0.95 \qquad \beta_1 = 0.20$$
$$\alpha_2 = 0.50 \qquad \beta_2 = 0.50$$

The rest of the pyramidal basis set was also found by trial and error. When the nonlinear parameters were too spread out ($M \geq 3$) the E_n were inaccurate and when the parameters were too close ($M \leq 1.5$) the larger basis sets would have numerical instability issues (the E_n couldn't be calculated in this case). The most accurately determined coefficients, deemed PYC5TGC68 (PY - pyramidal basis set, C5 - 25th trial, T - tridiagonalization method, G - exact ground state included, C68 - basis size of 1268 terms) were calculated using the pyramidal basis set displayed in table 4.5. The corresponding stability check coefficients were calculated and named PYS5TGC68. PYC5TGC68, PYS5TGC68 and the E_n from reference [1] are all compared in table 4.8. The pyramidal basis set is very different from the basis set used in reference [1], yet the coefficients still agree with each other consistently to 4-5 decimal digits even at 400th order. This is very strong evidence that both the coefficients of Baker *et al.* and PYC5TGC68 are accurate to at least 4 decimal digits up to 400th order. Comparing PYC5TGC68 with PYS5TGC68 further suggests that the PYC5TGC68 coefficients are accurate to 7 decimal digits at 400th order then progressively become less accurate as the order is increased until they are only accurate to a single decimal digits place at 1000th order.

Table 4.8: Comparison of different E_n. D+01 represents 10^1.

Order	PYC5TGC68	PYS5TGC68	Baker *et al.*
0	-0.100000000000000000D+01	-0.100000000000000000D+01	-0.1000000000D+01
1	0.625000000000000000D+00	0.625000000000000000D+00	0.6250000000D+00
2	-0.157666429469061186D+00	-0.157666429469064706D+00	-0.1576664295D+00
3	0.869093152779249933D-02	0.869093152779037790D-02	0.8699031528D-02
4	-0.888707284437038512D-03	-0.888707284433329529D-03	-0.8887072842D-03

5	-0.10363718475625541D-02	-0.10363718475362083 6D-02	-0.1036371848D-02
6	-0.61294052156893232D-03	-0.61294052156485635 9D-03	-0.6129405205D-03
7	-0.37217557390372628 6D-03	-0.37217557396588952 7D-03	-0.3721755765D-03
8	-0.24287797603667808 7D-03	-0.24287797608923006 3D-03	-0.2428779732D-03
9	-0.16566105256763777 4D-03	-0.16566105250002934 3D-03	-0.1656610547D-03
10	-0.11617920405395959 6D-03	-0.11617920392950023 7D-03	-0.1161792026D-03
11	-0.83301350473994357 7D-04	-0.83301350475136145 3D-04	-0.8330135003D-04
12	-0.60880276020447351 0D-04	-0.60880276184209402 4D-04	-0.6088027632D-04
13	-0.45230718668734732 6D-04	-0.45230718796866222 6D-04	-0.4523072242D-04
14	-0.34079663934582257 6D-04	-0.34079663837049489 1D-04	-0.3407966122D-04
15	-0.25991069480644613 2D-04	-0.25991069234577348 8D-04	-0.2599106570D-04
16	-0.20033067980747972 9D-04	-0.20033067860872197 9D-04	-0.2003307002D-04
17	-0.15585371985120826 8D-04	-0.15585372149835648 6D-04	-0.1558537543D-04
18	-0.12225842823574284 1D-04	-0.12225843134596420 8D-04	-0.1222584280D-04
19	-0.96616386310211029 7D-05	-0.96616388002389640 0D-05	-0.9661636835D-05
20	-0.76861639175584310 0D-05	-0.76861637938572523 9D-05	-0.7686162634D-05
21	-0.61514687643747040 0D-05	-0.61514684561153589 7D-05	-0.6151468041D-05
22	-0.49501696594639648 7D-05	-0.49501694075515855 9D-05	-0.4950169803D-05
23	-0.40033790749354202 9D-05	-0.40033790420728413 1D-05	-0.4003380609D-05
24	-0.32525066671537008 0D-05	-0.32525068379407056 6D-05	-0.3252508668D-05
25	-0.26536027884384231 2D-05	-0.26536030249929553 8D-05	-0.2653603522D-05
26	-0.21734003451571354 8D-05	-0.21734005077640654 6D-05	-0.2173399140D-05
27	-0.17865089703105338 8D-05	-0.17865089986509220 1D-05	-0.1786506716D-05
28	-0.14734022236965689 4D-05	-0.14734021423807047 8D-05	-0.1473400370D-05
29	-0.12189578035429164 7D-05	-0.12189576793175007 6D-05	-0.1218957262D-05
30	-0.10113881558416123 7D-05	-0.10113880506565704 6D-05	-0.1011388955D-05
31	-0.84144981636207708 0D-06	-0.84144976235002822 3D-06	-0.8414513883D-06
32	-0.70185382581436521 7D-06	-0.70185382423140092 4D-06	-0.7018554629D-06
33	-0.58682257644774619 1D-06	-0.58682260983492653 8D-06	-0.5868237564D-06
34	-0.49175423940032964 4D-06	-0.49175428554813330 5D-06	-0.4917547384D-06

35	-0.41296885458207460D-06	-0.41296926801937862D-06	-0.4129667397D-06
36	-0.34750210257937454 2D-06	-0.34750212976428433 2D-06	-0.3475015037D-06
37	-0.29297335877010255 9D-06	-0.29297336997046185 8D-06	-0.2929725474D-06
38	-0.24744824839615309 1D-06	-0.24744824666006045 5D-06	-0.2474474379D-06
39	-0.20935656230020876 8D-06	-0.20935655268880973 1D-06	-0.2093558999D-06
40	-0.17741815809490643 9D-06	-0.17741814555291850 7D-06	-0.1774177169D-06
41	-0.15058609816528832 5D-06	-0.15058608637065330 0D-06	-0.1505858883D-06
42	-0.12800162331701947 4D-06	-0.12800161435559310 0D-06	-0.1280016120D-06
43	-0.10895834779085526 7D-06	-0.10895834235373680 1D-06	-0.1089584800D-06
44	-0.92873673126095289 4D-07	-0.92873670938939806 7D-07	-0.9287388845D-07
45	-0.79265878826494133 7D-07	-0.79265879103152294 2D-07	-0.7926612330D-07
46	-0.67735769631978537 7D-07	-0.67735769819897374 19D-07	-0.6773592858D-07
47	-0.57951438655142434 7D-07	-0.57951441148442602 5D-07	-0.5795163168D-07
48	-0.49636959433423464 5D-07	-0.49636961975810531 4D-07	-0.4963709996D-07
49	-0.42561874680116823 4D-07	-0.42561876869274730 3D-07	-0.4256196029D-07
50	-0.36533596995800606 0D-07	-0.36533598637685304 8D-07	-0.3653363293D-07
51	-0.31390829040106175 3D-07	-0.31390830097029290 5D-07	-0.3139082506D-07
52	-0.26998234421668653 3D-07	-0.26998234955773986 4D-07	-0.2699820214D-07
53	-0.23242061828062462 0D-07	-0.23242061952183025 2D-07	-0.2324201270D-07
54	-0.20026543108300202 0D-07	-0.20026542949322436 2D-07	-0.2002648718D-07
55	-0.17270921490326458 4D-07	-0.17270921165630452 9D-07	-0.1727086666D-07
56	-0.14906994206911487 4D-07	-0.14906993811956633 9D-07	-0.1490694605D-07
57	-0.12877076128225312 4D-07	-0.12877075732375107 2D-07	-0.1287703797D-07
58	-0.11132308801016177 3D-07	-0.11132308448680544 2D-07	-0.1113228206D-07
59	-0.96312535345867273 7D-08	-0.96312532492417577 3D-08	-0.9631238139D-08
60	-0.83387186000673031 6D-08	-0.83387183893666172 0D-08	-0.8338713427D-08
61	-0.72247798048603427 8D-08	-0.72247796656852984 5D-08	-0.7224783083D-08
62	-0.62639611250687593 9D-08	-0.62639610478823287 1D-08	-0.6263970780D-08
63	-0.54345480839168115 9D-08	-0.54345480561602478 3D-08	-0.5434562009D-08
64	-0.47180114364278180 6D-08	-0.47180114449400658 9D-08	-0.4718027681D-08

65	-0.409852268363810097D-08	-0.40985271621201413D-08	-0.4098539575D-08
66	-0.35625461709039 4743D-08	-0.35625462171514 0752D-08	-0.3562562376D-08
67	-0.309849516567166405D-08	-0.309849521737911556D-08	-0.3098509705D-08
68	-0.26964414731968 6601D-08	-0.26964415243350 4557D-08	-0.2696453705D-08
69	-0.234786992438430075D-08	-0.234786997090607519D-08	-0.2347879506D-08
70	-0.204547053062605147D-08	-0.204547057015378724D-08	-0.2045477367D-08
71	-0.178296230455110627D-08	-0.178296233602515444D-08	-0.1782966493D-08
72	-0.155494374000641995D-08	-0.155494376334150539D-08	-0.1554945518D-08
73	-0.135676576741796094D-08	-0.135676578319510258D-08	-0.1356765460D-08
74	-0.118442368277793996D-08	-0.118442369198560513D-08	-0.1184421664D-08
75	-0.103446511493911648D-08	-0.103446511876778550D-08	-0.1034461773D-08
76	-0.903911567084674087D-09	-0.903911566772909495D-09	-0.9039072781D-09
77	-0.790191460845980139D-09	-0.790191457572568186D-09	-0.7901865701D-09
78	-0.691082939189583036D-09	-0.691082934004594687D-09	-0.6910777500D-09
79	-0.604664958058827129D-09	-0.604664951845942807D-09	-0.6046597253D-09
80	-0.529275426006756198D-09	-0.529275419469469962D-09	-0.5292703540D-09
81	-0.463475343241838931D-09	-0.463475336906883963D-09	-0.4634705874D-09
82	-0.406018052846502340D-09	-0.406018047078796500D-09	-0.4060137233D-09
83	-0.355822852556487192D-09	-0.355822847580933030D-09	-0.3558190191D-09
84	-0.311952329654871943D-09	-0.311952325581360713D-09	-0.3119490281D-09
85	-0.273592877758075833D-09	-0.273592874606978336D-09	-0.2735901158D-09
86	-0.240037935473324460D-09	-0.240037933199568534D-09	-0.2400356987D-09
87	-0.210673555515960931D-09	-0.210673554030480709D-09	-0.2106718132D-09
88	-0.184965970911903613D-09	-0.184965970099796992D-09	-0.1849646810D-09
89	-0.162450874060698851D-09	-0.162450873795853660D-09	-0.1624499872D-09
90	-0.142724166105046664D-09	-0.142724166261305102D-09	-0.1427236294D-09
91	-0.125433969419854956D-09	-0.125433969878995606D-09	-0.1254337293D-09
92	-0.110273726082821028D-09	-0.110273726739765063D-09	-0.1102737305D-09
93	-0.969762307450737191D-10	-0.969762315107837627D-10	-0.9697643063D-10
94	-0.853084680777960385D-10	-0.853084688803484585D-10	-0.8530881854D-10

95	-0.750671435116977509D-10	-0.75067144295986172 7D-10	-0.7506760448D-10
96	-0.660748118011126965D-10	-0.66074812527594487 2D-10	-0.6607534835D-10
97	-0.581765214465512599D-10	-0.58176522089389582 6D-10	-0.5817710380D-10
98	-0.512369045472992300D-10	-0.51236905092188872 1D-10	-0.5123750794D-10
99	-0.451376515234818643D-10	-0.45137651965383171 9D-10	-0.4513825588D-10
100	-0.397753185937754456D-10	-0.39775318934721348 7D-10	-0.3977590813D-10
101	-0.350594231312823748D-10	-0.35059423378371163 0D-10	-0.3505998589D-10
102	-0.309107882244509907D-10	-0.30910788388093462 0D-10	-0.3091131557D-10
103	-0.272601030936749282D-10	-0.27260103186129141 7D-10	-0.2726058924D-10
104	-0.240466705858466850D-10	-0.24046670620046468 4D-10	-0.2404711213D-10
105	-0.212173168978633322D-10	-0.21217316886527177 9D-10	-0.2121771238D-10
106	-0.187254420587727667D-10	-0.18725442013766761 0D-10	-0.1872579156D-10
107	-0.165301926079873521D-10	-0.16530192539908201 4D-10	-0.1653049741D-10
108	-0.145957404111681750D-10	-0.14595740329109078 9D-10	-0.1459600269D-10
109	-0.128906537134755920D-10	-0.12890653624937606 1D-10	-0.1289087625D-10
110	-0.113873483909567250D-10	-0.11387348301870412 4D-10	-0.1138753438D-10
111	-0.100616089668191522D-10	-0.10061608881644938 6D-10	-0.1006176182D-10
112	-0.889217034606795414D-11	-0.88921702679480285 6D-11	-0.8892293565D-11
113	-0.786035242013594706D-11	-0.78603523510752834 1D-11	-0.7860449467D-11
114	-0.694974072898588531D-11	-0.69497406700446249 8D-11	-0.6949814948D-11
115	-0.614590726422574101D-11	-0.61459072157095213 5D-11	-0.6145961819D-11
116	-0.543616627236756619D-11	-0.54361662340062399 1D-11	-0.5436204106D-11
117	-0.480936058905505987D-11	-0.48093605601635457 7D-11	-0.4809384397D-11
118	-0.425567461712506826D-11	-0.42556745967427783 3D-11	-0.4255686832D-11
119	-0.376647056599447881D-11	-0.37664705530018985 7D-11	-0.3766473360D-11
120	-0.333414500760534003D-11	-0.33341450008179437 9D-11	-0.3334140293D-11
121	-0.295200318408034152D-11	-0.29520031823211645 6D-11	-0.2951992627D-11
122	-0.261414883214388951D-11	-0.26141488342968263 3D-11	-0.2614133867D-11
123	-0.231538757597849070D-11	-0.23153875810248146 2D-11	-0.2315369423D-11
124	-0.205114218931389675D-11	-0.20511421963546704 9D-11	-0.2051121873D-11

125	-0.181737824419410115D-11	-0.18173782524611338D-11	-0.1817356614D-11
126	-0.16105385235781373D-11	-0.16105386121566817D-11	-0.1610516602D-11
127	-0.14274873692363658D-11	-0.14274873781776932D-11	-0.1427465056D-11
128	-0.12654570734477894D-11	-0.12654570820839671D-11	-0.1265435134D-11
129	-0.11220069591397063D-11	-0.11220069671884627D-11	-0.1121985729D-11
130	-0.99498288702347696D-12	-0.99498289429486601D-12	-0.9949626143D-12
131	-0.88248343454049158D-12	-0.88248344092230980D-12	-0.8824642950D-12
132	-0.78282986812165862D-12	-0.78282987356511037D-12	-0.7828119767D-12
133	-0.69453973251448950D-12	-0.69453973702069345D-12	-0.6945231546D-12
134	-0.61630361502177421D-12	-0.61630361862950108D-12	-0.6162883760D-12
135	-0.54696469740420156D-12	-0.54696470017907222D-12	-0.5469507912D-12
136	-0.48550075617307180D-12	-0.48550075819831767D-12	-0.4854881522D-12
137	-0.43100831393013990D-12	-0.43100831529892917D-12	-0.4309969633D-12
138	-0.38268686810744137D-12	-0.38268686818836750D-12	-0.3826785214D-12
139	-0.33983565926398635D-12	-0.33983565960961486D-12	-0.3398266193D-12
140	-0.30182470608053666D-12	-0.30182470605382955D-12	-0.3018167088D-12
141	-0.26810338490473478D-12	-0.26810338458990023D-12	-0.2680963505D-12
142	-0.23818294551617831D-12	-0.23818294498874534D-12	-0.2381767935D-12
143	-0.21163089976810699D-12	-0.21163089909407587D-12	-0.2116255509D-12
144	-0.18806447319168756D-12	-0.18806447242726823D-12	-0.1880598504D-12
145	-0.16714482785058892D-12	-0.16714482704238995D-12	-0.1671408577D-12
146	-0.14857196444977105D-12	-0.14857196363531816D-12	-0.1485685773D-12
147	-0.13208022282610282D-12	-0.13208022203458328D-12	-0.1320773537D-12
148	-0.11743430970739569D-12	-0.11743430896054257D-12	-0.1174318984D-12
149	-0.10442579119074159D-12	-0.10442579050378781D-12	-0.1044237821D-12
150	-0.92869990490918796D-13	-0.92869994291829287D-13	-0.9286833743D-13
151	-0.82603273457454802D-13	-0.82603272914816897D-13	-0.8260192161D-13
152	-0.73480586446262545D-13	-0.73480585979750931D-13	-0.7347949878D-13
153	-0.65373636493007398D-13	-0.65373632574353261D-13	-0.6537250299D-13
154	-0.58167616184907365D-13	-0.58167615864038358D-13	-0.5816694939D-13

155	-0.517622666104688029D-13	-0.51762263554049946D-13	-0.5176176429D-13
156	-0.460676722690567722D-13	-0.46067672073599 6473D-13	-0.4606730848D-13
157	-0.410043192722821872D-13	-0.41004319129669 1137D-13	-0.4100407125D-13
158	-0.365016671819417192D-13	-0.36501667085204 1234D-13	-0.3650151503D-13
159	-0.324971268102919182D-13	-0.32497126752536 0866D-13	-0.3249705326D-13
160	-0.289351556337917047D-13	-0.28935155608410 8475D-13	-0.2893514575D-13
161	-0.257664571421624380D-13	-0.25766457142989 0552D-13	-0.2576649809D-13
162	-0.229472720536636222D-13	-0.22947272075071 1729D-13	-0.2294735286D-13
163	-0.204387507449192743D-13	-0.20438750781881 7737D-13	-0.2043886209D-13
164	-0.182063974925726398D-13	-0.18206397540690 2081D-13	-0.1820653153D-13
165	-0.162195782247847681D-13	-0.16219578280282 4032D-13	-0.1621972836D-13
166	-0.144510844509379339D-13	-0.14451084510643 9494D-13	-0.1445124522D-13
167	-0.128767468935003332D-13	-0.12876746954810 0463D-13	-0.1287691379D-13
168	-0.114750931005943352D-13	-0.11475093161423 7407D-13	-0.1147526245D-13
169	-0.102270439834599175D-13	-0.10227044042193 2783D-13	-0.1022721285D-13
170	-0.91156448103287 3258D-14	-0.91156448657632 7267D-14	-0.9115810857D-14
171	-0.812582670655095309D-14	-0.81258267578411 6334D-14	-0.8125988120D-14
172	-0.724419516834964038D-14	-0.72441952149531 1399D-14	-0.7244350579D-14
173	-0.645884250153117458D-14	-0.64588425431573 7353D-14	-0.6458990909D-14
174	-0.575918145320335288D-14	-0.57591814897662 7088D-14	-0.5759322166D-14
175	-0.513579761963165618D-14	-0.51357976512069 8156D-14	-0.5135930200D-14
176	-0.458031849171645413D-14	-0.45803185185035 4261D-14	-0.4580442711D-14
177	-0.408529724552931277D-14	-0.40852972678180 4817D-14	-0.4085413044D-14
178	-0.364410960271819883D-14	-0.36441096208606 4173D-14	-0.3644217054D-14
179	-0.325086227773815969D-14	-0.32508622921247 5350D-14	-0.3250961563D-14
180	-0.290031169874551878D-14	-0.29003117097855 3101D-14	-0.2900403077D-14
181	-0.258779183921797080D-14	-0.25877918473237 8907D-14	-0.2587875633D-14
182	-0.230915013022931688D-14	-0.23091501358041 8738D-14	-0.2309226703D-14
183	-0.206069054084306487D-14	-0.20606905442718 5043D-14	-0.2060760285D-14
184	-0.183912301808142667D-14	-0.18391230197239 6706D-14	-0.1839186344D-14

185	-0.16415185695225397D-14	-0.16415185701389289 1D-14	-0.1641575895D-14
186	-0.14652693564673995 2D-14	-0.14652693554965209 5D-14	-0.1465321098D-14
187	-0.13080532256895699 4D-14	-0.13080532238262618 6D-14	-0.1308099795D-14
188	-0.11678021956845605 9D-14	-0.11678021931608195 3D-14	-0.1167843994D-14
189	-0.10426744397884662 3D-14	-0.10426744368041317 2D-14	-0.1042711852D-14
190	-0.93102938266974889 0D-15	-0.93102937939414893 0D-15	-0.9310627789D-15
191	-0.83140555901993699 8D-15	-0.83140555559400833 4D-15	-0.8314352894D-15
192	-0.74250092600322642 5D-15	-0.74250092254194182 4D-15	-0.7425273210D-15
193	-0.66315535541659078 0D-15	-0.66315535201155533 8D-15	-0.6631787249D-15
194	-0.59233506237270340 0D-15	-0.59233505909480897 0D-15	-0.5923556954D-15
195	-0.52911875467278677 7D-15	-0.52911875157483746 8D-15	-0.5291369198D-15
196	-0.47268531128745488 7D-15	-0.47268530840669751 4D-15	-0.4727012569D-15
197	-0.42230281986615877 1D-15	-0.42230281722667000 2D-15	-0.4223167746D-15
198	-0.37731882226433437 7D-15	-0.37731881987923149 8D-15	-0.3773309961D-15
199	-0.33715163398982733 9D-15	-0.33715163186328209 8D-15	-0.3371622189D-15
200	-0.30128261847260631 3D-15	-0.30128261660165148 7D-15	-0.3012917896D-15
201	-0.26924931037181696 6D-15	-0.26924930874794346 9D-15	-0.2692572269D-15
202	-0.24063929394447980 5D-15	-0.24063929255502840 0D-15	-0.2406461000D-15
203	-0.21508475298107713 9D-15	-0.21508475181043356 6D-15	-0.2150905789D-15
204	-0.19225761811582898 7D-15	-0.19225761714643467 0D-15	-0.1922625813D-15
205	-0.17186524557725308 7D-15	-0.17186524479044583 4D-15	-0.1718694516D-15
206	-0.15364656877597674 0D-15	-0.15364656815267718 1D-15	-0.1536501123D-15
207	-0.13736867063652938 8D-15	-0.13736867015778947 2D-15	-0.1373716362D-15
208	-0.12282373036084164 9D-15	-0.12282373000827150 9D-15	-0.1228261934D-15
209	-0.10982630344567036 8D-15	-0.10982630320175943 1D-15	-0.1098283311D-15
210	-0.98210898337054342 2D-16	-0.98210898185401767 9D-16	-0.9821255006D-16
211	-0.87829817156785136 2D-16	-0.87829817082253656 0D-16	-0.8783114560D-16
212	-0.78551231536016335 8D-16	-0.78551231524822420 9D-16	-0.7855228316D-16
213	-0.70257467790299656 2D-16	-0.70257467830051684 9D-16	-0.7025828348D-16
214	-0.62843478513540682 7D-16	-0.62843478593235520 5D-16	-0.6284409414D-16

215	-0.562154801955283179D-16	-0.56215480305515464O-16	-0.5621592713D-16
216	-0.502897387142140926D-16	-0.50289738846135336O-16	-0.5029004434D-16
217	-0.449914865512054853D-16	-0.44991486697916873O-16	-0.4499167467D-16
218	-0.402539573548532144D-16	-0.40253957510335061O-16	-0.4025404859D-16
219	-0.360175250545781079D-16	-0.36017525213837818O-16	-0.3601753722D-16
220	-0.322289361346375363D-16	-0.32228936293609132O-16	-0.3222888454D-16
221	-0.288406249248463869D-16	-0.28840625080289854O-16	-0.2884052269D-16
222	-0.258101028771276989D-16	-0.25810103026530579O-16	-0.2580996118D-16
223	-0.230994137855183846D-16	-0.23099413927001469O-16	-0.2309924213D-16
224	-0.206746477870208374D-16	-0.20674647919249289O-16	-0.2067445417D-16
225	-0.185055077635708865D-16	-0.18505507885671710O-16	-0.1850529890D-16
226	-0.165649224621322544D-16	-0.16564922573618676O-16	-0.1656470394D-16
227	-0.148287012700723261D-16	-0.14828701370775356O-16	-0.1482847770D-16
228	-0.132752261350030041D-16	-0.13275226225010220O-16	-0.1327500129D-16
229	-0.118851766097173868D-16	-0.11885176689318805O-16	-0.1188495354D-16
230	-0.106412844404122901D-16	-0.10641284510053052O-16	-0.1064106557D-16
231	-0.952811450600743484D-17	-0.95281145662469243O-17	-0.9527901728D-17
232	-0.853186926334208918D-17	-0.85318693148190451O-17	-0.8531664030D-17
233	-0.764021416204933830D-17	-0.76402142054524752O-17	-0.7640017543D-17
234	-0.684212176815551375D-17	-0.68421218041991382O-17	-0.6841934515D-17
235	-0.612773258064290682D-17	-0.61277326100470178O-17	-0.6127555180D-17
236	-0.548823074365138166D-17	-0.54882307671257496O-17	-0.5488063463D-17
237	-0.491573305161693202D-17	-0.49157330698486685O-17	-0.4915575981D-17
238	-0.440318981806574794D-17	-0.44031898317099053O-17	-0.4403042901D-17
239	-0.394429633332544562D-17	-0.39442963429982147O-17	-0.3944159397D-17
240	-0.353341377414866653D-17	-0.35334137804227763O-17	-0.3533286556D-17
241	-0.316549855100812853D-17	-0.31654985544100865O-17	-0.3165380719D-17
242	-0.283603918825355135D-17	-0.28360391892623995O-17	-0.2835930358D-17
243	-0.254099992987659586D-17	-0.25409999289238931O-17	-0.2540899681D-17
244	-0.227677035060671847D-17	-0.22767703480774953O-17	-0.2276678237D-17

245	-0.204012032961281831D-17	-0.20401203258472815 1D-17	-0.2040035893D-17
246	-0.18281959813240182 71D-17	-0.18281959808535979 08D-17	-0.1828082589D-17
247	-0.16383028548842336 3D-17	-0.16383028494991101 3D-17	-0.1638232381D-17
248	-0.14682345475106389 6D-17	-0.14682345469261112 14D-17	-0.1468171296D-17
249	-0.13158686934158219 91D-17	-0.13158686928039641 12D-17	-0.1315828605D-17
250	-0.11794040528438783 8D-17	-0.11794040466080518 1D-17	-0.1179351144D-17
251	-0.10571282566927313 2D-17	-0.10571282504680105 9D-17	-0.1057080356D-17
252	-0.94757550532466633 51D-18	-0.94757504713671807 2D-18	-0.9475317669D-18
253	-0.84941568334604462 0D-18	-0.84941567743275255 9D-18	-0.8493766383D-18
254	-0.76146071503156431 8D-18	-0.76146070937774648 6D-18	-0.7614255588D-18
255	-0.68264537342832992 0D-18	-0.68264536808030603 3D-18	-0.6826137747D-18
256	-0.61201642206669186 0D-18	-0.61201641705664202 3D-18	-0.6119880706D-18
257	-0.54872043080889722 2D-18	-0.54872042615702258 0D-18	-0.5486950373D-18
258	-0.49199328314833731 2D-18	-0.49199327886481803 0D-18	-0.4919705785D-18
259	-0.44115079135739875 7D-18	-0.44115078744415214 2D-18	-0.4411305261D-18
260	-0.39558030198450211 7D-18	-0.39558029843674714 7D-18	-0.3955622457D-18
261	-0.35473318672245339 5D-18	-0.35473318353009050 5D-18	-0.3547171270D-18
262	-0.31811812485068487 5D-18	-0.31811812199950173 6D-18	-0.3181038664D-18
263	-0.28529509343771833 2D-18	-0.28529509091043359 0D-18	-0.2852824572D-18
264	-0.25586999040600755 5D-18	-0.25586998818316525 7D-18	-0.2558588125D-18
265	-0.22948908235240387 40D-18	-0.22948908215847664 83D-18	-0.2294799543D-18
266	-0.20583840550260164 3D-18	-0.20583840382524550 5D-18	-0.2058297087D-18
267	-0.18463250172484150 5D-18	-0.18463250028749052 2D-18	-0.1846248533D-18
268	-0.16561838281454877 1D-18	-0.16561838159546127 2D-18	-0.1656116705D-18
269	-0.14856873931683600 7D-18	-0.14856873829477948 9D-18	-0.1485628611D-18
270	-0.13327992029474670 4D-18	-0.13327991944926223 5D-18	-0.1332747842D-18
271	-0.11956946169230841 1D-18	-0.11956946100390971 2D-18	-0.1195649847D-18
272	-0.10727387393072142 6D-18	-0.10727387338103801 5D-18	-0.1072699811D-18
273	-0.96246661435846619 3D-19	-0.96246661007719507 5D-19	-0.9624328557D-19
274	-0.86356549683048927 9D-19	-0.86356549360586566 4D-19	-0.8635363038D-19

275	-0.774858979264746471D-19	-0.77485897676950759938D-19	-0.7748338107D-19
276	-0.695292780867566878D-19	-0.69529279331074919D-19	-0.6952711529D-19
277	-0.623922023332020808D-19	-0.62392022452497512D-19	-0.6239035038D-19
278	-0.559899837398328512D-19	-0.55989983706744587D-19	-0.5598840411D-19
279	-0.502467160425388421D-19	-0.50246716054647081 7D-19	-0.5024537447D-19
280	-0.450943599978758845D-19	-0.45094360046614512 0D-19	-0.4509322603D-19
281	-0.404719251612932998D-19	-0.40471925239127581 5D-19	-0.4047097181D-19
282	-0.363247370804009783D-19	-0.36324737180753665 0D-19	-0.3632394045D-19
283	-0.326037809521133659D-19	-0.32603781069289011 6D-19	-0.3260311994D-19
284	-0.292651137343767935D-19	-0.29265113863485950 1D-19	-0.2926456972D-19
285	-0.262693375455249603D-19	-0.26269337682409581 5D-19	-0.2626889416D-19
286	-0.235811279376801664D-19	-0.23581128078841267 1D-19	-0.2358077079D-19
287	-0.211688113044633918D-19	-0.21168811446991758 8D-19	-0.2116852779D-19
288	-0.190039862860268586D-19	-0.19003986427537396 8D-19	-0.1900376539D-19
289	-0.170611845736123393D-19	-0.17061184712182458 7D-19	-0.1706101666D-19
290	-0.153175669981991446D-19	-0.15317567132311439 4D-19	-0.1531744371D-19
291	-0.137526512193530972D-19	-0.13752651347842446 3D-19	-0.1375256528D-19
292	-0.123480677164978466D-19	-0.12348067838502959 9D-19	-0.1234801283D-19
293	-0.110873411303071980D-19	-0.11087341245226553 2D-19	-0.1108731187D-19
294	-0.995569431105600041D-20	-0.99556944185080485 4D-20	-0.9955685996D-20
295	-0.893987270740594633D-20	-0.89398728071934163 7D-20	-0.8939881327D-20
296	-0.802798697667253635D-20	-0.80279870687506316 5D-20	-0.8028009102D-20
297	-0.720937191918774898D-20	-0.72093720036360034 9D-20	-0.7209404633D-20
298	-0.647446003768186282D-20	-0.64744601146794085 6D-20	-0.6474500866D-20
299	-0.581466820010916005D-20	-0.58146682699131484 2D-20	-0.5814715059D-20
300	-0.522229604322809668D-20	-0.52222961061550140 5D-20	-0.5222347183D-20
301	-0.469043489647720254D-20	-0.46904349528868226 4D-20	-0.4690488862D-20
302	-0.421288613301641380D-20	-0.42128861832981364 1D-20	-0.4212941719D-20
303	-0.378408796879740891D-20	-0.37840880133587433 8D-20	-0.3784144188D-20
304	-0.339904983258786821D-20	-0.33990498718448323 4D-20	-0.3399105885D-20

305	-0.305329352125742726D-20	-0.30532935562664532D-20	-0.3053348764D-20
306	-0.27428004364591247 2D-20	-0.27428004663514227 2D-20	-0.2742854365D-20
307	-0.24639642721127285 2D-20	-0.24639642979280397 4D-20	-0.2464016496D-20
308	-0.22135485877130522 8D-20	-0.22135486098364612 8D-20	-0.2213598813D-20
309	-0.19886487612502629 6D-20	-0.19886487800490312 1D-20	-0.1988696777D-20
310	-0.17866578681586768 9D-20	-0.17866578839801077 8D-20	-0.1786703531D-20
311	-0.16052360798484646 9D-20	-0.16052360930184800 8D-20	-0.1605279303D-20
312	-0.14422832175962270 8D-20	-0.14422832284185406 1D-20	-0.1442323961D-20
313	-0.12959141353902655 5D-20	-0.12959141441460510 1D-20	-0.1295952397D-20
314	-0.11644366392051617 0D-20	-0.11644366461531265 1D-20	-0.1164472446D-20
315	-0.10463316805302123 3D-20	-0.10463316859069970 3D-20	-0.1046365085D-20
316	-0.94023558916627646 9D-21	-0.94023559318711164 5D-21	-0.9402666621D-21
317	-0.84492413466588786 2D-21	-0.84492413752544886 6D-21	-0.8449529608D-21
318	-0.75929822761764271 1D-21	-0.75929822949105107 1D-21	-0.7593249020D-21
319	-0.68237109153246715 2D-21	-0.68237109257639522 7D-21	-0.6823957166D-21
320	-0.61325675361325358 5D-21	-0.61325675396709573 4D-21	-0.6132794363D-21
321	-0.55115971839256782 8D-21	-0.55115971817964748 2D-21	-0.5511805679D-21
322	-0.49536570229550828 4D-21	-0.49536570162429563 6D-21	-0.4953848284D-21
323	-0.44523331979631294 0D-21	-0.44523331876163273 8D-21	-0.4452508314D-21
324	-0.40018662314014916 8D-21	-0.40018662182436217 3D-21	-0.4002026273D-21
325	-0.35970840773196046 6D-21	-0.35970840620610575 1D-21	-0.3597230084D-21
326	-0.32333420437431636 8D-21	-0.32333420269920470 3D-21	-0.3233475019D-21
327	-0.29064688767520095 1D-21	-0.29064688590245215 6D-21	-0.2906589785D-21
328	-0.26127183724245424 3D-21	-0.26127183541547362 6D-21	-0.2612828133D-21
329	-0.23487259482180663 7D-21	-0.23487259297669751 6D-21	-0.2348825433D-21
330	-0.21114696639863090 7D-21	-0.21114696456504175 4D-21	-0.2111559697D-21
331	-0.18982352354000412 7D-21	-0.18982352174191017 3D-21	-0.1898316592D-21
332	-0.17065846296641658 6D-21	-0.17065846122283672 8D-21	-0.1706658038D-21
333	-0.15343278756791698 1D-21	-0.15343278589356768 3D-21	-0.1534394015D-21
334	-0.13794977586819609 7D-21	-0.13794977427408457 2D-21	-0.1379557263D-21

335	-0.124032710337375098D-21	-0.12403270831334558D-21	-0.1240380561D-21
336	-0.111522838000657080D-21	-0.11152283658782717 6D-21	-0.1115276336D-21
337	-0.100277539521878386D-21	-0.10027753820513 4174D-21	-0.1002818354D-21
338	-0.901686853909359342D-22	-0.90168684171268 8436D-22	-0.9017252806D-22
339	-0.810811600412595537D-22	-0.81081158918113 8824D-22	-0.8108459233D-22
340	-0.729115366941023172D-22	-0.72911535665670 7699D-22	-0.7291459792D-22
341	-0.655668874938792387D-22	-0.65566865573609553D-22	-0.6556961370D-22
342	-0.589637150841040322D-22	-0.58963714235928 4549D-22	-0.5896613926D-22
343	-0.530269931954838028D-22	-0.53026992431503 5958D-22	-0.5302914547D-22
344	-0.476893050933084522D-22	-0.47689304408964 5292D-22	-0.4769121294D-22
345	-0.428900698755415156D-22	-0.42890069266003 0606D-22	-0.4289175829D-22
346	-0.385748476395407823D-22	-0.38574847099822 9650D-22	-0.3857633936D-22
347	-0.346947154562644382D-22	-0.34694714981326 3372D-22	-0.3469603110D-22
348	-0.312057069170470655D-22	-0.31205706501872 1255D-22	-0.3120686518D-22
349	-0.280683087593272747D-22	-0.28068308398988 4328D-22	-0.2806932654D-22
350	-0.252470087428319612D-22	-0.25247008432543 3986D-22	-0.2524790131D-22
351	-0.227098895445223566D-22	-0.22709889279679 6507D-22	-0.2271067068D-22
352	-0.204282639761235838D-22	-0.20428263752333 8693D-22	-0.2042894609D-22
353	-0.183763473086041915D-22	-0.18376347121707 7773D-22	-0.1837694156D-22
354	-0.165309629192048681D-22	-0.16530962765289 6063D-22	-0.1653147934D-22
355	-0.148712778636114457D-22	-0.14871277739021 0065D-22	-0.1487172545D-22
356	-0.133785653231776576D-22	-0.13378565224514 7349D-22	-0.1337895213D-22
357	-0.120359911888094893D-22	-0.12035991112934 8395D-22	-0.1203632442D-22
358	-0.108284223228858654D-22	-0.10828422266913 9697D-22	-0.1082870842D-22
359	-0.974225429169286950D-23	-0.97422542529849 1221D-23	-0.9742498999D-23
360	-0.876525658623529429D-23	-0.87652565623900 5356D-23	-0.8765465015D-23
361	-0.788643355160120435D-23	-0.78864335404443 7151D-23	-0.7886610250D-23
362	-0.709589942666145851D-23	-0.70958994262338 2596D-23	-0.7096048434D-23
363	-0.638476605891189502D-23	-0.63847660674567 8649D-23	-0.6384890957D-23
364	-0.574504200561750665D-23	-0.57450420215677 6360D-23	-0.5745145965D-23

365	-0.516954186380561771D-23	-0.51695418857704033 8D-23	-0.5169627687D-23
366	-0.465180478961310088D-23	-0.46518048163647367 3D-23	-0.4651874949D-23
367	-0.418602127339754508D-23	-0.41860213038585538 6D-23	-0.4186077948D-23
368	-0.376696733210901822D-23	-0.37669673653395123 6D-23	-0.3767012438D-23
369	-0.338994536579576336D-23	-0.33899454009812866 1D-23	-0.3389980583D-23
370	-0.305073100177809835D-23	-0.30507310382180023 1D-23	-0.3050757802D-23
371	-0.274552531886213344D-23	-0.27455253559585478 1D-23	-0.2745544990D-23
372	-0.247091190577926703D-23	-0.24709119430267034 5D-23	-0.2470925570D-23
373	-0.222381826354720356D-23	-0.22238183005228166 8D-23	-0.2223826898D-23
374	-0.200148111129819262D-23	-0.20014811476527086 4D-23	-0.2001485562D-23
375	-0.180141519988893296D-23	-0.18014152353382449 2D-23	-0.1801416202D-23
376	-0.162138527781341899D-23	-0.16213853121308390 6D-23	-0.1621383464D-23
377	-0.145938089005101109D-23	-0.14593809230601631 1D-23	-0.1459376805D-23
378	-0.131359372291551757D-23	-0.13135937544838473 3D-23	-0.1313587833D-23
379	-0.118239723710257215D-23	-0.11823972671354488 2D-23	-0.1182389942D-23
380	-0.106432835729912349D-23	-0.10643283857345026 9D-23	-0.1064319996D-23
381	-0.958071010222970597D-24	-0.95807103702658710 9D-24	-0.9580618691D-24
382	-0.862441324073573526D-24	-0.86244134923463092 3D-24	-0.8624316452D-24
383	-0.776374321341657939D-24	-0.77637434486898136 5D-24	-0.7763643068D-24
384	-0.698911953963297284D-24	-0.69891197588191592 5D-24	-0.6989017717D-24
385	-0.629192345110709132D-24	-0.62919236545883523 6D-24	-0.6291821333D-24
386	-0.566440115663371105D-24	-0.56644013448974322 9D-24	-0.5664299870D-24
387	-0.509957685757653591D-24	-0.50995770311921291 1D-24	-0.5099477310D-24
388	-0.459117452913210688D-24	-0.45911746887308045 2D-24	-0.4591077439D-24
389	-0.413354758207576469D-24	-0.41335477283331620 7D-24	-0.4133453509D-24
390	-0.372161560931456168D-24	-0.37216157429356382 3D-24	-0.3721524975D-24
391	-0.335080750209056109D-24	-0.33508076237969290 2D-24	-0.3350720613D-24
392	-0.301701029302934111D-24	-0.30170104035484865 4D-24	-0.3016927360D-24
393	-0.271652314824316395D-24	-0.27165232482994621 1D-24	-0.2716444300D-24
394	-0.244601598912195492D-24	-0.24460160794292580 6D-24	-0.2445941287D-24

395	-0.22024927694774095D-24	-0.22024923582033539D-24	-0.2202421727D-24
396	-0.19832555404065106651D-24	-0.19832556135309371 8D-24	-0.1983189105D-24
397	-0.17858792704314177 2D-24	-0.17858793355863956D-24	-0.1785816874D-24
398	-0.16081798380731136 4D-24	-0.16081798961261253 8D-24	-0.1608121378D-24
399	-0.14481921390393445 3D-24	-0.14481921905833681 0D-24	-0.1448137490D-24
400	-0.13041476822115758 3D-24	-0.13041477278082950 3D-24	-0.1304096702D-24
401	-0.11744548808110879 8D-24	-0.11744549209901262 7D-24	-0.1174407416D-24
402	-0.10576813229099178 5D-24	-0.10576813581685598 4D-24	
403	-0.95253782229371508 4D-25	-0.95253785309703462 5D-25	
404	-0.85786407053399087 4D-25	-0.85786409731531400 5D-25	
405	-0.77261572919097375 5D-25	-0.77261575235261334 8D-25	
406	-0.69585281730658538 0D-25	-0.69585283722079218 4D-25	
407	-0.62672926394479967 7D-25	-0.62672928095488156 6D-25	
408	-0.56448350865996895 D-25	-0.56448352308153759 2D-25	
409	-0.50843004457185903 2D-25	-0.50843005669416239 1D-25	
410	-0.45795180933320340 8D-25	-0.45795181942052753 8D-25	
411	-0.41249333881218579 1D-25	-0.41249334710528099 5D-25	
412	-0.37155460688648149 7D-25	-0.37155461360400513 9D-25	
413	-0.33468548245487724 7D-25	-0.33468548779482933 0D-25	
414	-0.30148074170429430 9D-25	-0.30148074584543181 8D-25	
415	-0.27157557990295977 3D-25	-0.27157558300617766 9D-25	
416	-0.24464157259508665 0D-25	-0.24464157480475590 5D-25	
417	-0.22038304111221657 9D-25	-0.22038304255747180 7D-25	
418	-0.19853378184839325 4D-25	-0.19853378264436435 5D-25	
419	-0.17885412282184109 0D-25	-0.17885412307082495 3D-25	
420	-0.16112827471090458 4D-25	-0.16112827450347424 4D-25	
421	-0.14516194684807940 4D-25	-0.14516194626412923 1D-25	
422	-0.13078020162026749 7D-25	-0.13078020072999394 2D-25	
423	-0.11782552338938138 1D-25	-0.11782552225419963 6D-25	
424	-0.10615608044519051 0D-25	-0.10615607911858808 9D-25	

425	-0.95644160658876491D-26	-0.95644159187216428 7D-26
426	-0.86174763445565973 6D-26	-0.86174761868774651 9D-26
427	-0.77644323884926034D-26	-0.77644330740801877 7D-26
428	-0.69959614447389112 5D-26	-0.69959612757912095 6D-26
429	-0.63036633084547961 3D-26	-0.63036631377858541 9D-26
430	-0.56799763912406752 1D-26	-0.56799762209058708 6D-26
431	-0.51180902608447956 5D-26	-0.51180900925447693 6D-26
432	-0.46118715870828106 4D-26	-0.46118714222063898 1D-26
433	-0.41557967112510311 7D-26	-0.41557965509140915 6D-26
434	-0.37448909423256308 4D-26	-0.37448907874061766 2D-26
435	-0.33746739076961674 2D-26	-0.33746737588659041 6D-26
436	-0.30411103534882349 6D-26	-0.30411102112409009 0D-26
437	-0.27405658500848536 8D-26	-0.27405657147615639 8D-26
438	-0.24697669129379552 2D-26	-0.24697667847498025 4D-26
439	-0.22257650977802938 1D-26	-0.22257649768284364 0D-26
440	-0.20059046734531262 1D-26	-0.20059045597465818 5D-26
441	-0.18077935152496219 7D-26	-0.18077934087209734 6D-26
442	-0.16292768973820839 1D-26	-0.16292767979012886 7D-26
443	-0.14684138953119032 4D-26	-0.14684138026983868 4D-26
444	-0.13234561375938104 3D-26	-0.13234560516270114 2D-26
445	-0.11928286729033654 3D-26	-0.11928285933318864 1D-26
446	-0.10751127413292371 1D-26	-0.10751126678787453 2D-26
447	-0.96903026008093142 3D-27	-0.96903019246094082 8D-27
448	-0.87342985272325874 2D-27	-0.87342979063291456 7D-27
449	-0.78727426811238518 4D-27	-0.78727421124536189 8D-27
450	-0.70962905056495826 2D-27	-0.70962899861357212 3D-27
451	-0.63965233661259804 8D-27	-0.63965228927122628 8D-27
452	-0.57658566613289113 1D-27	-0.57658562310078135 3D-27
453	-0.51974570684335512 6D-27	-0.51974566782690050 3D-27
454	-0.46851680122120081 5D-27	-0.46851676593574931 4D-27

455	-0.422344253981154210D-27	-0.42234422152413228D-27
456	-0.380728286406917572D-27	-0.38072825772009022D-27
457	-0.343218591179741473D-27	-0.34321856487956585D-27
458	-0.309409427961649175D-27	-0.30940940474946901D-27
459	-0.278935205944518498D-27	-0.27893518543780656 1D-27
460	-0.251466504935544585D-27	-0.25146464866967777 41D-27
461	-0.226706491374018568D-27	-0.22670647520414460 3D-27
462	-0.204387690017346184D-27	-0.20438767573012649 7D-27
463	-0.184269075943922834D-27	-0.18426906336565112 8D-27
464	-0.166133455040184026D-27	-0.16613344400932364 0D-27
465	-0.149785104307832465D-27	-0.14978509467459017 4D-27
466	-0.135047646179974241D-27	-0.13504763780582593 6D-27
467	-0.121762133603235477D-27	-0.12176212636041697 8D-27
468	-0.109785324955278322D-27	-0.10978531872625264 4D-27
469	-0.989881299490508773D-28	-0.98988124625961560 6D-28
470	-0.892542095495924771D-28	-0.89254205033711075 8D-28
471	-0.804787146169761791D-28	-0.80478710818150650 2D-28
472	-0.725671495086370989D-28	-0.72567146344746674 5D-28
473	-0.654343482426783401D-28	-0.65434345639099417 1D-28
474	-0.590035520558597564D-28	-0.59003549944946443 6D-28
475	-0.532055782994444403D-28	-0.53205576620026617 4D-28
476	-0.479780716151321832D-28	-0.47978070312033248 9D-28
477	-0.432648292329553314D-28	-0.43264828256531236 1D-28
478	-0.390151930431584070D-28	-0.39015192348859065 6D-28
479	-0.351835018236472665D-28	-0.35183501371601025 0D-28
480	-0.317285976616048709D-28	-0.31728597416226343 7D-28
481	-0.286133811995560875D-28	-0.28613381129177382 7D-28
482	-0.258044108690293678D-28	-0.25804410945554473 3D-28
483	-0.232715417548655969D-28	-0.23271541953447496 9D-28
484	-0.209876001654366552D-28	-0.20987600464176586 6D-28

485	-0.18928090373305216 3D-28	-0.18928090752973345 5D-28
486	-0.17070930341456667 0D-28	-0.17070930785233370 4D-28
487	-0.15396213566011410 2D-28	-0.15396214059248270 3D-28
488	-0.13885994450745343 9D-28	-0.13885994980744920 5D-28
489	-0.12524094884926949 6D-28	-0.12524095440740355 1D-28
490	-0.11295929926729395 9D-28	-0.11295930498970687 9D-28
491	-0.10188350702323853 0D-28	-0.10188351283000252 4D-28
492	-0.91895028179825053 4D-29	-0.91895034003394584 5D-29
493	-0.82886987511665223 7D-29	-0.82886993295466401 7D-29
494	-0.74763028384914079 7D-29	-0.74763034082063400 7D-29
495	-0.67436276153118639 9D-29	-0.67436281725261950 4D-29
496	-0.60828403849473352 7D-29	-0.60828409265736245 4D-29
497	-0.54868790066255820 8D-29	-0.54868795302297044 5D-29
498	-0.49493759912687059 8D-29	-0.49493764949846919 2D-29
499	-0.44645900843770670 2D-29	-0.44645905668306799 8D-29
500	-0.40273445964658102 2D-29	-0.40273450567061416 0D-29
501	-0.36329718146627377 3D-29	-0.36329722521011415 3D-29
502	-0.32772628949833675 1D-29	-0.32772633093390983 0D-29
503	-0.29564226941782110 9D-29	-0.29564230854301700 5D-29
504	-0.26670290535461361 1D-29	-0.26670294218901699 7D-29
505	-0.24059960953093702 2D-29	-0.24059964411206066 7D-29
506	-0.21705411355755351 5D-29	-0.21705414593752757 9D-29
507	-0.19581548570431853 7D-29	-0.19581551594699131 9D-29
508	-0.17665744198657990 8D-29	-0.17665747016498916 9D-29
509	-0.15937592208588541 6D-29	-0.15937594828006263 8D-29
510	-0.14378690398612431 1D-29	-0.14378692828119735 6D-29
511	-0.12972443378572527 1D-29	-0.12972445627028777 2D-29
512	-0.11703884947091643 2D-29	-0.11703887023563499 8D-29
513	-0.10559517952959021 0D-29	-0.10559519866602305 5D-29
514	-0.95271699172768284 5D-30	-0.95271716772371283 1D-30

515	-0.859586286315344147D-30	-0.85958644784832792 5D-30
516	-0.775569595300654879D-30	-0.77556974325971411 5D-30
517	-0.699773967166840043D-30	-0.69977410241942239 3D-30
518	-0.631394041796680878D-30	-0.63139416518413644 2D-30
519	-0.569703447963925521D-30	-0.56970356029805858 9D-30
520	-0.514047046754027172D-30	-0.51404714881449348 7D-30
521	-0.463833937622023532D-30	-0.46383403015445695 0D-30
522	-0.418531152007433370D-30	-0.41853123572219822 3D-30
523	-0.377657966827342638D-30	-0.37765804239881951 2D-30
524	-0.340780776839542546D-30	-0.34078084490586549 3D-30
525	-0.307508470879887404D-30	-0.30750853204306003 0D-30
526	-0.277488262397033453D-30	-0.27748831722335986 5D-30
527	-0.250401929592032888D-30	-0.25040197861280715 2D-30
528	-0.225962424872719022D-30	-0.22596246858512376 5D-30
529	-0.203910817301031107D-30	-0.20391085616920216 9D-30
530	-0.184013535288283294D-30	-0.18401356974450293 4D-30
531	-0.166059880017531448D-30	-0.16605991046351766 3D-30
532	-0.149859782978461633D-30	-0.14985980978672566 0D-30
533	-0.135241783619998506D-30	-0.13524180713524658 5D-30
534	-0.122051205487391608D-30	-0.12205122602795065 4D-30
535	-0.110148511339367606D-30	-0.11014852919861762 2D-30
536	-0.994078196600034753D-31	-0.99407835107802312 9D-31
537	-0.897155667099760768D-31	-0.89715579994064633 7D-31
538	-0.809692998214295383D-31	-0.80969311168807655 9D-31
539	-0.730765890466825341D-31	-0.73076598664947736 7D-31
540	-0.659540455385219076D-31	-0.65954053617164792 3D-31
541	-0.595264361825500046D-31	-0.59526442894201521 1D-31
542	-0.537258850322752980D-31	-0.53725890533902399 5D-31
543	-0.484911530264493240D-31	-0.48491157460496534 8D-31
544	-0.437669883055528298D-31	-0.43766991801028187 8D-31

545	-0.39503540199329057D-31	-0.39503542872833661D-31
546	-0.35655830637971977D-31	-0.35655832594673021D-31
547	-0.32183277353320609D-31	-0.32183278687868327D-31
548	-0.29049263789783854D-31	-0.29049264587173250D-31
549	-0.26220751143669508D-31	-0.26220751480048114D-31
550	-0.23667928399475712D-31	-0.23667928342898896D-31
551	-0.21363896637354150D-31	-0.21363896248489747D-31
552	-0.19284384251726473D-31	-0.19284383584510670D-31
553	-0.17407490050854176D-31	-0.17407489153100713D-31
554	-0.15713451504565985D-31	-0.15713450418530835D-31
555	-0.14184435675525602D-31	-0.14184434438429313D-31
556	-0.12804350611251770D-31	-0.12804349255761722D-31
557	-0.11558675192174492D-31	-0.11558673746849273D-31
558	-0.10434305627662479D-31	-0.10434304117360600D-31
559	-0.94194169692944399D-32	-0.94194154155495448D-32
560	-0.85033381705697415D-32	-0.85033365919344307D-32
561	-0.76764939366474599D-32	-0.76764377788349184D-32
562	-0.69300301763819448D-32	-0.69300285932445147D-32
563	-0.62562795105815670D-32	-0.62562663838118486D-32
564	-0.56480749903327351D-32	-0.56480734484867090D-32
565	-0.50990638533889791D-32	-0.50990623447888202D-32
566	-0.46034699696747797D-32	-0.46034685006983778D-32
567	-0.41560908360323848D-32	-0.41560894117671171D-32
568	-0.37522311556335953D-32	-0.37522297800362819D-32
569	-0.33876533374299325D-32	-0.33876520134709504D-32
570	-0.30585328317599704D-32	-0.30585315615528253D-32
571	-0.27614178291060828D-32	-0.27614166140236558D-32
572	-0.24931928953083683D-32	-0.24931917360869741D-32
573	-0.22510461583186927D-32	-0.22510450551510099D-32
574	-0.20324396992582419D-32	-0.20324386518761008D-32

575	-0.18350283452955153D-32	-0.18350184227749423D-32
576	-0.16569080063910296D-32	-0.16569070682914735D-32
577	-0.14960490270551140 3D-32	-0.14960481418660023 6D-32
578	-0.13508214463158072 4D-32	-0.13508206125812205 8D-32
579	-0.12197048352111256 4D-32	-0.12197040513058525 3D-32
580	-0.11013267985241161 4D-32	-0.11013260626925465 5D-32
581	-0.99444854723442311 7D-33	-0.99444785762442641 1D-33
582	-0.89795187854931443 9D-33	-0.89795123324160046 6D-33
583	-0.81082742604234858 5D-33	-0.81082682307578298 4D-33
584	-0.73216405586873635 2D-33	-0.73216349326204024 0D-33
585	-0.66113929715170069 9D-33	-0.66113877292192682 0D-33
586	-0.59701070557270439 3D-33	-0.59701021775084644 7D-33
587	-0.53910806906656941 9D-33	-0.53910761571062856 1D-33
588	-0.48682637342512117 2D-33	-0.48682595263092341 3D-33
589	-0.43961945364463507 0D-33	-0.43961906355466541 3D-33
590	-0.39699426409834871 4D-33	-0.39699390290884213 1D-33
591	-0.35850570715256941 0D-33	-0.35850537311907515 5D-33
592	-0.32375196574285168 7D-33	-0.32375165718446574 9D-33
593	-0.29237029074793603 9D-33	-0.29237000605037666 7D-33
594	-0.26403319880008680 9D-33	-0.26403293641776987 5D-33
595	-0.23844504050206891 0D-33	-0.23844479895932330 3D-33
596	-0.21533890292919469 5D-33	-0.21533868082074279 0D-33
597	-0.19447381382108748 7D-33	-0.19447360981190202 1D-33
598	-0.17563221804942190 5D-33	-0.17563203087405805 0D-33
599	-0.15861769981862656 5D-33	-0.15861752828011670 4D-33
600	-0.14325292664678368 6D-33	-0.14325276961517211 1D-33
601	-0.12937779351116565 3D-33	-0.12937764992175116 7D-33
602	-0.11684774765175789 2D-33	-0.11684761650310391 9D-33
603	-0.10553227642905440 5D-33	-0.10553215678081871 5D-33
604	-0.95313542349515811 5D-34	-0.95313433320145201 1D-34

605	-0.860851509215171183D-34	-0.86085051685846325 1D-34
606	-0.777510384027730957D-34	-0.77750948189561827 8D-34
607	-0.702244677618986375D-34	-0.70224385851335743 8D-34
608	-0.634271223152786408D-34	-0.63427048036478150 3D-34
609	-0.572882875278206018D-34	-0.57288202563305330 D-34
610	-0.517441123932999464D-34	-0.51744051548641395 4D-34
611	-0.467369426466778606D-34	-0.46736887689928882 2D-34
612	-0.422147188158109088D-34	-0.42214669247247064 2D-34
613	-0.381304328013537493D-34	-0.38130388158154878 5D-34
614	-0.344416372885739790D-34	-0.34441597142604721 9D-34
615	-0.311100028497415121D-34	-0.31109966805411341 0D-34
616	-0.281009180965795085D-34	-0.28100885788786493 3D-34
617	-0.253831286942529366D-34	-0.25383099786414140 1D-34
618	-0.229284114562913235D-34	-0.22928385638461585 1D-34
619	-0.207112801079952285D-34	-0.20711257095075117 6D-34
620	-0.187087196381423447D-34	-0.18708699168175241 4D-34
621	-0.168999464586906498D-34	-0.16899928291248213 6D-34
622	-0.152661918628323648D-34	-0.15266175577487073 6D-34
623	-0.137905065160347370D-34	-0.13790492310917699 9D-34
624	-0.124575839351844743D-34	-0.12457571425626334 5D-34
625	-0.112536011099534824D-34	-0.11253590127205918 8D-34
626	-0.101660746001191594D-34	-0.10166064990154252 5D-34
627	-0.918373060469317530D-35	-0.91837222270777252 7D-35
628	-0.829638764504417520D-35	-0.82963803718859287 1D-35
629	-0.749485063628146570D-35	-0.74948443512441252 6D-35
630	-0.677081524038754411D-35	-0.67708098377713868 9D-35
631	-0.611678150220082303D-35	-0.61167768860857422 7D-35
632	-0.552597586648730223D-35	-0.55259719499350982 9D-35
633	-0.499228076202210458D-35	-0.49922774663348891 0D-35
634	-0.451017101774999637D-35	-0.45101682717816287 7D-35

635	-0.40746564475396758D-35	-0.40746541870572259D-35
636	-0.36812300045400726D-35	-0.36812281716323636D-35
637	-0.33258209643653246D-35	-0.33258195068957736D-35
638	-0.30047526488896287D-35	-0.30047515199905881D-35
639	-0.27147042498753651D-35	-0.27147034074813894D-35
640	-0.24526763544855631D-35	-0.24526757609030678D-35
641	-0.22159598133941872D-35	-0.22159594349051016D-35
642	-0.20021076271103698D-35	-0.20021074336074968D-35
643	-0.18089095576415699D-35	-0.18089095222934798D-35
644	-0.16343692010660245D-35	-0.16343693000094215D-35
645	-0.14766832822649007D-35	-0.14766834943225138D-35
646	-0.13342229562483614D-35	-0.13342232626705192D-35
647	-0.12055169214401921D-35	-0.12055173056683475D-35
648	-0.10892361691819378D-35	-0.10892366166325118D-35
649	-0.98418021077753878D-36	-0.98418070864455224D-36
650	-0.88926463880184291D-36	-0.88926517587689935D-36
651	-0.80350989330232906D-36	-0.80351045981060615D-36
652	-0.72603111607842794D-36	-0.72603170352942068D-36
653	-0.65602989755832712D-36	-0.65602958861017071D-36
654	-0.59278145102767446D-36	-0.59278205936395435D-36
655	-0.53563623820517963D-36	-0.53563684842321174D-36
656	-0.48400411850337567D-36	-0.48400472601301142D-36
657	-0.43735280184595940D-36	-0.43735340277803794D-36
658	-0.39520143171491214D-36	-0.39520202283854586D-36
659	-0.35711561124208415D-36	-0.35711618989002363D-36
660	-0.32270291070526655D-36	-0.32270347470664756D-36
661	-0.29160880979589325D-36	-0.29160935741572146D-36
662	-0.26351303254669929D-36	-0.26351356243147775D-36
663	-0.23812623689011364D-36	-0.23812674801906454D-36
664	-0.21518702450449678D-36	-0.21518751614587245D-36

665	-0.19445923993401742 6D-36	-0.19445971160603568 0D-36
666	-0.17572953097372810 8D-36	-0.17572998240970482 3D-36
667	-0.15880514502560188 9D-36	-0.15880557614288868 6D-36
668	-0.14351193858223941 9D-36	-0.14351234945460670 9D-36
669	-0.12969257920820329 4D-36	-0.12969297004133920 1D-36
670	-0.11720492138755910 8D-36	-0.11720529249738268 1D-36
671	-0.10592053941103086 3D-36	-0.10592089120454386 0D-36
672	-0.95723402106020501 8D-37	-0.95723735064445939 1D-37
673	-0.86508675684578034 7D-37	-0.86508990348555777 7D-37
674	-0.78181642313571538 3D-37	-0.78181939270201575 6D-37
675	-0.70656723211637699 4D-37	-0.70657003083180523 8D-37
676	-0.63856596161491813 9D-37	-0.63856859595552605 6D-37
677	-0.57711398305125899 9D-37	-0.57711645966165100 6D-37
678	-0.52158005973513866 6D-37	-0.52158238535541328 1D-37
679	-0.47139384100873383 2D-37	-0.47139602241196667 4D-37
680	-0.42603998494612019 2D-37	-0.42604202888521704 7D-37
681	-0.38505284883310957 5D-37	-0.38505476199597049 4D-37
682	-0.34801169253245696 8D-37	-0.34801348150449521 9D-37
683	-0.31453634515125055 1D-37	-0.31453801638440420 4D-37
684	-0.28428329022469428 0D-37	-0.28428485001215403 1D-37
685	-0.25694212896332880 6D-37	-0.25694358341928382 5D-37
686	-0.23223238502403723 0D-37	-0.23223374006781213 4D-37
687	-0.20990061779960485 2D-37	-0.20990187914362569 9D-37
688	-0.18971781441386009 7D-37	-0.18971898755494627 4D-37
689	-0.17147703349267039 3D-37	-0.17147812370620275 7D-37
690	-0.15499127638523958 5D-37	-0.15499228872180376 5D-37
691	-0.14009156386228766 5D-37	-0.14009250314643538 2D-37
692	-0.12662519844220255 8D-37	-0.12662606927301360 8D-37
693	-0.11445419441518447 3D-37	-0.11445500116834795 0D-37
694	-0.10345385936866526 9D-37	-0.10345460619983105 4D-37

695	-0.93511512582858256 5D-38	-0.93512203432039048 4D-38
696	-0.84525327079414985 1D-38	-0.84525965676245453 1D-38
697	-0.76403283383498295 6D-38	-0.76403873253181612 7D-38
698	-0.69062242421336800 71D-38	-0.69062768683161256 1D-38
699	-0.62427000353776430 9D-38	-0.62427502559885411 4D-38
700	-0.56429698910886317 9D-38	-0.56430161805657318 5D-38
701	-0.51008945996808301 4D-38	-0.51009372356119617 9D-38
702	-0.46109276660017976 5D-38	-0.46109669090787527 0D-38
703	-0.41680656557181077 20D-38	-0.41680926519548240 7D-38
704	-0.37677512605771483 6D-38	-0.37677844362114153 5D-38
705	-0.34059178013464621 7D-38	-0.34059482723645570 5D-38
706	-0.30788562411053070 0D-38	-0.30788842081258815 3D-38
707	-0.27832272725361989 05D-38	-0.27832483758201993 4D-38
708	-0.25159951891382882 3D-38	-0.25160186979894549 4D-38
709	-0.22744423679072273 3D-38	-0.22744638983106730 3D-38
710	-0.20560957950389249 0D-38	-0.20561154990201666 7D-38
711	-0.18587244977199923 9D-38	-0.18587425168099050 9D-38
712	-0.16803121311127934 9D-38	-0.16803285969627381 0D-38
713	-0.15190363156363224 7D-38	-0.15190513506085617 2D-38
714	-0.13732499649400839 9D-38	-0.13732636826730897 4D-38
715	-0.12414644126406587 2D-38	-0.12414769185891565 1D-38
716	-0.11223341644094177 4D-38	-0.11223455563592191 6D-38
717	-0.10146431187304213 5D-38	-0.10146534872882675 5D-38
718	-0.91729211476271142 9D-39	-0.91730154382149579 8D-39
719	-0.82928767939707929 4D-39	-0.82929624657693677 0D-39
720	-0.74973185734961114 D-39	-0.74973963500080902 5D-39
721	-0.67781302396374733 0D-39	-0.67782007721994090 4D-39
722	-0.61279757407354101 5D-39	-0.61280396473636795 6D-39
723	-0.55402242215918977 3D-39	-0.55402820670797486 7D-39
724	-0.50088821627212667 6D-39	-0.50089344677975124 0D-39

725	-0.452853208413992954D-39	-0.452857932857656699D-39
726	-0.409427714374786565D-39	-0.409431976927852745D-39
727	-0.370169106781590453D-39	-0.370172948087360375D-39
728	-0.334677290002298265D-39	-0.334680747430559533D-39
729	-0.302590610498648526D-39	-0.302593718385833870D-39
730	-0.273582160695319020D-39	-0.273584950569100221D-39
731	-0.247356438472910403D-39	-0.247358939262035448D-39
732	-0.223646328043998434D-39	-0.223648566274160386D-39
733	-0.202210371270672150D-39	-0.202212371247175978D-39
734	-0.182830301463082161D-39	-0.182832085441051450D-39
735	-0.165308814392198260D-39	-0.165310402735037852D-39
736	-0.149467553683953344D-39	-0.149468965010756976D-39
737	-0.135145289961287590D-39	-0.135146541283851805D-39
738	-0.122196275087939802D-39	-0.122197381938017254D-39
739	-0.110488754663613402D-39	-0.110489731211010263D-39
740	-0.999036235428494532D-40	-0.999044827049433593D-40
741	-0.903332106162619438D-40	-0.903339641594888396D-40
742	-0.816801804178131404D-40	-0.816808390516437717D-40
743	-0.738565403191556423D-40	-0.738571137830553528D-40
744	-0.667827431540540277D-40	-0.667832402978931083D-40
745	-0.603868760936459485D-40	-0.603873049520021170D-40
746	-0.546039274768601091D-40	-0.546042953376298530D-40
747	-0.493751240987570236D-40	-0.493754375664685570D-40
748	-0.446473321811019873D-40	-0.446475972352995057D-40
749	-0.403725159015311065D-40	-0.403727379505778812D-40
750	-0.365072479469282116D-40	-0.365074318775548768D-40
751	-0.330122670891447515D-40	-0.330124173120488982D-40
752	-0.298520782624343732D-40	-0.298521987542182715D-40
753	-0.269945910568795482D-40	-0.269946853985944757D-40
754	-0.244107929351236190D-40	-0.244108643476718485D-40

755	-0.22074453834921829 6D-40	-0.22074505211550816 2D-40
756	-0.19961859141034191 9D-40	-0.19961893077141873 1D-40
757	-0.18051568300094962 7D-40	-0.18051587120550313 2D-40
758	-0.16324196614284074 3D-40	-0.16324202398453126 5D-40
759	-0.14762217986584274 2D-40	-0.14762212591238678 9D-40
760	-0.13349786604563943 5D-40	-0.13349771684836787 9D-40
761	-0.12072575743175390 2D-40	-0.12072552771717370 7D-40
762	-0.10917632041986022 5D-40	-0.10917602326464161 8D-40
763	-0.98732437703582098 9D-41	-0.98732084694290751 0D-41
764	-0.89288217369830474 9D-41	-0.89287818748628409 9D-41
765	-0.80747916293178030 5D-41	-0.80747481090627249 3D-41
766	-0.73024966851996149 8D-41	-0.73024503008015071 4D-41
767	-0.66041097044046586 0D-41	-0.66040611517991032 9D-41
768	-0.59725535032729703 0D-41	-0.59725033903497017 9D-41
769	-0.54014290017008149 9D-41	-0.54013778573994827 8D-41
770	-0.48849502096972670 0D-41	-0.48848984922652343 6D-41
771	-0.44178854511069433 2D-41	-0.44178335555898896 0D-41
772	-0.39955042257371923 7D-41	-0.39954524907677852 8D-41
773	-0.36135291686467296 2D-41	-0.36134778825915197 4D-41
774	-0.32680926173422535 1D-41	-0.32680420238621938 0D-41
775	-0.29556973446218428 8D-41	-0.29556476476974286 4D-41
776	-0.26731810572796042 9D-41	-0.26731324257475416 8D-41
777	-0.24176842992795100 5D-41	-0.24176368709240339 1D-41
778	-0.21866214327102405 2D-41	-0.21865753179486950 5D-41
779	-0.19776544012019305 5D-41	-0.19776096864009807 9D-41
780	-0.17886869008406860 6D-41	-0.17886257592965272 6D-41
781	-0.16177534732473948 6D-41	-0.16177117358605532 0D-41
782	-0.14631790346556318 2D-41	-0.14631388403283889 5D-41
783	-0.13233842423766078 11D-41	-0.13233437895481882 1D-41
784	-0.11969500100857895 8D-41	-0.11969129410919778 4D-41

785	-0.108260346957323169D-41	-0.10825679606939539 6D-41
786	-0.979186825879017472D-42	-0.979152863304109985D-42
787	-0.885654733455701890D-42	-0.885622296028846808D-42
788	-0.801061883450569884D-42	-0.801030943870935218D-42
789	-0.724553424722145133D-42	-0.724523950608116985D-42
790	-0.655356302650772867D-42	-0.655328257479374507D-42
791	-0.592771427751509623D-42	-0.592744771685886658D-42
792	-0.536166594538966106D-42	-0.536141285155202029D-42
793	-0.484970078724817361D-42	-0.484946071648321299D-42
794	-0.438664847727258820D-42	-0.438642097188030376D-42
795	-0.396783325708106879D-42	-0.396761785023324883D-42
796	-0.358902659991114720D-42	-0.358882281982711430D-42
797	-0.32464044081188251 1D-42	-0.32462117816604656 0D-42
798	-0.293650830957445363D-42	-0.293632636532340324D-42
799	-0.265621066019189243D-42	-0.265603893106575048D-42
800	-0.240268289748627770D-42	-0.240252092294524992D-42
801	-0.217336692410146152D-42	-0.217321425199183929D-42
802	-0.196594923102769835D-42	-0.196580541910403246D-42
803	-0.177833749805700175D-42	-0.177820211522068440D-42
804	-0.160863943418120579D-42	-0.160851206146940248D-42
805	-0.145514364338234865D-42	-0.145502387473779136D-42
806	-0.131630232182814886D-42	-0.131618976467718396D-42
807	-0.119071561107642215D-42	-0.119060988673987571D-42
808	-0.107711744870054005D-42	-0.107701819265939432D-42
809	-0.974362772944535695D-43	-0.974269634980081850D-43
810	-0.881415951755868770D-43	-0.881328595981891466D-43
811	-0.797340318965970362D-43	-0.797258423768610694D-43
812	-0.721288711619879602D-43	-0.721211969519096773D-43
813	-0.652494912610803857D-43	-0.652423030055796659D-43
814	-0.590265911956562874D-43	-0.590198609066104867D-43

815	-0.53397490835598072D-43	-0.53391191861335447D-43
816	-0.48305498016877283D-43	-0.48299605007984613D-43
817	-0.43699336174864297D-43	-0.43693825047060241D-43
818	-0.39532626719513841D-43	-0.39527474614247229D-43
819	-0.35763420913767259D-43	-0.35758606157116682D-43
820	-0.32353776518139220D-43	-0.32349278578516012D-43
821	-0.29269374918020756D-43	-0.29265174363111038D-43
822	-0.26479174860340184D-43	-0.26475253313662245D-43
823	-0.23955099297044288D-43	-0.23951439394444600D-43
824	-0.21671752168160489D-43	-0.21668337514524472D-43
825	-0.19606162260381427D-43	-0.19602977386793113D-43
826	-0.17737551551254965D-43	-0.17734581872802477D-43
827	-0.16047125696948052D-43	-0.16044357471338840D-43
828	-0.14517884545698573D-43	-0.14515304832819210D-43
829	-0.13134450761750058D-43	-0.13132047384279727D-43
830	-0.11882914827836822D-43	-0.11880676333001041D-43
831	-0.10750694860011318D-43	-0.10748610482542666D-43
832	-0.97264098184624501D-44	-0.97244694448177850D-44
833	-0.87997648334836137D-44	-0.87979589673522144D-44
834	-0.79614474882864488D-44	-0.79597672174104885D-44
835	-0.72030340111635931D-44	-0.72014709754810969D-44
836	-0.65169044297045158D-44	-0.65154507908153043D-44
837	-0.58961658303787070D-44	-0.58948142423255967D-44
838	-0.53345829487386039D-44	-0.53333265300891642D-44
839	-0.48265153895911136D-44	-0.48253476967994341D-44
840	-0.43668608434923783D-44	-0.43657758455154373D-44
841	-0.39510037265144507D-44	-0.39499957806536935D-44
842	-0.35747687250287240D-44	-0.35738325539642457D-44
843	-0.32343778768043800D-44	-0.32335094467865698D-44
844	-0.29264170645326853D-44	-0.29256099646942446D-44

845	-0.264779263841351937D-44	-0.264704346116333780D-44
846	-0.239570932108941692D-44	-0.239501404354881246D-44
847	-0.216763758135571105D-44	-0.216699244779695154D-44
848	-0.196128909304859093D-44	-0.196069059829535970D-44
849	-0.177459372261942717D-44	-0.177403859636892954D-44
850	-0.160567871341790569D-44	-0.160516390544459103D-44
851	-0.145284985687641249D-44	-0.145237252307777123D-44
852	-0.131457446083804171D-44	-0.131413195008359476D-44
853	-0.118946594340339620D-44	-0.118905578514879536D-44
854	-0.107626989707043195D-44	-0.107588978969950861D-44
855	-0.973851482772826019D-45	-0.973499282631437699D-45
856	-0.881184026835704397D-45	-0.880857737922315787D-45
857	-0.797338705998680564D-45	-0.797036470277757836D-45
858	-0.721475216627671411D-45	-0.721195304933152547D-45
859	-0.652833334159784729D-45	-0.652574137657099256D-45
860	-0.590725277800004720D-45	-0.590485299976342964D-45
861	-0.534528803605136259D-45	-0.534306652758900730D-45
862	-0.483680956431522985D-45	-0.483475338633124253D-45
863	-0.437672417862599256D-45	-0.437482130359978522D-45
864	-0.396042393237445868D-45	-0.395866318280910206D-45
865	-0.358373986332851454D-45	-0.358211085394990275D-45
866	-0.324290015163790145D-45	-0.324139323531398708D-45
867	-0.293449226810318893D-45	-0.293309848526383045D-45
868	-0.265542873197536830D-45	-0.265413976332430097D-45
869	-0.240291613390005845D-45	-0.240172425622113136D-45
870	-0.217442711249597163D-45	-0.217332515736607254D-45
871	-0.196767500279285376D-45	-0.196665631802385800D-45
872	-0.178059090164968276D-45	-0.177964931529130480D-45
873	-0.161130291960087398D-45	-0.161043270634546677D-45
874	-0.145811741058205034D-45	-0.145731326042118673D-45

875	-0.131950199088956464D-45	-0.13187589798806487 7D-45
876	-0.119407017673016912D-45	-0.119338373973936667D-45
877	-0.108056748600057641D-45	-0.107993339129602709D-45
878	-0.977858864665355609D-46	-0.977273190241945305D-46
879	-0.884917311424168292D-46	-0.884376422948100459D-46
880	-0.800813586410089218D-46	-0.800314116678114344D-46
881	-0.724706900561154655D-46	-0.724245730375602619D-46
882	-0.655836492167207610D-46	-0.655410732533931196D-46
883	-0.593514006012933662D-46	-0.593120981574923165D-46
884	-0.537116598605578406D-46	-0.536753832230358467D-46
885	-0.486080700273494304D-46	-0.485745898717476286D-46
886	-0.439896371522901302D-46	-0.439587412100649200D-46
887	-0.398102197011557738D-46	-0.397817115202444363D-46
888	-0.360280665899569098D-46	-0.360017643828563599D-46
889	-0.326053992223709848D-46	-0.325811347957058922D-46
890	-0.295080333361599360D-46	-0.294856510961953886D-46
891	-0.267050368650358698D-46	-0.266843928939466071D-46
892	-0.241684203841232058D-46	-0.241493815821672878D-46
893	-0.218728570343492107D-46	-0.218553003234098479D-46
894	-0.197954291170692367D-46	-0.197792407013254131D-46
895	-0.179153988179767731D-46	-0.179004734977422155D-46
896	-0.162140007615557296D-46	-0.162002412965876638D-46
897	-0.146742543164400783D-46	-0.146615708352649790D-46
898	-0.132807937702582953D-46	-0.132691032222923527D-46
899	-0.120197146718507180D-46	-0.120089403193088566D-46
900	-0.108784348009604045D-46	-0.108685057477501978D-46
901	-0.984556837224359837D-47	-0.983641912723010099D-47
902	-0.891081221320002484D-47	-0.890238228540512477D-47
903	-0.806484277572067075D-47	-0.805707629918674869D-47
904	-0.729922294959874897D-47	-0.729206833580188809D-47

905	-0.660631774464030302D-47	-0.659972736048365476D-47
906	-0.597921799693223429D-47	-0.597314786648601699D-47
907	-0.541167133527102585D-47	-0.540608086355258499D-47
908	-0.489801971653341472D-47	-0.489287143373934965D-47
909	-0.443314290461192441D-47	-0.442840222932499859D-47
910	-0.401240732710493824D-47	-0.400804234710182600D-47
911	-0.363161979784119608D-47	-0.362760106722353635D-47
912	-0.328698564207347319D-47	-0.328328599353463525D-47
913	-0.297507080528536053D-47	-0.297166517640918608D-47
914	-0.269276756646141390D-47	-0.268963283902737202D-47
915	-0.243726351277513450D-47	-0.243437836411717341D-47
916	-0.220601346531372665D-47	-0.220335823084797278D-47
917	-0.199671407501122571D-47	-0.199427062111088831D-47
918	-0.180728083469900495D-47	-0.180503244115369693D-47
919	-0.163582727373317415D-47	-0.163375852872464245D-47
920	-0.148064615266470847D-47	-0.147874283776194769D-47
921	-0.134019239329987930D-47	-0.133844141246403260D-47
922	-0.121306770125435159D-47	-0.121145698048791849D-47
923	-0.109800659951387229D-47	-0.109652501122976605D-47
924	-0.993863810020379982D-48	-0.992501099804515181D-48
925	-0.899602831651694476D-48	-0.898349550608232272D-48
926	-0.814285604088753135D-48	-0.813133046350070620D-48
927	-0.737063154287023364D-48	-0.736003299301074146D-48
928	-0.667167132097137036D-48	-0.666192591333292886D-48
929	-0.603902150472483972D-48	-0.603006118213341122D-48
930	-0.546638853747598739D-48	-0.545815061658736921D-48
931	-0.494807644751314608D-48	-0.494050319943742677D-48
932	-0.447893008105792910D-48	-0.447196834426923785D-48
933	-0.405428373022665731D-48	-0.404788455331249345D-48
934	-0.366991464300366564D-48	-0.366403295498978782D-48

935	-0.33220095106289410D-48	-0.33165925721826730D-48
936	-0.30070835942587157D-48	-0.30021156960844017D-48
937	-0.27220318698941369 2D-48	-0.27174660364307656D-48
938	-0.24640122383423743 1D-48	-0.24598172400567802 9D-48
939	-0.22304601146670215 0D-48	-0.22266055973354657 7D-48
940	-0.20190543237813154 6D-48	-0.20155128748420488 1D-48
941	-0.18276939888279526 9D-48	-0.18244403828463935 2D-48
942	-0.16544776140128249 8D-48	-0.16514886399619680 1D-48
943	-0.14976841543901779 9D-48	-0.14949384564112406 0D-48
944	-0.13557558837704654 2D-48	-0.13532338143759907 9D-48
945	-0.12272828898756743 5D-48	-0.12249663746359187 4D-48
946	-0.11109890421126089 8D-48	-0.11088614549388106 4D-48
947	-0.10057192920350706 1D-48	-0.10037653402405519 7D-48
948	-0.91042817986811151 2D-49	-0.90863379825049937 6D-49
949	-0.82416943250462353 6D-49	-0.82252168575014832 9D-49
950	-0.74608654927683234 7D-49	-0.74457354204102783 4D-49
951	-0.67540428166172925 0D-49	-0.67401507573021399 7D-49
952	-0.61142092199864029 5D-49	-0.61014545997731477 0D-49
953	-0.55350132436817953 1D-49	-0.55233035939439077 0D-49
954	-0.50107058808544599 7D-49	-0.49995619090707966D-49
955	-0.45360834086950782 8D-49	-0.45262155296045495 7D-49
956	-0.41064356473202936 3D-49	-0.40973777428964105 9D-49
957	-0.37174991304010907 6D-49	-0.37091851716807662 0D-49
958	-0.33654147210609015 0D-49	-0.33577840208769189 0D-49
959	-0.30466892508921767 2D-49	-0.30396860353839779 7D-49
960	-0.27581608000482626 9D-49	-0.27517338142149820 3D-49
961	-0.24969672726631586 7D-49	-0.24910694172838296 1D-49
962	-0.22605179546976516 4D-49	-0.22551059521510774 2D-49
963	-0.20464677710344737 4D-49	-0.20415018577429480 4D-49
964	-0.18526939855443463 0D-49	-0.18481376289424312 7D-49

965	-0.16772751121876621 4D-49	-0.16730947502806795 4D-49
966	-0.15184718272461648 9D-49	-0.15146366289739555 8D-49
967	-0.13747096927152393 5D-49	-0.13711913374760442 9D-49
968	-0.12445635189293424 6D-49	-0.12413359937472314 8D-49
969	-0.11267432108207613 3D-49	-0.11237826237586969 1D-49
970	-0.10200809569882394 4D-49	-0.10173653655183632 1D-49
971	-0.92351963412452105 7D-50	-0.92102888726828689 2D-50
972	-0.83610231145396269 0D-50	-0.83381790459795623 9D-50
973	-0.75696275078379448 7D-50	-0.75486769216307048 0D-50
974	-0.68531680768464796 1D-50	-0.68339549560473567 2D-50
975	-0.62045464828647506 2D-50	-0.61869275822835844 8D-50
976	-0.56173370429444067 8D-50	-0.56011808511428505 3D-50
977	-0.50857229617674395 4D-50	-0.50709087467435185 1D-50
978	-0.46044386112588291 2D-50	-0.45908555431322145 5D-50
979	-0.41687172841292623 7D-50	-0.41562636286694989 3D-50
980	-0.37742439020089703 0D-50	-0.37628262793363781 0D-50
981	-0.34171122081270389 5D-50	-0.34066449113653462 7D-50
982	-0.30937860191031164 1D-50	-0.30841903881770133 3D-50
983	-0.28010641507949375 0D-50	-0.27922679969473940 5D-50
984	-0.25360486696879191 0D-50	-0.25279857466437991 6D-50
985	-0.22961161543864035 1D-50	-0.22887256724129494 8D-50
986	-0.20788916816994971 7D-50	-0.20721178611128061 4D-50
987	-0.18822252789061041 4D-50	-0.18760169398477449 1D-50
988	-0.17041706083035836 9D-50	-0.16984807938648451 9D-50
989	-0.15429656723367213 2D-50	-0.15377513023413261 5D-50
990	-0.13970153476894353 8D-50	-0.13922369006604569 6D-50
991	-0.12648755749008903 5D-50	-0.12604967959355178 1D-50
992	-0.11452390465214896 1D-50	-0.11412266789795206 2D-50
993	-0.10369222517164138 4D-50	-0.10332457907961478 9D-50
994	-0.93885374870323096 5D-51	-0.93548521513291576 6D-51

995	-0.85006354860981824 8D-51	-0.84697728082501493 8D-51
996	-0.76967350538085207 9D-51	-0.76684596868899290 2D-51
997	-0.69688861635534191 8D-51	-0.69429822770924686 5D-51
998	-0.63098914718358338 1D-51	-0.62861611429659889 7D-51
999	-0.57132350293950249 0D-51	-0.56914967657698207 0D-51
1000	-0.51730177469513223 3D-51	-0.51531051307089270 5D-51

We applied Neville-Richardson Extrapolation to the ratios r_n of the PYC5TGC68 and PYS5TGC68 coefficients in table 4.8 and performed linear least squares fits to the resulting series as was described in section 4.1. The r_n agreed with Baker's to 5 decimal digits, the s_n to 4 decimal digits and the t_n to 3-4 decimal digits for all n up to $n \sim 400$. A simple calculation can be done to estimate the precision of the Neville-Richardson extrapolations. For example, at 100th order we know the PYC5TGC68 E_n are accurate to 8 decimal digits from the comparison with the stability check PYS5TGC68 coefficients. This means

$$r_{100} = \frac{E_{101}}{E_{100}} = \frac{-0.350594231 \times 10^{-10}}{-0.397753186 \times 10^{-10}} = 0.8814366\underline{3}8 \tag{4.26}$$

where the underline denotes the last significant digit of a number. So the r_n are accurate to 8 decimal digits at 100th order. Now the s_n and t_n are calculated

$$\begin{aligned} s_{100} &= (101)r_{101} - (100)r_{100} \\ &= 101 \times 0.8816684\underline{7}6 - 100 \times 0.8814366\underline{3}8 \\ &= 89.0485\underline{1}6076 - 88.1436\underline{3}6800 \\ &= 0.90485\underline{2}2276 \end{aligned}$$

$$\begin{aligned} t_{100} &= 2[(100 + \frac{1}{2})r_{101} - (100)r_{100}] \\ &= 2[100.5 \times 0.8816684\underline{7}6 - 100 \times 0.8814366\underline{3}8] \\ &= 2[88.6076\underline{1}838 - 88.1436\underline{3}6800] \\ &= 0.92803\underline{6}0076 \end{aligned}$$

Lastly the v_n are calculated

$$\begin{aligned} v_{100} &= (102)t_{101} - (101)t_{100} \\ &= 102 \times 0.927872\underline{6} - (101) \times 0.928036\underline{1} \\ &= 94.643\underline{0}052 - 93.731\underline{6}461 \\ &= 0.911\underline{3}591 \end{aligned} \tag{4.27}$$

Table 4.9: Accuracy of the series coefficients

Order	E_n	r_n	s_n	t_n	v_n
100	8	8	6	6	4
200	8	8	6	6	3
300	7	7	5	5	2
400	7	7	4	4	1
600	6	6	2	2	0
800	4	4	1	1	0
1000	1	1	0	0	0

So the 100th order E_n are accurate to 8 decimal digits, the r_n to 8 decimal digits, the s_n and t_n to 6 decimal digits and the v_n to 4 decimal digits. Table 4.9 shows the estimated accuracy of the coefficients of each of these series for a range of different orders.

Figures 4.1 - 4.13 are plots of the coefficients of the various Neville-Richardson extrapolations and their least squares fits. Each of the series began at 100th order because only the asymptotic behaviour of the $1/Z$ expansion was of interest in this work. Multiple different ranges of coefficients (e.g. $n = 100$ to $n = 400$) were analyzed for each series in order to estimate the uncertainty in the resulting λ^*. In order to have λ^* accurate to 4 decimal digits, the coefficients in the series must be accurate to about 4 decimal digits and so naturally the coefficient ranges $n = 100$ to 300, $n = 100$ to 400 and $n = 100$ to 500 were analyzed for the s_n and t_n series. Figures 4.1, 4.3, 4.7 and 4.11 display all of the coefficients in the series r_n s_n t_n respectively which contain at least 1 significant figure. The values of the parameters used in the fits are displayed below each of the figures and the radius of convergence of the $1/Z$ expansion is estimated by $\lambda^* = 1/a$. Only every 10th series coefficient was plotted in order to allow the fit lines to be clearly visible. All of the uncertainties recorded below are only from the least squares fitting procedure. The largest source of error comes from the assumption that the true asymptotic behaviour of each of the series is

fully revealed within the range of terms that were analyzed and thus that the fit lines can be trusted as $n \to \infty$. There is no estimate to this error and so the uncertainties displayed below serve only as a testament to how well the fit lines agree with the data.

Figure 4.1: Least squares fit to the ratios from $n = 100$ to 999

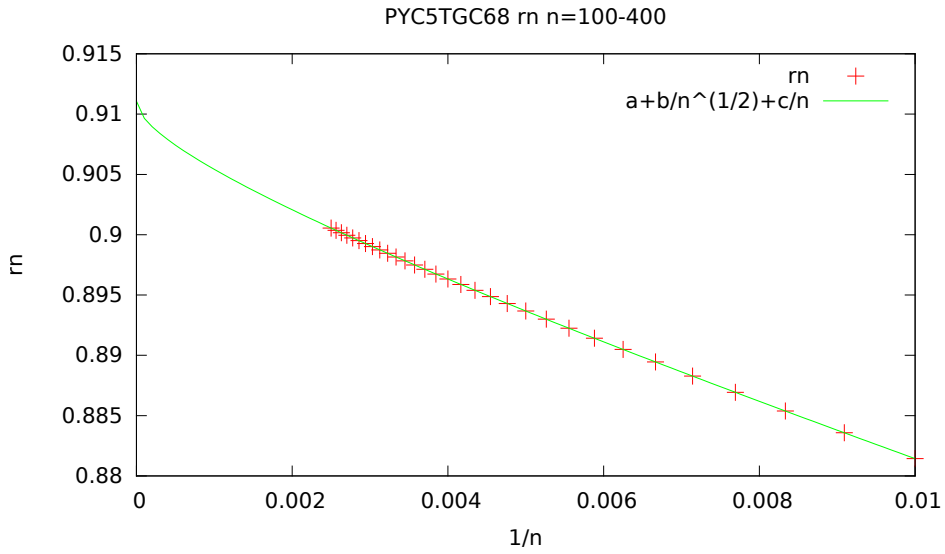

The key in the top right corner of the graph shows the fit function that was used to fit the coefficients. For this graph and those that follow, the intersection of the fit line and the y-axis yields an estimate to $Z^* = \dfrac{1}{\lambda^*}$.

$$a = 0.911\,213 \pm 2 \times 10^{-6} \implies \lambda^* = 1.097\,438 \pm 2 \times 10^{-6}$$

$$b = -0.128\,62 \pm 6 \times 10^{-5}$$

$$c = -1.6898 \pm 0.0005$$

Figure 4.2: Least squares fit to the ratios from $n = 100$ to 400

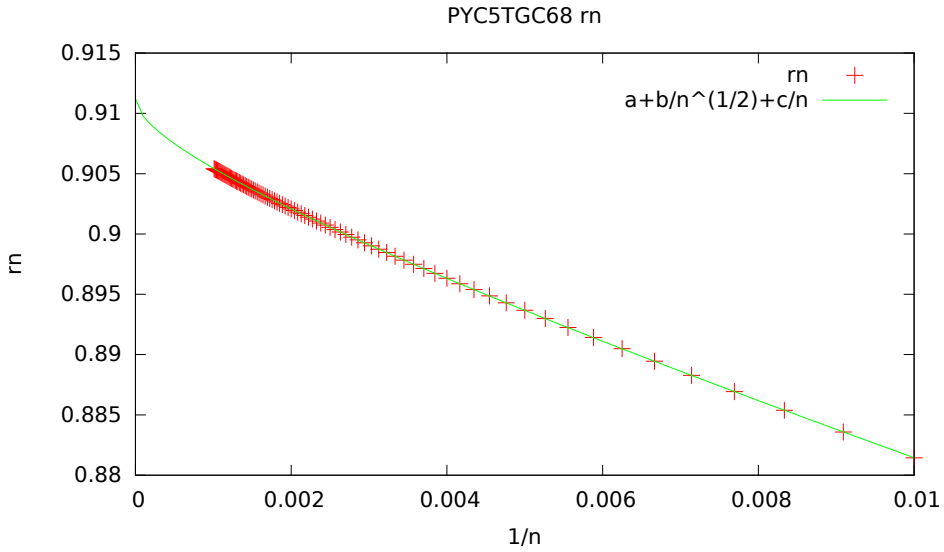

$$a = 0.911\,076 \pm 1 \times 10^{-6} \implies \lambda^* = 1.097\,603 \pm 1 \times 10^{-6}$$

$$b = -0.124\,56 \pm 3 \times 10^{-5}$$

$$c = -1.7183 \pm 0.0002$$

Figure 4.3: Least squares fit to the s_n from $n = 100$ to 800

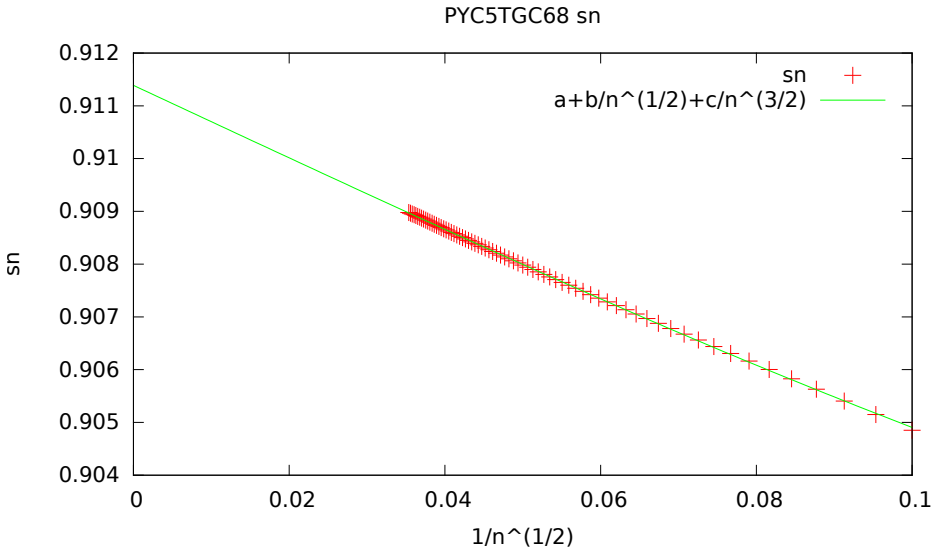

$$a = 0.911\,389 \pm 4 \times 10^{-6} \implies \lambda^* = 1.097\,226 \pm 5 \times 10^{-6}$$

$$b = -0.068\,90 \pm 0.0001$$

$$c = 0.407 \pm 0.008$$

Figure 4.4: Least squares fit to the s_n from $n = 100$ to 300

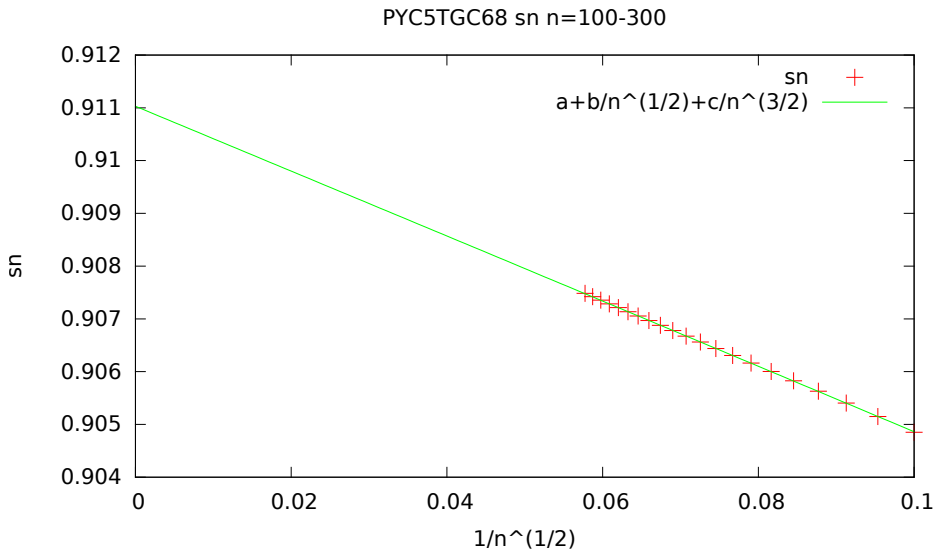

$$a = 0.911\,030 \pm 6 \times 10^{-6} \implies \lambda^* = 1.097\,659 \pm 7 \times 10^{-6}$$

$$b = -0.0614 \pm 0.0001$$

$$c = -0.024 \pm 0.007$$

Figure 4.5: Least squares fit to the s_n from $n = 100$ to 400

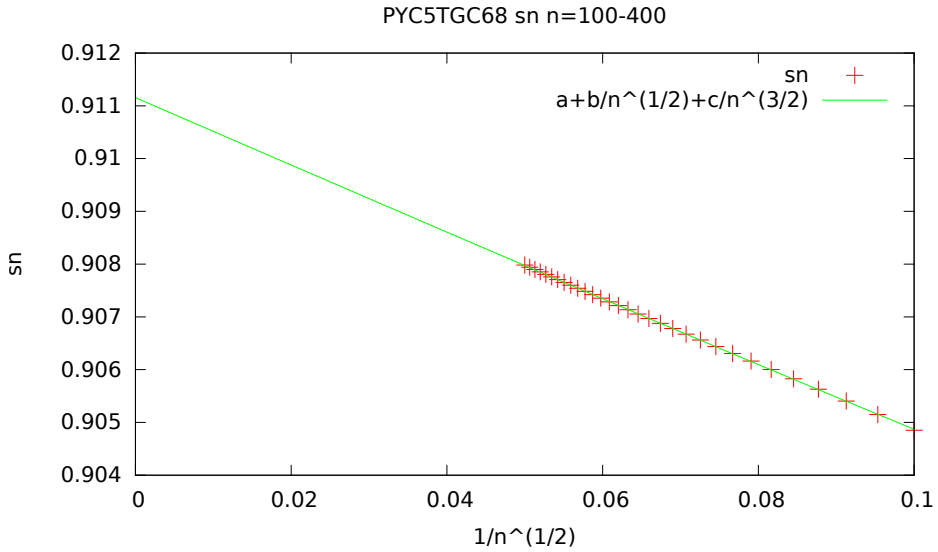

$$a = 0.911\,156 \pm 6 \times 10^{-6} \implies \lambda^* = 1.097\,506 \pm 7 \times 10^{-6}$$

$$b = -0.0638 \pm 0.0001$$

$$c = 0.104 \pm 0.007$$

Figure 4.6: Least squares fit to the s_n from $n = 100$ to 500

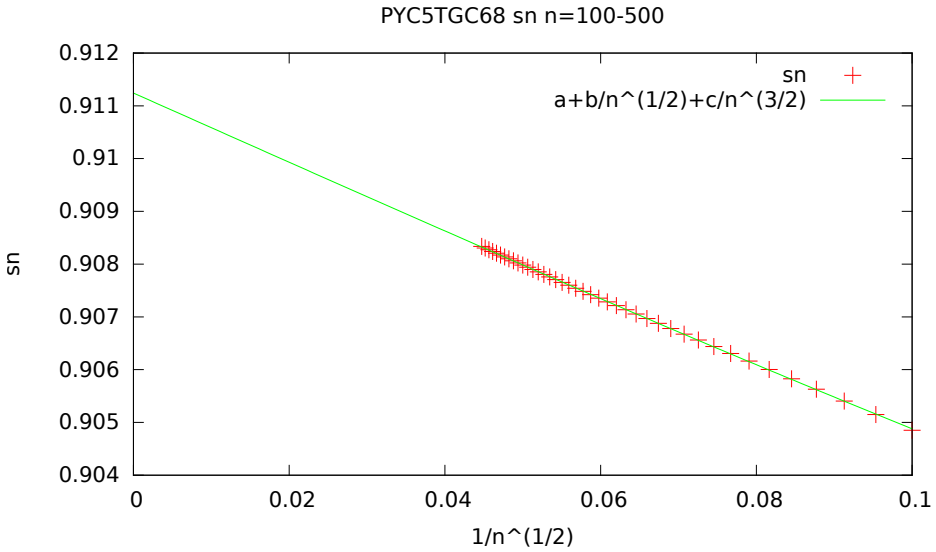

$$a = 0.911\,243 \pm 5 \times 10^{-6} \implies \lambda^* = 1.097\,402 \pm 6 \times 10^{-6}$$

$$b = -0.0657 \pm 0.0001$$

$$c = 0.205 \pm 0.008$$

Figure 4.7: Least squares fit to the t_n from $n = 100$ to 800

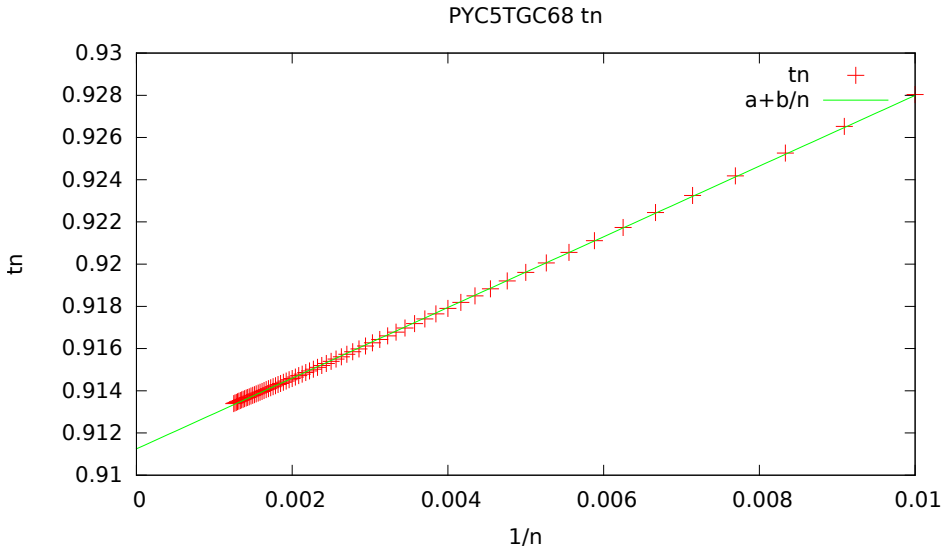

$$a = 0.911\,248 \pm 3 \times 10^{-6} \implies \lambda^* = 1.097\,396 \pm 4 \times 10^{-6}$$

$$b = 1.6746 \pm 0.0007$$

Figure 4.8: Least squares fit to the t_n from $n = 100$ to 300

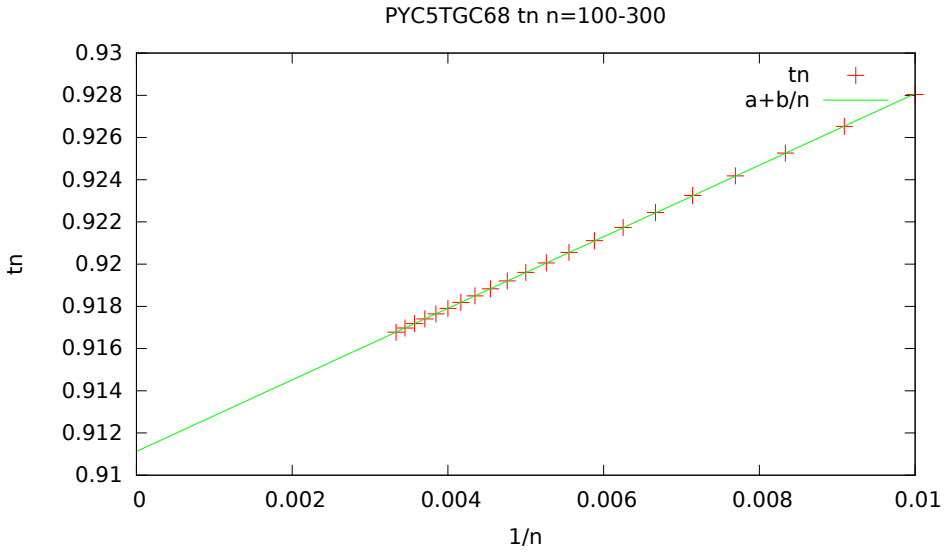

$$a = 0.911\,130 \pm 2 \times 10^{-6} \implies \lambda^* = 1.097\,538 \pm 2 \times 10^{-6}$$

$$b = 1.6951 \pm 0.0004$$

Figure 4.9: Least squares fit to the t_n from $n = 100$ to 400

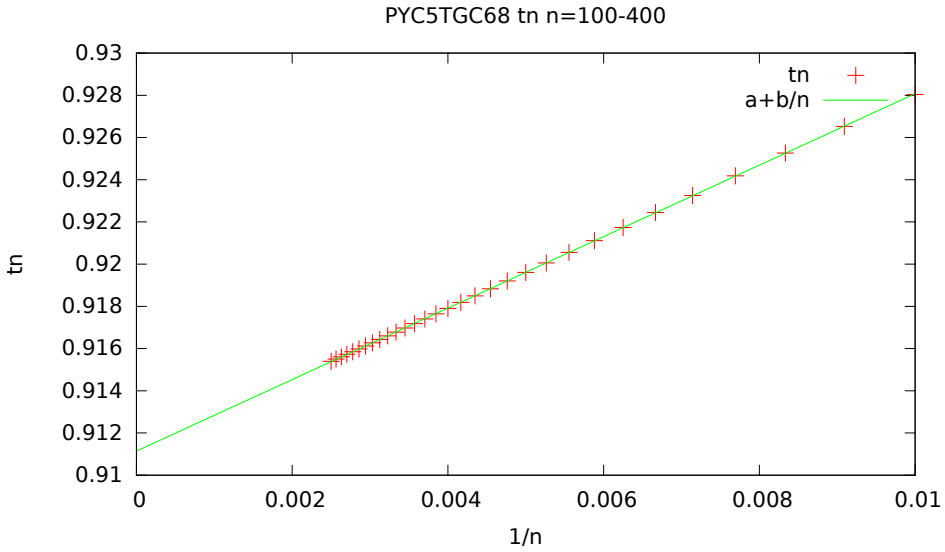

$$a = 0.911\,143 \pm 2 \times 10^{-6} \implies \lambda^* = 1.097\,522 \pm 2 \times 10^{-6}$$

$$b = 1.6932 \pm 0.0003$$

Figure 4.10: Least squares fit to the t_n from $n = 100$ to 500

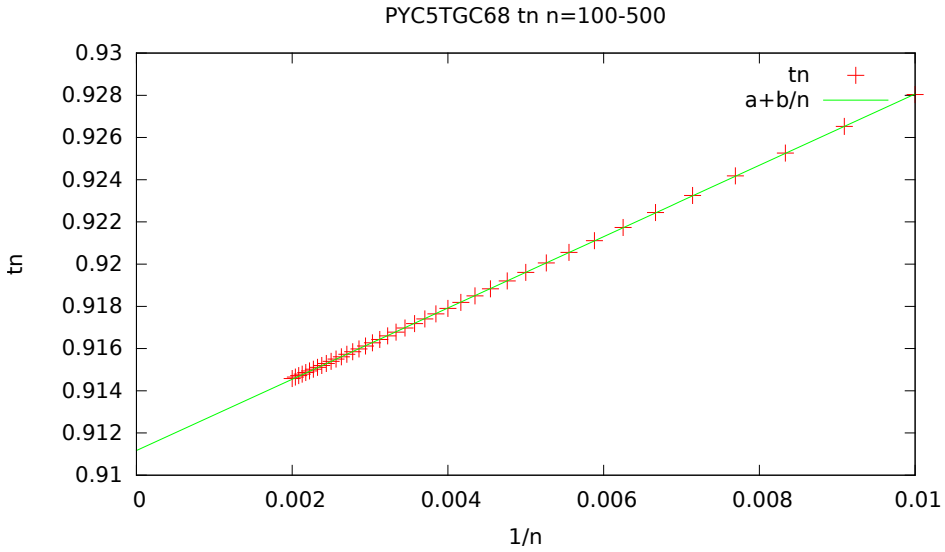

$$a = 0.911\,169 \pm 2 \times 10^{-6} \implies \lambda^* = 1.097\,491 \pm 2 \times 10^{-6}$$

$$b = 1.6889 \pm 0.0004$$

Figure 4.11: Least squares fit to the v_n from $n = 100$ to 400

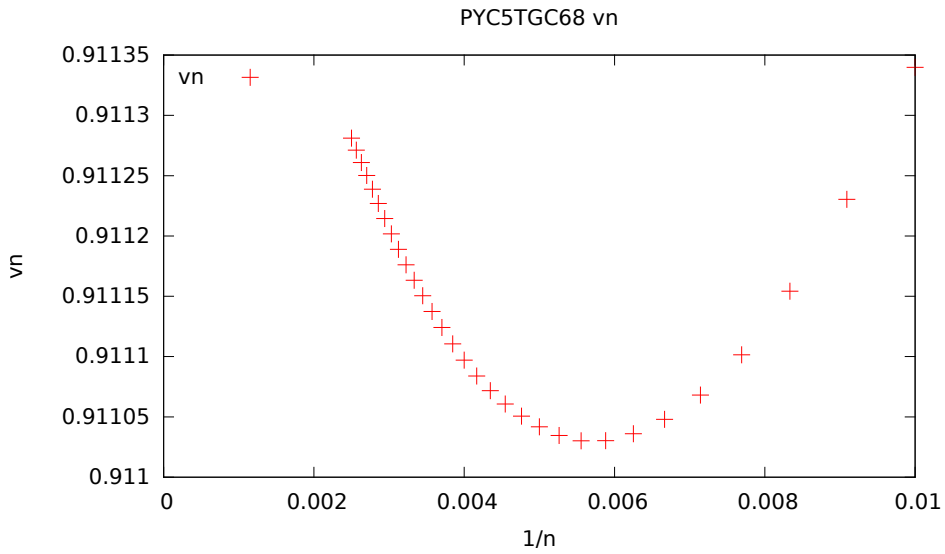

The fits for this range of coefficients were not consistent and so there is no fit line plotted in the above image. The fits tended to be more unreliable for the v_n series because it has many less significant figures and spans a much smaller range of values than the s_n and t_n series.

Figure 4.12: Least squares fit to the v_n from $n = 100$ to 150

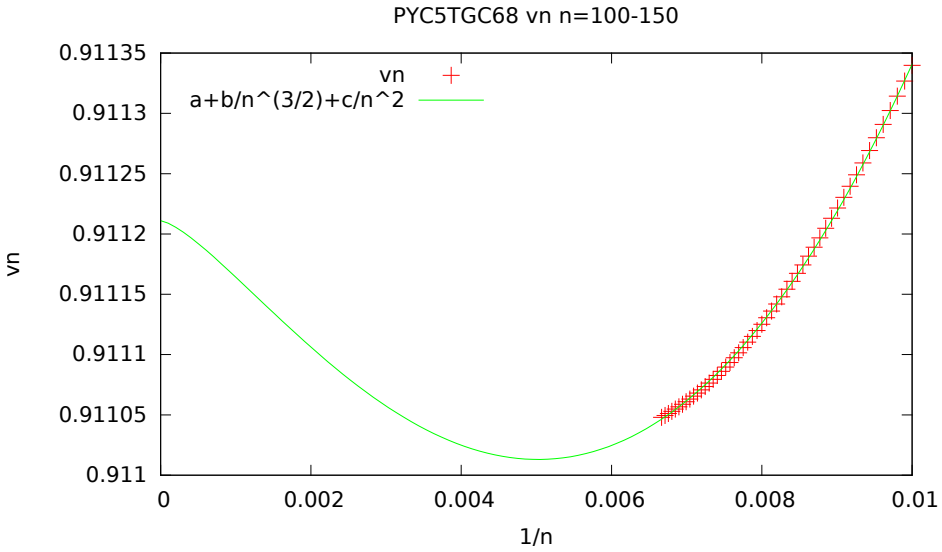

$$a = 0.911\,21 \pm 3 \times 10^{-5} \implies \lambda^* = 1.097\,44 \pm 3 \times 10^{-5}$$

$$b = -2.2 \pm 0.2$$

$$c = 23 \pm 1$$

Figure 4.13: The v_n from $n = 100$ to 200

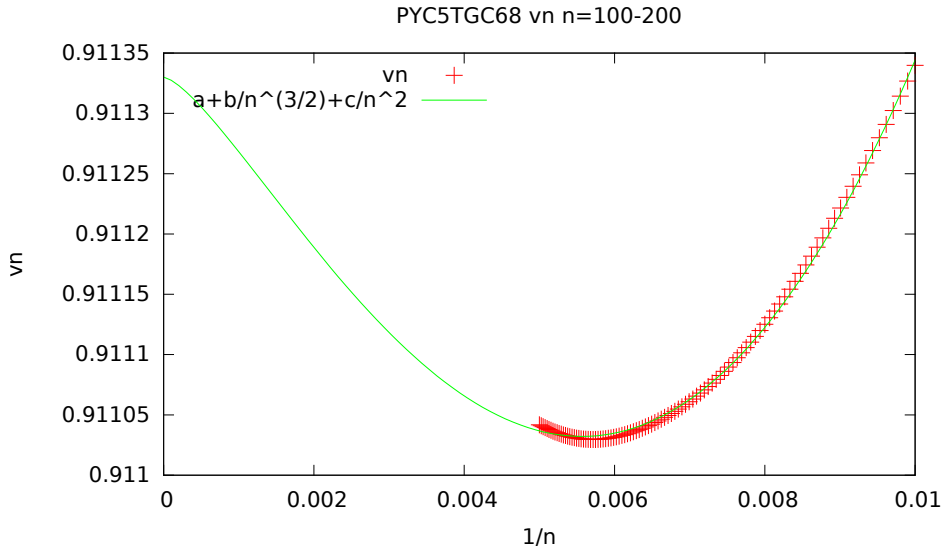

$$a = 0.911\,33 \pm 2 \times 10^{-5} \implies \lambda^* = 1.097\,30 \pm 2 \times 10^{-5}$$

$$b = -2.9 \pm 0.1$$

$$c = 29 \pm 1$$

It is interesting to compare the values of fit parameter b for the above r_n and s_n plots to the value of b found by Baker *et al.* in reference [1]. Their estimated value is $b = -0.124$ and they state that the true value of b might be exactly $-\frac{1}{8}$ but the accuracy of their fits did not allow them to say for certain if this was the case. The fit of r_n from $n = 100$ to 400 in figure 4.2 resulted in $b = -0.124\,56 \pm 3 \times 10^{-5}$ which on its own would seem to be conclusive evidence that $b \neq -\frac{1}{8}$. However, using different ranges of n in the fitting procedure resulted in many estimates for b which all varied from each other by an appreciable amount.

Although each of the best fit lines fit the respective data sets very well, the values for the fitting parameters had significant differences. For instance, the

value for b in the range $n = 100$ to 999 from figure 4.1 is $b = -0.128\,62 \pm 6 \times 10^{-5}$. This is close to the value $b = -0.124\,56 \pm 3 \times 10^{-5}$ from r_n in the range $n = 100$ to 400 yet these two values are in disagreement. It does make sense that this value for b could differ from the b found using $n = 100$ to 400 because the r_n series dropped in significant figures from 7 at $n = 400$ to roughly 1 at $n = 999$ so the tail end of this series was not very accurate (meaning that even a very good fit to this series may be completely incorrect in predicting what the true values of the series coefficients should be and therefore is untrustworthy). The value of b obtained in the s_n series should be exactly double the value of b in the r_n series. This results in the following estimates for b

$$n = 100 - 300 : \; b = -0.1314 \pm 0.0002$$
$$n = 100 - 400 : \; b = -0.1228 \pm 0.0002$$
$$n = 100 - 500 : \; b = -0.1276 \pm 0.0002$$

Clearly we still cannot say that b is exactly equal to $-\frac{1}{8}$, however we learned something important from this analysis. We can conclude that the largest error in the fitting parameters comes not from the least squares fitting procedure, but in choosing the range of series coefficients to fit, and that this quirk is due to the fact that even at 500th order the behaviour of the E_n is still changing very gradually.

All of the independent estimates of λ^* from each of the above fits suggest that

$$\lambda^\star = 1.0975(2) \tag{4.28}$$

Thus we find that our results agree with those of references [1] and [19]. Recall from reference [23] that $\lambda_c = \dfrac{1}{Z_c} = 1.097\,66$ and so $\lambda^\star = \lambda_c$ agree to all 4 decimal digits within the estimated uncertainty. Thus this work concludes that λ^* and λ_c are equivalent. This means that as Z is continuously reduced, the ground state of the two-electron atom is no longer a bound state when $Z < Z^* = Z_c$. Therefore

the ground state cannot exist as a bound state embedded in the continuum for $Z < Z_c$. However, it is still possible that the ground state becomes a resonant state at $Z = Z_c$ as the work of Drake *et al.* in reference [23] strongly suggests.

4.3 Interesting Findings

This section explains some results that are not directly relevant to determining the radius of convergence of the $1/Z$ expansion, but are still intriguing or useful to know.

4.3.1 Diagonalization Scheme Comparison

In calculating the eigenvalues and eigenvectors with the variational method, the Hamiltonian was diagonalized using two different techniques – the Jacobi method (Appendix C.1) and the Tridiagonalization method (Appendix C.2). The Jacobi method takes $O(n^4)$ operations to complete while the tridiagonalization method takes $O(n^3)$ operations with n being the dimension of the Hamiltonian matrix. The computation times of each of these methods for different matrix dimensions are compared in figure 4.14

Dall2016.f used the Jacobi method and dtridlz2016.f used the tridiagonalization method. Both programs needed to perform two separate diagonalizations among many other necessary calculations. The diagonalization procedures take the majority of the runtime for larger basis sets and can safely be assumed to take the full time for $n > 500$. The tridiagonalization method was found to have the same numerical stability as the Jacobi method, but take much less time for large n. The tridiagonalization method should always be implemented for computations involving matrix diagonalization with large matrices.

4.3.2 Oscillating Coefficients

As was explained in reference [1] the coefficients of a perturbation expansion can exhibit oscillatory behaviour even when no such behaviour should be present.

Figure 4.14: Runtime for dall2016.f and dtridlz2016.f

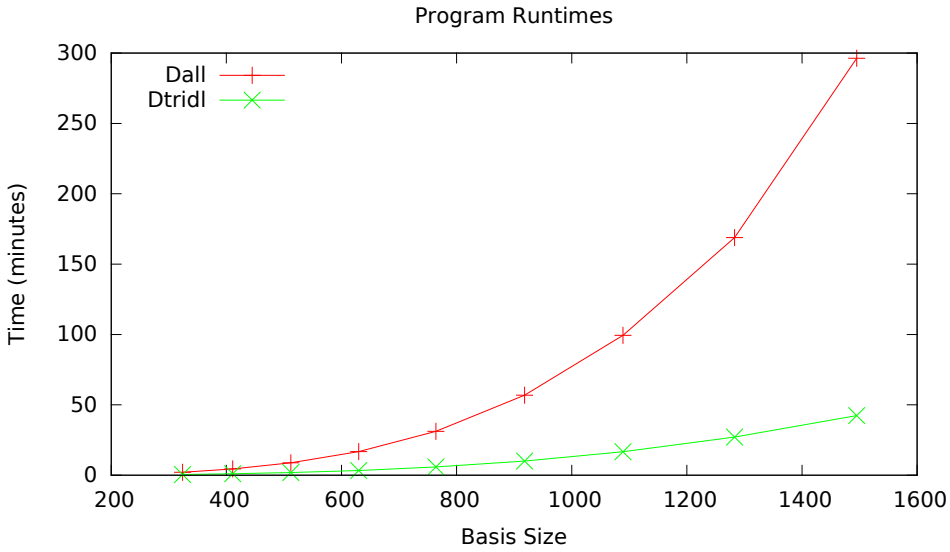

This is a result of using a finite size basis set in the perturbation theory procedure to calculate the E_n. Baker *et al.* showed that a Hamiltonian matrix with a perturbation, when expanded in a basis set of size two

$$\begin{pmatrix} a_{11} & 0 \\ 0 & a_{22} \end{pmatrix} + \lambda \begin{pmatrix} b_{11} & b_{12} \\ b_{21} & b_{22} \end{pmatrix} \tag{4.29}$$

have eigenvalues $E_\pm$ with perturbation expansion coefficients that behave like

$$E_\pm^n = \pm\lambda_0^{-n}\left[(\frac{2}{\pi n}\sin\theta)^{1/2}\frac{\sin((n-\frac{1}{2})\theta-\frac{\pi}{4})}{n-\frac{1}{2}} + O(n^{-5/2})\right] \tag{4.30}$$

for large n where n is the order of the perturbation expansion and λ_0 and θ are the modulus and argument of the complex conjugate pair of values $\lambda = \lambda_0 e^{i\theta}, \lambda^* = \lambda_0 e^{-i\theta}$ for which $E_+ = E_-$ (a singularity occurs at these two points in the λ plane). From this equation it is seen that the perturbation expansion coefficients for E_+ and E_- oscillate with constant period $2\pi/\theta$. Of course for basis sizes larger than two the asymptotic behaviour of the eigenvalues of the

Hamiltonian matrix may differ from that of equation (4.30). The purpose of equation (4.30) is simply to show that oscillations in perturbation expansion coefficients naturally occur as a result of using finite size basis sets to diagonalize a Hamiltonian matrix.

The $1/Z$ expansion coefficients were found to oscillate with increasing period as $n \to \infty$. The following figures are plots of the absolute value of the differences between the $1/Z$ expansion coefficients E_n that were calculated using three different sizes of basis sets. Baker *et al.* used a 450 term basis set while PYC5TG974 and PYC5TGC68 from this work used 974 and 1268 terms respectively.

Figure 4.15: PYC5TG974 vs. PYC5TGC68

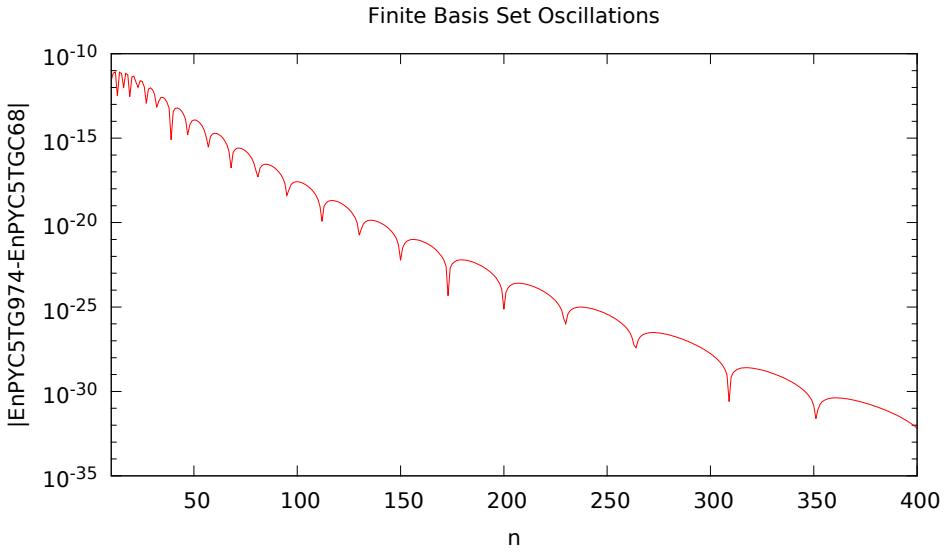

A graph of the absolute value of the differences between the $1/Z$ expansion coefficients calculated using the PYC5TG974 basis set and those of the PYC5TGC68 basis set. In order to make the oscillatory behaviour more clear, a smooth line was used to plot this data instead of a series of data points.

Figure 4.16: Baker vs. PYC5TG974

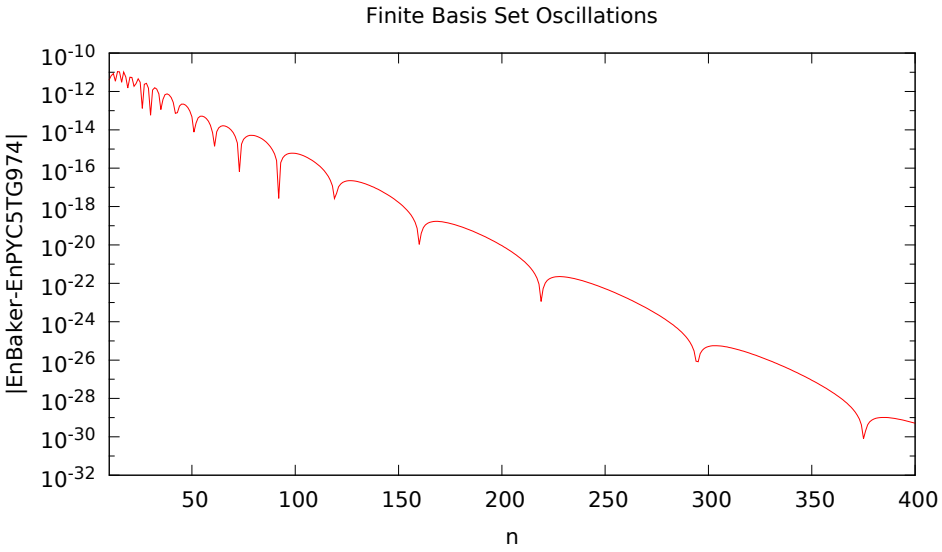

Figure 4.17: Baker vs. PYC5TGC68

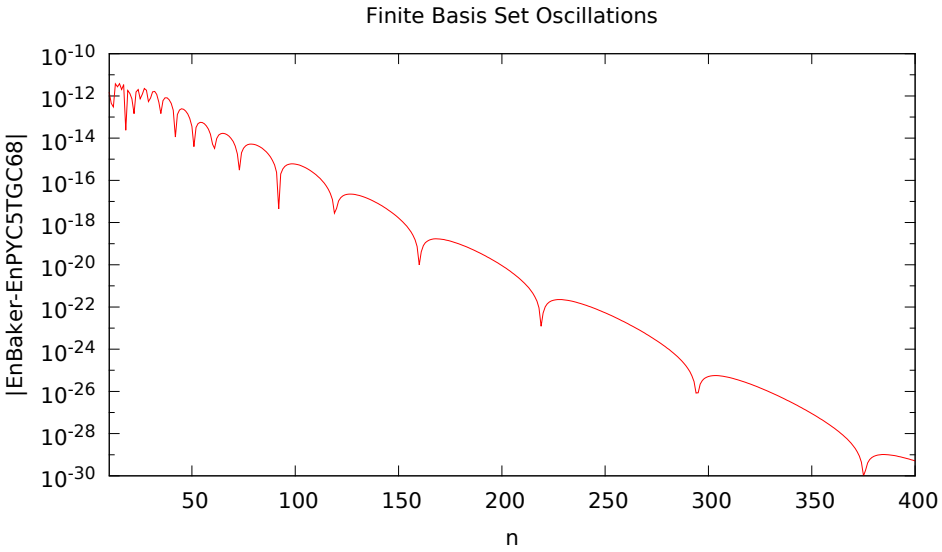

It can be clearly seen from these graphs that all of the calculated coefficients exhibit oscillatory behaviour. Although the amplitude of the oscillations has a very similar dependence on n regardless of the basis set being used, the period of the oscillations differ. Most notably, we can conclude from these graphs that the oscillations in the coefficients of Baker et al. had much longer periods than the larger pyramidal basis sets. The oscillations are most likely a result of the finite basis size, and so it seems that by increasing the number of terms in the basis set the gradual increase in the period of oscillations in the coefficients is decreased. Thus, if these oscillations are not identifiable at higher orders then it may be an indication that either the perturbation coefficients need to be calculated with higher precision (coefficients with errors larger than the amplitude of oscillations would mask the underlying oscillatory behaviour) or the size of the variational basis sets must be increased (as we have seen from the graphs, increasing the basis size decreases period of coefficient oscillations).

4.3.3 Decay of Coefficients

When a basis set did not include the correct long range behaviour to describe the higher order terms, there would be a point in the sequence of E_n after which these coefficients would begin to rapidly decrease in magnitude. This can be clearly seen in the E_n that were calculated using the He basis sets.

At 200th order, the He E_n are 2 orders of magnitude smaller than the PYC5TGC68 E_n and at 400th order they are 6 orders of magnitude smaller. This separation continues to increase rapidly as n is increased.

A similar phenomenon can be seen from comparing the E_n calculated from different basis set sizes. A larger basis set will allow for higher order terms in the $1/Z$ expansion to be found more accurately than those calculated with a smaller basis set. Increasing basis size does not have as large an effect on the E_n as changing the nonlinear parameters within the basis set. The differences in the various E_n are small, but can be seen clearly by plotting the respective accelerated series s_n for the different basis sizes together as was done in figure

Figure 4.18: Helium E_n rapid decrease

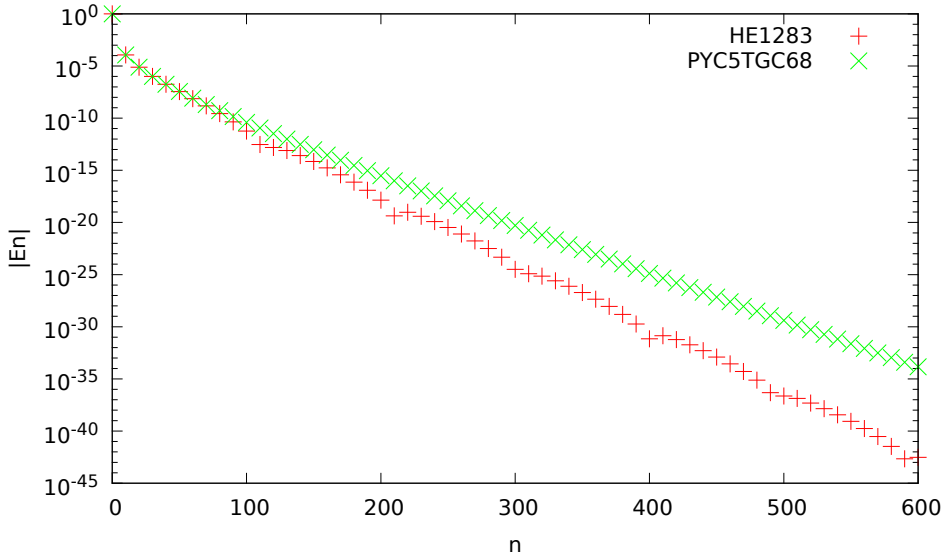

4.19.

Figure 4.19: s_n decay for different H^- triple basis set sizes

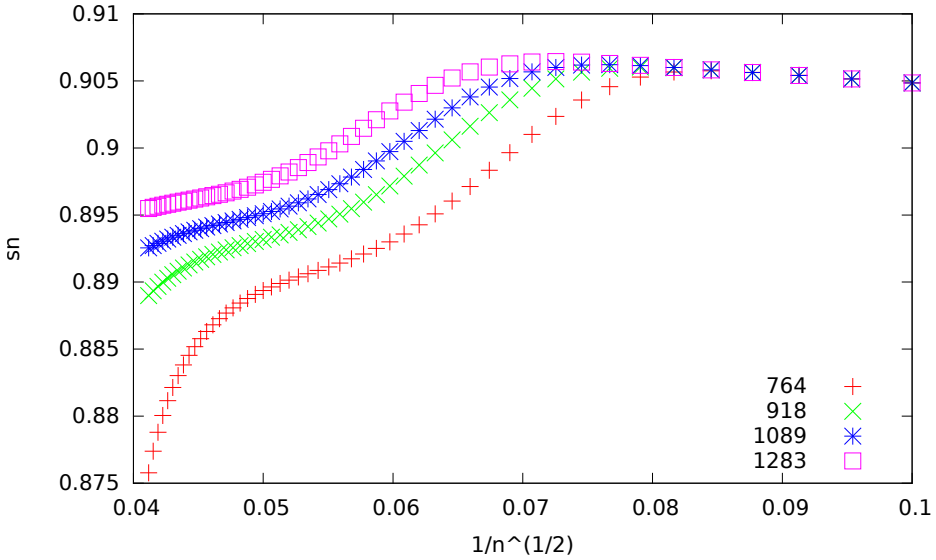

Chapter 5

Conclusion

The $1/Z$ expansion coefficients of Baker *et al.* in reference [1] were shown to be accurate to 5 decimal digits even at high orders as they had originally claimed. This proves that Turbiner and Guevara's assertion that these E_n contain no significant figures once $n \geq 135$ (from reference [21]), is incorrect. The pyramidal basis sets employed in this work successfully found more accurate E_n that still contained a single significant figure even at 1000th order. Using these coefficients the radius of convergence was found $\lambda^* = 1.0975(2)$ in agreement with references ([1, 19, 22]). Table 5.1 lists the previous determinations of λ^* up to and including this work. Some of the errors in various λ^* have been adjusted from what the original authors claimed due to the knowledge obtained in this work, of the accuracy of the coefficients in reference [1] which were used in many other works. The estimate of λ^* from Baker *et al.* in reference [1] was not included in table 5.1 because it was not calculated but instead came directly from their assumption that $\lambda^* = \lambda_c$ (this assumption was still uncertain at the time). The result of Zamastil *et al.* disagrees with this work because they analyzed only the first 20 coefficients of the $1/Z$ expansion whereas this work analyzed the coefficients from 100th order up to 1000th order. While it is true that the first 20 coefficients are more accurate than the higher order coefficients, the $1/Z$ expansion is a very slowly converging series and so the first 20 coefficients do

Table 5.1: Important estimates of the radius of convergence of the $1/Z$ expansion

year	reference	λ^*
1962	Knight and Scherr [5]	1.33
1966	Stillinger [8]	1.1184
1970	Brändas and Goscinski [12]	1.118
1972	Brändas and Goscinski [13]	1.119
1986	Arteca *et al.* [18]	1.1056(40)
1995*	Ivanov [19]	1.0976(1)
2010*	Zamastil *et al.* [20]	1.1085(2)
2015*	Karr [22]	1.0973(1)
2017	This work	1.0975(2)

The * indicates works that used the $1/Z$ expansion coefficients from reference [1] and thus needed to have their error's readjusted. Only the order of magnitude of the errors is known in these cases (and so the real errors are most likely larger than 1×10^{-4}).

not capture the proper asymptotic behaviour of the series. Any analysis on just the first 20 coefficients is bound to yield inaccurate estimates of λ^*.

The critical nuclear charge Z_c has recently been calculated to very high precision $Z_c = 0.911\,028\,224\,077\,255\,73(4)$ by Drake *et al.* in reference [23] corresponding to $\dfrac{1}{Z_c} = 1.097\,660\,833\,738\,559\,80(5)$. The main result is that $\lambda^* = \dfrac{1}{Z_c}$ for up to 4 decimal digits and within the estimated uncertainty and thus it is concluded that the ground state cannot become a bound state embedded in the continuum as Z is reduced below $Z^* = Z_c*$.

Chapter 6

Future Work

The Hamiltonian used in this work was the nonrelativistic, infinite nuclear mass Z-scaled two-electron atom Hamiltonian. In reference [33] the critical nuclear charge in the finite nuclear mass case was found for a range of different values of reduced mass. It would be interesting to investigate whether the radius of convergence of the $1/Z$ expansion of the ground state energy for the finite mass Hamiltonian is equivalent to $\frac{1}{Z_c}$ for these different values of reduced mass.

There has not been much research into the three-electron atom critical values (Z_c and λ^*) due to both the complexity of this problem and the greater interest in the two-electron atom critical values. λ^* has been found to appreciable accuracy for two-electron atoms and so the next logical step is to analyze three-electron atoms to see if the result $\lambda^* = \frac{1}{Z_c}$ still holds (Z_c in this case would be the charge at which the three-electron atom ground state would have the same energy as the two-electron atom ground state).

Lastly, a more precise determination of λ^* could be attempted by either trying different basis sets, increasing the size of the existing basis sets, or by using a different series acceleration technique. The E_n were determined with high accuracy in this thesis and so it is likely the best of these options would be to use a different series acceleration technique such as those applied in reference [19].

Appendices

A Linear Variational Method

We start off assuming that the trial wave function, ψ_{tr} depends only linearly on a known, complete set of basis functions, χ_i

$$|\psi_{tr}\rangle = \sum_{i=0}^{N} c_i |\chi_i\rangle \tag{6.1}$$

We will inspect the more general case that the complete set of basis functions is not orthonormal. The expectation value of the energy of ψ_{tr} is

$$\tilde{E}_{tr} = \frac{\langle\psi_{tr}|H|\psi_{tr}\rangle}{\langle\psi_{tr}|\psi_{tr}\rangle} = \frac{\sum_{i,j=0}^{N} c_i^* c_j H_{ij}}{\sum_{i,j=0}^{N} c_i^* c_j O_{ij}} = \frac{f}{g} \tag{6.2}$$

where H_{ij} and O_{ij} are the matrix elements of $\mathbf{H}$ and $\mathbf{O}$ in the χ basis, *i.e.* $H_{ij} = \langle\chi_i|H|\chi_j\rangle$ and $O_{ij} = \langle\chi_i|\chi_j\rangle$.

Now, we want to minimize (6.2) with respect to the linear variational parameters, c_i^* (minimizing with respect to the c_i's independently yields the same final result, so we are free to chose either the c_i^*'s or c_i's)

$$\begin{aligned}\frac{\partial \tilde{E}_{tr}}{\partial c_k^*} &= \frac{\partial}{\partial c_k^*}\frac{f}{g} \\ &= \frac{\dfrac{\partial f}{\partial c_k^*}g - \dfrac{\partial g}{\partial c_k^*}f}{g^2} = 0\end{aligned}$$

$g = \langle\psi_{tr}|\psi_{tr}\rangle$ is nonzero so we can multiply both sides by g

$$\frac{\partial \tilde{E}_{tr}}{\partial c_k^*} = \frac{\dfrac{\partial f}{\partial c_k^*} g - \dfrac{\partial g}{\partial c_k^*} f}{g}$$

$$= \frac{\partial f}{\partial c_k^*} - \frac{\partial g}{\partial c_k^*} \tilde{E}_{tr} \tag{6.3}$$

$$= \sum_{j=0}^{N} c_j H_{kj} - \tilde{E}_{tr} \sum_{j=0}^{N} c_j O_{kj} \tag{6.4}$$

$$= \sum_{j=0}^{N} c_j (H_{kj} - \tilde{E}_{tr} O_{kj}) = 0 \tag{6.5}$$

In order to transition from (6.3) to (6.4) we used the fact that the c_i's are independent of each other and thus, $\dfrac{\partial c_i^*}{\partial c_k^*} = \delta_{ik}$. Equation (6.5) is what results after requiring that the energy be minimized with respect to only the k'th coefficient c_k^*. Requiring a full optimization over all linear parameters produces equation (6.5) for all k, which is equivalent to solving the following familiar matrix equation

$$\mathbf{H}|\psi_{tr}\rangle = \tilde{E}_{tr}\mathbf{O}|\psi_{tr}\rangle \tag{6.6}$$

Equation 6.6 is called the generalized eigenvalue problem. This is a more general Schrödinger equation which is used when the chosen basis set is not orthogonal. If $\mathbf{O} = \mathbf{I}$ then we are working in an orthonormal basis set. In this case (6.6) reduces to the regular Schrödinger equation. The energy, $\tilde{E}_{tr}$, are found by looking for nontrivial solutions to this equation ($|\psi_{tr}\rangle$ is nonzero) which is done by solving

$$|\mathbf{H} - \tilde{E}_{tr}\mathbf{O}| = 0 \tag{6.7}$$

Solving the above equation is equivalent to finding the orthonormal basis in which $\mathbf{H}$ is diagonal. The eigenvectors of a Hamiltonian matrix which correspond to different eigenvalues are always orthogonal (this is a property of Hermitian matrices in general). The orthonormal basis which solves 6.7 is simply the basis of normalized eigenvectors of $\mathbf{H}$. Recall that we arrived at this

equation by trying to find the optimal linear parameters which minimized the variational energy for a general trial wave function. Therefore we have shown that applying the variational method to a trial wave function that only depends on linear parameters is equivalent to diagonalizing the Hamiltonian matrix.

B Hylleraas Undheim Macdonald Theorem

The goal of this section is to help the reader understand what the HUM theorem is and what it implies. We begin by proving that the N old eigenvalues of a Hermitian matrix $\mathbf{H}$ fall between the $N+1$ new eigenvalues. Let's assume $\mathbf{H}^{(n)}$ is a Hamiltonian matrix of dimension n which is in diagonal form with eigenvalues ordered from smallest to largest, $E_1 < E_2 < \dots E_n$.

$$\mathbf{H}^{(n)} = \begin{pmatrix} E_1 & 0 & \dots & 0 \\ 0 & E_2 & \dots & 0 \\ \vdots & \vdots & \ddots & \vdots \\ 0 & 0 & \dots & E_n \end{pmatrix} \tag{6.8}$$

Now we add a row and column onto $\mathbf{H}^{(n)}$ (which is the same as increasing the size of the basis in which we are describing $\mathbf{H}$ by one). Recalling that the Hamiltonian is Hermitian

$$\mathbf{H}^{(n+1)} = \begin{pmatrix} E_1 & 0 & \dots & 0 & v_1 \\ 0 & E_2 & \dots & 0 & v_2 \\ \vdots & \vdots & \ddots & \vdots & \vdots \\ 0 & 0 & \dots & E_n & v_n \\ v_1 & v_2 & \dots & v_n & v_{n+1} \end{pmatrix} \tag{6.9}$$

We need to find the eigenvalues of this new matrix. To do this we solve the characteristic equation

$$D = |\mathbf{H}^{(n+1)} - \lambda I| = (E_1 - \lambda) M_{1,1}^{(n)} + (-1)^{(n)} v_1 M_{1,n+1}^{(n)} = 0 \tag{6.10}$$

with $M^n_{i,j}$ being the determinant of the matrix of size $n \times n$ that results from removing the ith and jth rows and columns of $\mathbf{H}^{(n+1)}$ respectively. That is

$$M^{(n)}_{(1,1)} = \begin{vmatrix} E_2 - \lambda & 0 & \dots & v_2 \\ 0 & E_3 - \lambda & \dots & v_3 \\ \vdots & \vdots & \ddots & \vdots \\ v_2 & v_3 & \dots & v_{n+1} \end{vmatrix} \tag{6.11}$$

$$M^{(n)}_{(1,n+1)} = \begin{vmatrix} 0 & E_2 - \lambda & 0 & \dots & 0 \\ 0 & 0 & E_3 - \lambda & \dots & 0 \\ \vdots & \vdots & \vdots & \ddots & \vdots \\ v_1 & v_2 & \dots & v_n & \end{vmatrix} = (-1)^{(n-1)} v_1 \prod_{i=2}^{n} (E_i - \lambda) \tag{6.12}$$

To find the determinant of $M^{(n)}_{(1,1)}$ we use the same expansion as was done in calculating the determinant of $\mathbf{H}^{(n+1)}$

$$M^{(n)}_{(1,1)} = (E_2 - \lambda) M^{(n-1)}_{(11)} + (-1)^{(n-1)} v_2 M^{(n-1)}_{(1,n)} \tag{6.13}$$

where $M^{(n-1)}_{(i,j)}$ is the determinant of the $(n-1) \times (n-1)$ dimensional matrix resulting from removing the ith row and jth column of $M^{(n)}_{(1,1)}$ respectively. Once again we can end up with a formula for one of the determinants

$$M^{(n-1)}_{(1,n)} = \begin{vmatrix} 0 & E_3 - \lambda & 0 & \dots & 0 \\ 0 & 0 & E_4 - \lambda & \dots & 0 \\ \vdots & \vdots & \vdots & \ddots & \vdots \\ v_2 & v_3 & \dots & v_n & \end{vmatrix} = (-1)^{(n-2)} v_2 \prod_{i=3}^{n} (E_i - \lambda) \tag{6.14}$$

but we are left to expand the $M^{(n-1)}_{(1,1)}$ determinant. After finishing this sequence of determinant expansions, the end result is

$$D(\lambda) = (v_{(n+1)} - \lambda) \prod_{i=1}^{n} (E_i - \lambda) - \sum_{i=1}^{n} v_i^2 \prod_{j \neq i}^{n} (E_j - \lambda) \tag{6.15}$$

where D is a function of λ. If we put $\lambda = E_k$ in equation (6.15) we find that

$$D(E_k) = -v_k^2 \prod_{j \neq k}^{n} (E_j - E_k) \tag{6.16}$$

If we put $\lambda = E_{k+1}$ in then

$$D(E_{k+1}) = -v_{(k+1)}^2 \prod_{j \neq k}^{n} (E_j - E_{k+1}) \tag{6.17}$$

We know that $E_1 < E_2 \cdots < E_n$, so equations (6.16) and (6.17) show that the products $\prod_{j \neq k}^{n}(E_j - E_k)$ and $\prod_{j \neq k}^{n}(E_j - E_{k+1})$ will have opposite signs (while $-v_k^2$ and $-v_{(k+1)}^2$ are both negative). This implies that $D(E_{k+1})$ is guaranteed to have the opposite sign of $D(E_k)$ for all k. Then $D(\lambda)$ has at least one root in each of the intervals $(E_1, E_2), (E_2, E_3) \ldots (E_{n-1}, E_n)$.

We know the characteristic equation for a Hermitian matrix of size $(n \times n)$ always has n real roots. For our $n+1$ dimensional matrix we have found $n-1$ of these roots so we must find the last two. To do this, we analyze the behaviour of $D(\lambda)$ as the magnitude of λ grows large. Looking at (6.15) it is clear that

$$\lim_{|\lambda| \to \infty} D(\lambda) = (-\lambda)^{(n+1)} \tag{6.18}$$

so if $\lambda \to -\infty$ then $D(\lambda)$ is positive. If $\lambda \to \infty$ then $D(\lambda)$ is a product of $(n+1)$ negative numbers. Using equation (6.16) we can see that

$$D(E_1) = -v_1^2 (E_2 - E_1)(E_3 - E_1) \cdots (E_n - E_1) \tag{6.19}$$

which is a product of $(n-1)$ positive numbers and one negative number, $-v_1^2$. Thus $D(E_1)$ and $\lim_{\lambda \to -\infty} D(\lambda)$ have opposite signs therefore there is a root of $D(\lambda)$ in the range $(-\infty, E_1)$. Similarly

$$D(E_n) = -v_n^2 (E_1 - E_n)(E_2 - E_n) \cdots (E_{n-1} - E_n) \tag{6.20}$$

which is a product of (n) negative numbers so that $D(E_n)$ and $\lim_{\lambda \to \infty} D(\lambda)$ have opposite sign, and thus there is a root of $D(\lambda)$ in (E_n, ∞). Therefore we have found all of the $(n+1)$ eigenvalues of our Hamiltonian matrix $\mathbf{H}^{(n+1)}$ and

have also seen that the n eigenvalues E_i of the old matrix $\mathbf{H}^{(n)}$ are sandwiched between the $n+1$ eigenvalues λ_i of $\mathbf{H}^{(n+1)}$

$$\lambda_1 < E_1 < \lambda_2 < E_2 < \cdots < E_n < \lambda_{n+1} \tag{6.21}$$

If the basis set used to construct the Hamiltonian matrix is complete in the limit $\lim_{n\to\infty}$ (where n is the basis set size) then we must reproduce the exact energy spectrum as $n \to \infty$. Also, the i'th eigenvalue of the Hamiltonian matrix can only decrease in value as n is increased as we have just shown (6.21). This implies the λ_i's cannot decrease past the true energies $E_i^\star$ for any basis size n or else they would not be able to converge to the correct values as $n \to \infty$ which is required by the completeness of the basis functions. Therefore, the HUM theorem states that all of the variational energies λ_i, not just the ground state λ_0, are upper bounds to the true energies E_i^* as long as the basis set being used is complete as $\lim_{n\to\infty}$. Each increase in n is guaranteed to yield smaller upper bounds to the energies and so by simply increasing the size of our basis sets we will find a more accurate approximation to the entire spectrum (disregarding issues of numerical stability in trying to find the spectrum of course).

C Matrix Diagonalization

For large Hamiltonian matrices, it is not feasible to solve the characteristic equation to find the eigenvalues and eigenvectors. Instead, we can apply a known matrix diagonalization method to put the Hamiltonian in diagonal form. The eigenvalues and eigenvectors become trivial once the Hamiltonian is in this form. Diagonalization of a Hamiltonian is equivalent to applying linear variational method as is shown in Appendix A and so it is critical to know how to diagonalize a Hamiltonian. The Hamiltonian matrices used in this work were real symmetric matrices, so in all of the following sections $\mathbf{H}$ will be assumed to be a real symmetric matrix. Most of the information from reference [25] was used in the sections on the Jacobi method, the tridiagonalization method and

Given's method.

C.1 Jacobi Method

In linear algebra, it is a well known and very useful fact that if we rotate any matrix $\mathbf{A}$ with a rotation matrix $\mathbf{R}$ *i.e.*

$$\mathbf{A}' = \mathbf{R}^t \mathbf{A} \mathbf{R} \tag{6.22}$$

then the rotated matrix, $\mathbf{A}'$, will have the same eigenvectors and eigenvalues as the original matrix. The idea of the Jacobi method is to make use of this fact by applying a series of rotations to $\mathbf{H}$ that sequentially zero the off-diagonal matrix elements until it is in diagonal form. Then the eigenvectors and eigenvalues of this transformed matrix will be the same as those for $\mathbf{H}$ except they will be trivial to find.

$$\mathbf{H}' = \mathbf{R}_n^t \mathbf{R}_{n-1}^t \dots \mathbf{R}_1^t \mathbf{H} \mathbf{R}_1 \dots \mathbf{R}_{n-1} \mathbf{R}_n = \mathbf{V}^t \mathbf{H} \mathbf{V} = \mathbf{\Lambda} \tag{6.23}$$

$\mathbf{\Lambda}$ is a diagonal matrix which contains the eigenvectors $\lambda_1 = \Lambda_{11}, \lambda_2 = \Lambda_{22} \dots$. The eigenvalues are contained in the columns of $\mathbf{V}$; $v_m^n = V_{mn}$. So we see that once we have diagonalized $\mathbf{H}$ by applying this set of rotation matrices, we will have found the eigenvalues and eigenvectors we were looking for. Now we must ask the question: which rotations do we use to diagonalize $\mathbf{H}$? Lets define a general Jacobi rotation matrix as

$$\begin{aligned} J(p,q,\theta)_{ii} &= 1 \,\forall\, i \neq p,q \\ J(p,q,\theta)_{ij} &= 0 \,\forall\, i,j \neq p,q \\ J(p,q,\theta)_{pp} &= J(p,q,\theta)_{qq} = \cos(\theta) \\ J(p,q,\theta)_{pq} &= -J(p,q,\theta)_{qp} = \sin(\theta) \end{aligned} \tag{6.24}$$

This matrix looks like

$$J(p,q,\theta) = \begin{pmatrix} 1 & 0 & \dots & & & & & & \\ 0 & \ddots & & & & & & & \\ \vdots & & \dots & \cos(\theta) & \dots & \sin(\theta) & \dots & & \\ & & & \vdots & & \vdots & & & \\ & & \dots & -\sin(\theta) & \dots & \cos(\theta) & \dots & & \\ & & & \vdots & & \vdots & & & \vdots \\ & & & & & & & \ddots & 0 \\ & & & & & & \dots & 0 & 1 \end{pmatrix} \tag{6.25}$$

which is just an identity matrix except for the matrix elements $J_{pp}, J_{pq}, J_{qp}, J_{qq}$. $J(p,q,\theta)$ is the matrix operator representing a rotation by θ in the (e_p, e_q) plane (where e_i is a unit vector in the i'th direction). After applying one of these rotations to $\mathbf{H}$, the new matrix elements are

$$\begin{aligned} H'_{ij} &= H_{ij} \,\forall\, i,j \neq p,q \\ H'_{ip} &= H'_{pi} = cH_{ip} - sH_{iq} \,\forall\, i \neq p,q \\ H'_{iq} &= H'_{qi} = cH_{iq} + sH_{ip} \,\forall\, i \neq p,q \\ H'_{pq} &= H'_{qp} = (c^2 - s^2)H_{pq} + cs(H_{pp} - H_{qq}) \\ H'_{pp} &= c^2 H_{pp} + s^2 H_{qq} - 2csH_{pq} \\ H'_{qq} &= s^2 H_{pp} + c^2 H_{qq} - 2csH_{pq} \end{aligned} \tag{6.26}$$

($c = \cos(\theta)$ and $s = \sin(\theta)$)

We know that rotations do not change the determinant of a matrix, but we need to check if the Frobenius norm is invariant under rotations

$$||\mathbf{H}|| = \sum_{i,j}^{N} H_{ij}^2 \tag{6.27}$$

The squares of the rotated matrix elements are

$$
\begin{aligned}
&{H'_{ij}}^2 = H_{ij}^2 \,\forall\, i,j \neq p,q \\
&{H'_{ip}}^2 = {H'_{pi}}^2 = c^2 H_{ip}^2 + s^2 H_{iq}^2 - 2cs(H_{ip}H_{iq}) \,\forall\, i \neq p,q \\
&{H'_{iq}}^2 = {H'_{qi}}^2 = c^2 H_{iq}^2 + s^2 H_{ip}^2 + 2cs(H_{ip}H_{iq}) \,\forall\, i \neq p,q \\
&{H'_{pq}}^2 = {H'_{qp}}^2 = (c^2 - s^2)^2 H_{pq}^2 + c^2 s^2 (H_{pp} - H_{qq})^2 + 2cs(c^2 - s^2)[H_{pq}(H_{pp} - H_{qq})] \\
&{H'_{pp}}^2 = c^4 H_{pp}^2 + s^4 H_{qq}^2 + 4c^2 s^2 H_{pq}^2 + 2c^2 s^2 (H_{pp}H_{qq}) - 4cs[H_{pq}(c^2 H_{pp} + s^2 H_{qq})]
\end{aligned}
\tag{6.28}
$$

$$
{H'_{qq}}^2 = c^4 H_{qq}^2 + s^4 H_{pp}^2 + 4c^2 s^2 H_{pq}^2 + 2c^2 s^2 (H_{pp}H_{qq}) + 4cs[H_{pq}(c^2 H_{qq} + s^2 H_{pp})] \tag{6.29}
$$

From these equations, it is easy to see that

$$
\begin{aligned}
{H'_{ip}}^2 + {H_{iq}}'^2 &= H_{ip}^2 + H_{iq}^2 \\
{H'_{pi}}^2 + {H_{qi}}'^2 &= H_{pi}^2 + H_{qi}^2
\end{aligned}
$$

where the second equation can be found just by using the fact that both $\mathbf{H}'$ and $\mathbf{H}$ are symmetric matrices. After some tedious algebra, we can find the relationship

$$
{H'_{pp}}^2 + {H'_{qq}}^2 + {H'_{pq}}^2 + {H'_{qp}}^2 = H_{pp}^2 + H_{qq}^2 + H_{pq}^2 + H_{qp}^2 \tag{6.30}
$$

combining this with the previous two expressions, we discover that the Frobenius norm for our real symmetric matrix, $\mathbf{H}$, is invariant under rotations

$$
\sum_{ij}^{N} {H'_{ij}}^2 = \sum_{ij}^{N} H_{ij}^2 \tag{6.31}
$$

Finally, we notice that for each Jacobi rotation, we have the freedom to zero two of the off-diagonal elements by finding the θ such that $H'_{pq} = H'_{qp} = 0$. From (6.26) we find

$$
\tan(2\theta) = \frac{(2H_{pq})}{H_{qq} - H_{pp}} \tag{6.32}
$$

Using (6.28) and (6.29) we have

$$H'^{\,2}_{pp}+H'^{\,2}_{qq} = (c^4+s^4)(H^2_{pp}+H^2_{qq})+8c^2s^2H^2_{pq}+4c^2s^2(H_{pp}H^{\star}_{qq})+4cs[H_{pq}(c^2-s^2)(H_{qq}-H_{pp})] \tag{6.33}$$

Inserting (6.32) into (6.33) results in

$$\begin{aligned} H'^{\,2}_{pp} + H'^{\,2}_{qq} &= H^2_{pp} + H^2_{qq} + 2\sin^2(2\theta)H^2_{pq} + \frac{1}{2}\sin^2(2\theta)(H_{qq} - H_{pp})^2 \\ &= H^2_{pp} + H^2_{qq} + \epsilon,\ \epsilon \geq 0 \\ &\implies H'^{\,2}_{pp} + H'^{\,2}_{qq} \geq H^2_{pp} + H^2_{qq} \end{aligned} \tag{6.34}$$

Equation (6.34) states that the diagonal elements will increase while (6.31) states that the sum of the magnitudes of all the elements in the matrix must stay the same after each rotation matrix is applied. Therefore with each Jacobi rotation, the off-diagonal terms must gradually diminish while the diagonal terms become larger. Given that we are retaining enough significant figures in the matrix elements to avoid large numerical cancellations, we can continue applying these rotations until the off-diagonal elements are all zero to within the desired precision and thus we will have obtained our diagonal matrix.

The Jacobi method is a slow but reliable procedure requiring arithmetic operations $\mathbf{O}(n^4)$ to complete (where n is the dimension of the matrix being diagonalized). The convergence of the Jacobi method can be accelerated by finding the largest off-diagonal matrix before each iteration and applying the corresponding Jacobi matrix to zero it.

C.2 Tridiagonalization

The code used in the programs for diagonalizing matrices with the tridiagonalization method was taken from reference [31], and can be found online using reference [32] (we used the TRED2 and IMTQL2 subroutines in F77). The code and was modified from double precision ($\sim$ 16 decimal digits) to quadruple precision ($\sim$ 30 decimal digits).

We begin the tridiagonalization method with the real symmetric matrix, $\mathbf{H}$. We need to put our matrix in tridiagonal form

$$\mathbf{A} = \begin{pmatrix} a_{11} & a_{12} & & & \\ a_{21} & a_{22} & a_{23} & & \\ & a_{32} & a_{33} & a_{34} & \\ & & \ddots & \ddots & \ddots \end{pmatrix} \tag{6.35}$$

(All unlabeled elements are assumed to be 0)

This is what we refer to as tridiagonalizing a matrix and we used the Householder method for this purpose. A Householder matrix has the form

$$\mathbf{P} = \mathbf{I} - 2ww^t \tag{6.36}$$

where $\mathbf{I}$ is the identity matrix and w is an arbitrary unit vector. $\mathbf{P}$ is symmetric

$$\begin{aligned} \mathbf{P}^t &= \mathbf{I}^t - 2(ww^t)^t \\ &= \mathbf{I} - 2(w^{t^t}w^t) \\ &= \mathbf{P} \end{aligned}$$

and is orthogonal

$$\begin{aligned} \mathbf{P}^2 &= (\mathbf{I} - 2(ww^t))(\mathbf{I} - 2(ww^t)) \\ &= \mathbf{I}^2 - 4(ww^t) + 4(ww^t)(ww^t) \\ &= \mathbf{I} - 4(ww^t) + 4w(w^tw)w^t \\ &= \mathbf{I} - 4(ww^t) + 4ww^t \\ &= \mathbf{I} \\ \implies \mathbf{P} &= \mathbf{P}^{-1} = \mathbf{P}^t \end{aligned} \tag{6.37}$$

Let a vector, x, be orthogonal to w, *i.e.* $w^tx = 0$. Then

$$\mathbf{P}x = (\mathbf{I} - 2ww^t)x = x - 2w(w^tx) = x \tag{6.38}$$

Now let u be a vector in the direction of the unit vector w. Then $w^t u = |u|$ and $w|u| = u$, hence

$$\mathbf{P}u = (\mathbf{I} - 2ww^t)u = u - 2u = -u \tag{6.39}$$

Equations (6.38) and (6.39) illuminate the action of $\mathbf{P}$ on a general vector q. $\mathbf{P}$ will leave any components of q orthogonal to w invariant while reversing the sign of any components of q that align with the w unit vector. $\mathbf{P}$ is a reflection operator.

A series of $\mathbf{P}$'s can be used to put a real symmetric matrix $\mathbf{H}$ in tridiagonal form. We can define $\mathbf{P}_1$ using the following vectors, u,v and w

$$u = \begin{pmatrix} H_{21} \\ H_{31} \\ \vdots \\ H_{n1} \end{pmatrix} \tag{6.40}$$

i.e. u is the vector such that

$$\mathbf{H} = \begin{pmatrix} H_{11} & u^t \\ u & \mathbf{H}^{(n-1)} \end{pmatrix} \tag{6.41}$$

where $\mathbf{H}^{(n-1)}$ is the bottom right $(n-1) \times (n-1)$ submatrix contained in $\mathbf{H}$.

$$v = \begin{pmatrix} |u| \\ 0 \\ \vdots \\ 0 \end{pmatrix} \tag{6.42}$$

$$w = \frac{u - v}{|u - v|} \tag{6.43}$$

With these vectors we can construct an $(n \times n)$ matrix,

$$\mathbf{A}_1 = \begin{pmatrix} 1 & \mathbf{0}^t \\ \mathbf{0} & \mathbf{P}_1 \end{pmatrix} \tag{6.44}$$

so that when $\mathbf{A_1}$ is applied to $\mathbf{H}$, the first row and column of the resulting matrix $\mathbf{H'}$ will be in tridiagonal form

$$\mathbf{H'} = \mathbf{A}_1^t \mathbf{H} \mathbf{A}_1 = \begin{pmatrix} H_{11} & v^t \\ v & \mathbf{P}_1 \mathbf{H}^{(n-1)} \mathbf{P}_1 \end{pmatrix} \tag{6.45}$$

To put the second row and column of $\mathbf{H'}$ in tridiagonal form we use

$$u = \begin{pmatrix} H_{32} \\ H_{42} \\ \vdots \\ H_{n2} \end{pmatrix} \tag{6.46}$$

$$v = \begin{pmatrix} |u| \\ 0 \\ \vdots \\ 0 \end{pmatrix} \tag{6.47}$$

then calculate $\mathbf{P} = \mathbf{I} - 2ww^t$ (recall that $w = \frac{u-v}{|u-v|}$) for the new u and v vectors

$$\mathbf{A}_2 = \begin{pmatrix} \mathbf{I}_2 & \mathbf{0^t} \\ \mathbf{0} & \mathbf{P}_2 \end{pmatrix} \tag{6.48}$$

$\mathbf{I}_2$ is the 2×2 unit matrix. This procedure can be repeated column by column until $\mathbf{H}$ is in tridiagonal form.

The Householder method tridiagonalizes a real symmetric matrix with just $\mathbf{O}(n^3)$ arithmetic operations. Of course, the end goal is to put $\mathbf{H}$ in diagonal form. Why then, do we not use Householder reflection matrices $\mathbf{P}$ that zero all of the elements below the diagonal instead of putting the matrix in tridiagonal form? Attempting to diagonalize the first row and column of $\mathbf{H}$ makes answers this question. First, we set

$$u = \begin{pmatrix} H_{11} \\ H_{21} \\ \vdots \\ H_{n1} \end{pmatrix} \tag{6.49}$$

so that

$$\mathbf{H} = \begin{pmatrix} u_1 & u_2 & \dots & u_n \\ u_2 & H_{22} & \dots & H_{2n} \\ \vdots & \vdots & \vdots & \vdots \\ u_n & H_{n2} & \dots & H_{nn} \end{pmatrix} \tag{6.50}$$

and as usual

$$v = \begin{pmatrix} |u| \\ 0 \\ \vdots \\ 0 \end{pmatrix} \tag{6.51}$$

$$w = \frac{u - v}{|u - v|} \tag{6.52}$$

The corresponding Householder reflection matrix, $\mathbf{P} = \mathbf{I} - 2ww^t$ will be a full $(n \times n)$ matrix; $\mathbf{A}_1 = \mathbf{P}$. Now we can calculate the transformed matrix $\mathbf{H}' = \mathbf{PHP}$. Multiplying on the left by $\mathbf{P}$ yields

$$\mathbf{PH} = \begin{pmatrix} |u| & x^t \\ \mathbf{0} & \mathbf{P}^{(n-1)}\mathbf{H}^{(n-1)} \end{pmatrix} \tag{6.53}$$

where $\mathbf{P}^{(n-1)}$ and $\mathbf{H}^{(n-1)}$ are the matrices resulting from removing the first row and column from $\mathbf{H}$ and $\mathbf{P}$ respectively. The components of the vector, x are $x_i = \mathbf{P}_{11}u_i + \sum_{j=2}^{n} \mathbf{P}_{1j}H_{ji}$ defined from $i = 2, n$.

At this point, the problem is apparent. Although we have successfully zeroed the off-diagonal elements of the first column of $\mathbf{PH}$, we have also altered the first row so that it is no longer equal to u^t. When the $\mathbf{P}$ matrix is applied on the right side, it will not zero the off-diagonal elements in the first row. Worse yet, upon application of $\mathbf{P}$ from the right the elements in the first column will be adjusted in the same way as the elements in the first row were, thereby becoming nonzero. Therefore the diagonalization process is not as simple as applying $n - 1$ Householder reflection matrices.

Now that we have a tridiagonal matrix $\mathbf{H}^0$ resulting from the application of the Householder method to $\mathbf{H}$, we can use another procedure to find the eigenvectors and eigenvalues of $\mathbf{H}^0$. The programs used in this work implemented the implicit QL factorization method for this purpose. First, the tridiagonal matrix is factored into an orthogonal matrix, $\mathbf{Q}_0$ and a lower triangular matrix $\mathbf{L}^0$.

$$\mathbf{H}^0 = \mathbf{Q}_0\mathbf{L}^0 \tag{6.54}$$

which can be done by applying a series of $n-1$ Givens rotations (see Appendix D) to $\mathbf{H}^0$. If the sequence

$$\mathbf{Q}_0^t = \mathbf{G}(2,2)\mathbf{G}(3,3)\ldots\mathbf{G}(n,n) \tag{6.55}$$

is applied to $\mathbf{H}^0$ on the left, the result is a lower triangular matrix L^0 (each $\mathbf{G}(i,i)$ zeros a single superdiagonal element of $\mathbf{H}^0$). Thus from this sequence of Givens rotations we obtain both $\mathbf{L}^0$ and $\mathbf{Q}_0 = \mathbf{G}(n,n)\ldots\mathbf{G}(3,3)\mathbf{G}(2,2)$. Now we can find $\mathbf{H}^1$ using

$$\mathbf{H}^1 = \mathbf{L}^0\mathbf{Q}_0 = \mathbf{Q}_0^t\mathbf{H}^0\mathbf{Q}_0 \tag{6.56}$$

$\mathbf{Q}_0$ is orthogonal (any composition of Givens rotation matrices will be orthogonal because the Givens rotations themselves are orthogonal), so $\mathbf{H}^1$ is similar to $\mathbf{H}^0$ and therefore they share the same eigenvectors and eigenvalues. This transformation also preserves the tridiagonal form of $\mathbf{H}^0$ – if $\mathbf{H^0}$ is a tridiagonal matrix then $\mathbf{H}^1$ will also be a tridiagonal matrix. The implicit QL method is continued by factoring $\mathbf{H}^1$ into a new orthogonal matrix $\mathbf{Q}_1$ and a new lower triangular matrix $\mathbf{L}^2$ then uses these to find the next tridiagonal matrix $\mathbf{H}^2 = \mathbf{L}^1\mathbf{Q}_1$. The sequence of matrices $\mathbf{H}^k$ gradually become diagonalized as k is incremented (k is the number of iterations of the implicit QL algorithm).

Each iteration of the implicit QL method, when applied to a tridiagonal matrix, takes $O(n)$ operations to perform. Depending on the precision requirement for which the off-diagonal elements must agree with zero, each eigenvalue and

eigenvector found take roughly 1 to 2 iterations on average. Thus, finding all of the eigenvalues and eigenvectors of a tridiagonal matrix with the implicit QL algorithm is of $O(n^2)$ operations. For large n the slowest part of the tridiagonalization method is putting the initial matrix $\mathbf{H}$ in tridiagonal form and is of $O(n^3)$ operations (if the Householder method is used). Givens' method can also be used to tridiagonalize a matrix (Appendix D) but it takes about 50% more operations to complete than the Householder method for large matrices.

C.3 Power Method and Inverse Iteration Method

The information from reference [26] was used to complete this section. The power and inverse iteration methods are very simple and effective ways to solve the generalized eigenvalue problem. The power method begins with a single arbitrary starting vector, χ that can be expanded as a linear combination of the true eigenvectors ψ_i of the Hamiltonian matrix $\mathbf{H}$

$$\chi = \sum_{i=0}^{N} c_i \psi_i \tag{6.57}$$

Then we can write

$$\mathbf{H}\chi = \sum_{i=0}^{N} c_i \mathbf{H}\psi_i = \sum_{i=0}^{N} c_i E_i \mathbf{O}\psi_i \tag{6.58}$$

where $\mathbf{O}$ is the overlap matrix. Left multiply both sides by $\mathbf{O}^{-1}$ to get

$$\mathbf{O}^{-1}\mathbf{H}\chi = \sum_{i=0}^{N} c_i E_i \psi_i \tag{6.59}$$

Now, if $\mathbf{O}^{-1}\mathbf{H}$ is applied n times to χ the result is

$$(\mathbf{O}^{-1}\mathbf{H})^n \chi = \sum_{i}^{N} (E_i^n) c_i \psi_i \tag{6.60}$$

Repeated application of $\mathbf{O}^{-1}\mathbf{H}$ to χ will make the sum on the right hand side of (6.60) converge to

$$\lim_{n\to\infty}(\mathbf{O}^{-1}\mathbf{H})^n\chi = (E_j)^n c_j\psi_j \tag{6.61}$$

where E_j is the largest eigenvalue in the spectrum. One would think that there might be a way we could find all the eigenvalues and eigenvectors using the power method. Certainly we could find the next largest eigenvalue and the corresponding eigenvector by using an initial vector χ_2 that is orthogonal to ψ_j so that $c_j = 0$. Repeated application of $\mathbf{O}^{-1}\mathbf{H}$ on χ_2 would isolate the second largest eigenvector and eigenvalue of the spectrum of $\mathbf{H}$. The next starting vector χ_3 would use an initial vector that is orthogonal to the first two eigenvectors allowing the discovery of the third largest eigenvalue and eigenvector upon repeated application of $\mathbf{O}^{-1}\mathbf{H}$. In theory, we could continue this procedure all the way down to the ground state, but in practice this most likely would not work due to issues with numerical stability. As we continue the algorithm, the number of vectors that the initial vector χ_i must be orthogonal to increases. Eventually, the orthogonalization routine will begin to become inaccurate and there will be small components of the higher eigenvectors left in χ_i. Even if the surviving components of the higher eigenvectors are small, the corresponding eigenvalues are large and so using the power method would not guarantee convergence to the desired eigenvalue and eigenvector pair.

The power method works but may have slow convergence in the case that the eigenvalues are all close together. Also, as we have just shown above, it is also only useful for finding the largest eigenvalue and eigenvector in a spectrum.

The inverse power method is an improvement of the power method. From reference [26]

$$\begin{aligned}
\mathbf{H}\psi_i &= E_i\mathbf{O}\psi_i \\
(\mathbf{H} - E_g\mathbf{O})\psi_i &= (E_i - E_g)\mathbf{O}\psi_i \\
\mathbf{G}\psi_i &= \frac{1}{E_i - E_g}\psi_i
\end{aligned}$$

with $\mathbf{G} = (\mathbf{H} - E_g\mathbf{O})^{-1}\mathbf{O}$ and E_g is a guessed value for the energy eigenvalue

that is desired. The idea is that the eigenvalue closest to E_g, which we will denote by E_j, will result in a much larger value for $\dfrac{1}{E_i - E_g}$ than the rest of the E_i so that the sequence

$$\begin{aligned} \chi_1 &= \mathbf{G}\chi \\ \chi_2 &= \mathbf{G}\chi_1 \\ \chi_3 &= \mathbf{G}\chi_2 \\ &\vdots \end{aligned} \tag{6.62}$$

will quickly converge to

$$\chi_n \approx c_j \left(\frac{1}{E_j - E_g} \right)^n \psi_j \tag{6.63}$$

By varying E_g, eventually all of the eigenvalues and eigenvectors of $\mathbf{H}$ can be found.

There are two minor details to be aware of when using the inverse power method. First, if the initial energy guess is exactly equal to one of the true eigenvalues then the inverse matrix $\mathbf{G}$ becomes singular. This issue almost never occurs and can easily be avoided by using a slightly adjusted E_g for the next attempt. Second, if by chance $c_j = 0$ in the trial wave function χ then the sequence will not converge to the desired results, E_j, ψ_j but instead to the next closest eigenvalue and eigenfunction with $c_k \neq 0$. This highly unlikely event can be handled by trying different initial wave functions for the same E_g and making sure the final values E_j for each different χ are consistent.

In the inverse power method a matrix inversion needs to take place in order to obtain the $\mathbf{G}$ matrix. In fact each time E_g is changed the $\mathbf{G}$ matrix will need to be recalculated. The inverse iteration method is almost the same as the inverse power method except it replaces matrix inversion with solving a matrix equation. We start by constructing the sequence

$$\mathbf{F}\chi_n = (E - E_g)\mathbf{O}\chi_{n-1}$$

with $\mathbf{F} = (\mathbf{H} - E_g)\mathbf{O}$. This is equivalent to the sequence we had from the inverse power method, but now there is no inverse matrix to calculate. We can simplify this further by noting that the factor of $(E - E_g)$ only affects the normalization of χ_n. So we can instead solve

$$\mathbf{F}\chi_n = \mathbf{O}\chi_{n-1}$$

which will provide the eigenvector $\chi_n \approx \psi_j$. The corresponding E_j is found by solving

$$E_j = \frac{\langle \chi_n | \mathbf{H} | \chi_n \rangle}{\langle \chi_n | \chi_n \rangle}$$

The inverse iteration method was used in one of the programs (dpoldl.f) which found the optimal nonlinear parameters for our Hylleraas basis sets. It is a quick method for finding a single eigenvalue and eigenvector pair and is very useful for finding the optimal nonlinear parameters for a variational basis set in a reasonable amount of time. The Jacobi and Tridiagonalization methods generally take more time to complete than the inverse iteration method. Also, the optimal nonlinear parameters corresponding to different eigenvectors are distinct from each other. This means that if we are trying to minimize a single variational energy there is no benefit in calculating all of the eigenvectors and eigenvalues of the Hamiltonian matrix – a single nonlinear parameter set can only be used to minimize one eigenvalue at a time. For these reasons, the inverse iteration method is chosen for finding the optimal nonlinear parameters of a variational basis set.

D Givens' Method

Givens' method is a method used to tridiagonalize a matrix. The Givens rotation matrices introduced in this section are commonly used in the implicit QL method as was done in this work.

The tridiagonalization of a real symmetric matrix $\mathbf{H}$ using Givens' method

is similar to the Jacobi method for diagonalizing matrices. We apply a series of Jacobi matrices $J(p,q,\theta)$ to $\mathbf{H}$, but instead of setting θ so that $H'_{pq} = H'_{qp} = 0$ we use θ such that $H'_{q(p-1)} = H'_{(p-1)q} = 0$. From equations (6.26) in section C.1 we have

$$H'_{iq} = H'_{qi} = cH_{iq} + sH_{ip} \,\forall\, i \neq p, q \tag{6.64}$$

and so the θ used in $J(p,q,\theta)$ required to zero $H'_{q(p-1)}$ and $H'_{(p-1)q}$ is

$$\tan(\theta) = -\frac{H_{q(p-1)}}{H_{p(p-1)}} \tag{6.65}$$

which is easily found by setting $i = (p-1)$ in equation (6.64). To simplify the notation, we can define the Jacobi rotation matrices that use the θ from equation (6.65) to be Givens rotation matrices and denote these by $\mathbf{G}(p,q)$. The Givens rotation matrices are orthogonal because the Jacobi matrices are orthogonal. Also, as can be seen from equations (6.26) in Appendix (C.1), when transforming a matrix $\mathbf{H}$ with a Jacobi rotation matrix (or a Givens rotation matrix) only rows and columns p and q are altered in the transformed matrix $\mathbf{H}'$. So if we have a matrix $\mathbf{H}$ which already has $H_{ij} = 0, ij \neq p, q$ then after applying $\mathbf{G}(p,q)$ to $\mathbf{H}$, $H'_{ij} = 0, ij \neq p, q$. Allowing the following series of Givens rotations

$$\mathbf{Q} = \mathbf{G}(2,3)\mathbf{G}(2,4)\ldots\mathbf{G}(2,n) \tag{6.66}$$

to act on $\mathbf{H}$

$$\mathbf{H}' = \mathbf{Q}^t\mathbf{H}\mathbf{Q} \tag{6.67}$$

will result in $H'_{31} = H'_{41} = \cdots = H'_{n1} = 0$. $\mathbf{H}'$ is a symmetric matrix (because $\mathbf{H}$ was assumed to be symmetric) so $H'_{13} = H'_{14} = \cdots = H'_{1n} = 0$ and thus both the first row and column of $\mathbf{H}$ are in tridiagonal form.

To put the second row and column in tridiagonal form we use the next series of Givens rotations

$$\mathbf{G}(3,4)\mathbf{G}(3,5)\dots\mathbf{G}(3,n) \tag{6.68}$$

Now the second rows and columns are in tridiagonal form, but we have to double-check that any zeros in the first row and column of the transformed matrix are not undone. Using

$$H'_{pi} = cH_{pi} - sH_{qi} \tag{6.69}$$

from equations (6.26) and setting $i = 1$, it is clear that the H'_{p1}'s that are not tridiagonal elements remain zero since the H_{n1}'s were all zeroed from applying the previous sequence of Givens rotations $\mathbf{Q}$.

To put an entire real symmetric matrix in tridiagonal form we use the sequence of Givens rotations

$$\begin{aligned}
&\mathbf{G}(2,3)\mathbf{G}(2,4)\dots\mathbf{G}(2,n)\\
\times&\mathbf{G}(3,4)\mathbf{G}(3,5)\dots\mathbf{G}(3,n)\\
&\vdots\\
\times&\mathbf{G}(n-2,n-1)\mathbf{G}(n-2,n)\\
\times&\mathbf{G}(n-1,n)
\end{aligned}$$

where each individual Givens rotation matrix zeros a single element in the transformed matrix. This procedure ends up resulting in $\mathbf{O}(n^4)$ total floating point operations as opposed to the $\mathbf{O}(n^3)$ operations the Householder method takes. Although it is slower than the Householder method when computing in series, unlike the Householder method, it has the advantage that it can be computed in parallel. However, even with parallel computing Givens' method takes about the same runtime as the Householder method and so the Householder method is more commonly used.

E Number of terms in a single Hylleraas basis set

Recall that a single Hylleraas basis is

$$\Psi = \sum^{\Omega} c_{ijk}[r_1^i r_2^j r_{12}^k e^{-\alpha r_1} e^{-\beta r_2} \pm r_2^i r_1^j r_{12}^k e^{-\alpha r_2} e^{-\beta r_1}] \tag{6.70}$$

with the truncation

$$i + j + k \leq \Omega \tag{6.71}$$

We can write out a matrix of the sums of all possible combinations for the first two numbers, i and j

$$\mathbf{M^0} = \begin{pmatrix} 0 & 1 & \dots & \Omega \\ 1 & 2 & \dots & (\Omega+1) \\ \vdots & \vdots & & \vdots \\ \Omega & (\Omega+1) & \dots & 2\Omega \end{pmatrix} \tag{6.72}$$

where the row number minus 1 represents the value of i, the column number minus 1 represents the value of j, and the elements M_{ij}^0 are the corresponding sums $i + j$. Only the upper left triangle (including the diagonal part) of this matrix is permitted by the restriction (6.71). The number of elements in a triangular section of a $(n \times n)$ matrix is

$$N = \frac{n(n+1)}{2} \tag{6.73}$$

which comes from taking half of all the n^2 elements in a $(n \times n)$ matrix and adding the missing half of the n diagonal elements to complete the triangle. $\mathbf{M^0}$ is a $((\Omega+1) \times (\Omega+1)$ matrix and therefore it contains $N_0 = \frac{(\Omega+1)(\Omega+2)}{2}$ possible basis set terms.

If we include the third index k we get a rank 3 tensor containing all of the possible permutations of i, j, and k. This rank 3 tensor can be represented by

a set of matrices of the same form as $\mathbf{M^0}$ in equation (6.72) – each k will have a unique $\mathbf{M^k}$ associated with it

$$\mathbf{M^k} = \begin{pmatrix} k & k+1 & \dots & k+\Omega \\ k+1 & K+2 & \dots & k+(\Omega+1) \\ \vdots & \vdots & & \vdots \\ k+\Omega & k+(\Omega+1) & \dots & k+2\Omega \end{pmatrix} \tag{6.74}$$

So all we need to do now is add up all of the allowed terms in each of these $\mathbf{M^k}$ matrices. We have already analyzed $\mathbf{M^0}$ so the next step is to look at $\mathbf{M^1}$.

$$\mathbf{M^1} = \begin{pmatrix} 1 & 2 & \dots & 1+\Omega \\ 2 & 3 & \dots & 1+(\Omega+1) \\ \vdots & \vdots & & \vdots \\ 1+\Omega & 1+(\Omega+1) & \dots & 1+2\Omega \end{pmatrix} \tag{6.75}$$

By equation (6.71), the only allowed terms contained in $\mathbf{M^1}$ are within the upper left triangular part of $\mathbf{M^1}$ with its bottom row and right-most column removed. The following is a $(\Omega+1)\times(\Omega+1)$ matrix illustrating the possible i, j combinations for $k=1$. The 1's represent the location of allowed permutations and the 0's are the prohibited permutations.

$$\begin{pmatrix} 1 & 1 & \dots & 1 & 0 \\ 1 & 1 & \dots & 0 & 0 \\ \vdots & \vdots & & \vdots & \vdots \\ 1 & 0 & \dots & 0 & 0 \\ 0 & 0 & \dots & 0 & 0 \end{pmatrix} \tag{6.76}$$

By equation (6.73), $\mathbf{M^1}$ provides $N_1 = \dfrac{\Omega(\Omega+1)}{2}$ terms to the Hylleraas basis set.

For the $\mathbf{M^2}$ matrix, the possible i and j permutations appear in the upper left triangle of $\mathbf{M^2}$ after removing its bottom two rows and right-most two columns. Then we get $N_2 = \dfrac{(\Omega-1)\Omega}{2}$ terms from $\mathbf{M^2}$. The crucial pattern to

notice here is that $\mathbf{M^k}$ provides $N_k = \dfrac{\Omega + 1 - k}{\Omega + 2 - k}$ more terms to the basis set. The total number of terms is

$$\begin{aligned} N &= \sum_{k=0}^{\Omega} N_k \\ &= \sum_{k=0}^{\Omega} \frac{(\Omega + 1 - k)(\Omega + 2 - k)}{2} \\ &= \sum_{k=0}^{\Omega} \frac{(\Omega^2 + 3\Omega + 2) + (k^2 - 2k\Omega - 3k)}{2} \\ &= \frac{(\Omega + 1)(\Omega^2 + 3\Omega + 2)}{2} + \frac{1}{2}\left[\sum_{k=0}^{\Omega} k^2 - (2\Omega + 3)\sum_{k=0}^{\Omega} k\right] \end{aligned} \tag{6.77}$$

There are formulas for the last two sums that appear in equation (6.77)

$$\sum_{i=0}^{n} i = \frac{n(n+1)}{2} \tag{6.78}$$

$$\sum_{i=0}^{n} i^2 = \frac{n(n+1)(2n+1)}{6} \tag{6.79}$$

putting these into (6.77)

$$\begin{aligned} N &= \frac{(\Omega + 1)(\Omega^2 + 3\Omega + 2)}{2} + \frac{1}{2}\left[\frac{\Omega(\Omega + 1)(2\Omega + 1)}{6} - (2\Omega + 3)\frac{\Omega(\Omega + 1)}{2}\right] \\ &= \frac{(\Omega + 1)}{2}\left[\frac{6(\Omega^2 + 3\Omega + 2) + \Omega(2\Omega + 1) - 3\Omega(2\Omega + 3)}{6}\right] \\ &= \frac{(\Omega + 1)}{2}\left[\frac{2\Omega^2 + 10\Omega + 12)}{6}\right] \\ &= \frac{(\Omega + 1)(\Omega + 2)(\Omega + 3)}{6} \end{aligned}$$

and we have the formula for the total number of terms in a single Hylleraas basis set.

Bibliography

[1] Jonathan D. Baker, David E. Freund, R. N. Hill and John D. Morgan III, Phys. Rev. A **41**, 1247 (1990).

[2] E. A. Hylleraas, Z. Phys. **65**, 209 (1930).

[3] T. Kato, J. Fac. Sci. Univ. Tokyo Sect. **I 6**, 145 (1951).

[4] T. Kato, *Perturbation Theory for Linear Operators*, 2nd ed., (Springer, New York, 1976), pp. 410-413.

[5] R. E. Knight and C. W. Scherr, Phys. Rev. **128**, 2675 (1962).

[6] R. E. Knight and C. W. Scherr, Rev. Mod. Phys. **35**, 436 (1963).

[7] J. Midtdal, Phys. Rev. **138**, A1010 (1965).

[8] F. H. Stillinger, J. Chem. Phys. **45**, 3623 (1966).

[9] F. C. Sanders and C. W. Scherr, Phys. Rev. **181**, 84 (1969).

[10] J. Midtdal, K. Aashamar, and G. Lyslo, Phys. Norv. **3**, 11 (1968).

[11] J. Midtdal, K. Aashamar, and G. Lyslo, Phys. Norv. **3**, 163 (1969).

[12] E. Brändas and O. Goscinski, Int. J. Quantum Chem. **4**, 571 (1970).

[13] E. Brändas and O. Goscinski, Int. J. Quantum Chem. Symp. **6**, 59 (1972).

[14] F. H. Stillinger and D. K. Stillinger, Phys. Rev. A **10**, 1109 (1974).

[15] F. H. Stillinger and T. A. Weber, Phys. Rev. A **10**, 1122 (1974).

[16] W. P. Reinhardt, Phys. Rev. A **15**, 802 (1977).

[17] F. H. Stillinger, Phys. Rev. A **15**, 806 (1977).

[18] G. A. Arteca, F. M. Fernández, and E. A. Castro, J. Chem. Phys. **84**, 1624 (1986).

[19] I. A. Ivanov, Phys. Rev. A **51**, 1080 (1995).

[20] J. Zamastil, J. Cizek, L. Skala, and M. Simanek, Phys. Rev. A **81**, 032118 (2010).

[21] A. V. Turbiner and J. C. Lopez Vieyra, Can. J. Phys. **94**, 3 (2015) pp. 249-253.

[22] J.-P. Karr, Phys. Rev. A **92**, 042505 (2015).

[23] C. S. Estienne, M. Busuttil, A. Moini and G. W. F. Drake, Phys. Rev. Lett. **112**, 173001 (2014).

[24] R. N. Hill, Phys. Rev. Lett. **38**, 643 (1977).

[25] W. H. Press, S. A. Teukolsky, W. T. Vetterling, B. P. Flannery, *Numerical Recipes in C: The Art of Scientific Computing*, 2nd ed., (Cambridge University Press, Cambridge, 1988), pp. 456-493.

[26] G. W. F. Drake, Notes on solving the Schrödinger equation in Hylleraas coordinates for heliumlike atoms (2016). http://drake.sharcnet.ca/mediawiki/index.php/Theory_Notes

[27] G. W. F. Drake, W. Baylis, J. Louck, J. Paldus, B. Judd, K. Bartschat, D. Schultz, . . . , M. Inokuti, *Springer Handbook of Atomic Molecular and Optical Physics* 2nd ed. (Springer, New York, 2006) pp. 201.

[28] E. A. Hylleraas and B. Undheim, Z. Phys. **65**, 759 (1930).

[29] J. K. L. MacDonald, Phys. Rev. Lett. **43**, 830 (1933).

[30] G. W. F. Drake, Mark M. Cassar and Razvan A. Nistor, Phys. Rev. A **65**, 054501 (2002).

[31] B. T. Smith, J. M. Boyle, J. J. Dongarra, B. S. Garbow, Y. Ikebe, V. C. Klema, C. B. Moler, *Matrix Eigensystem Routines - EISPACK Guide*, Lecture Notes in Computer Science (Springer-Verlag, Berlin, 1976) Vol. 6.

[32] EISPACK. http://www.netlib.org/eispack/

[33] A. Moini, *Critical Nuclear Charge of the Quantum Mechanical Three-Body Problem* (Masters thesis, University of Windsor, Windsor, Ontario), retrieved from http://scholar.uwindsor.ca/cgi/viewcontent.cgi?article=6048&context=etd (2014).

Vita Auctoris

Ryan Peck was born in Sudbury, Ontario in 1991. He moved to Maple Ridge, British Columbia in 2002. He received his BSc with a double major in math and physics from the University of the Fraser Valley in 2014. He began his MSc program at the University of Windsor in the fall of 2014 and hopes to graduate in August 2017.